2-16-2021 1:30 PM

A critical review and finite element study of structural relaxation in veneered 3Y-TZP dental structures

Prashant S. Shelar, *Western University*

Supervisor: Abdolvand, Hamidreza, *The University of Western Ontario*
Co-Supervisor: Butler, Sheila, *The University of Western Ontario*
A thesis submitted in partial fulfillment of the requirements for the Master of Engineering Science degree in Mechanical and Materials Engineering

Abstract

Yttria stabilized Tetragonal Zirconia Polycrystal (3Y-TZP) materials veneered with porcelain are preferred for clinical practice due to their bio-functionality, biocompatibility, and affordability. However, these materials are often subjected to premature clinical failures due to combination of subsurface flaws and tensile stresses within porcelains. This work focuses on performing a critical literature review and evaluating veneer characteristics, i.e. structural relaxation, to form a suitable explanation for the development of subsurface stresses. User material subroutines, UEXPAN and UTRS are developed, validated and integrated in ABAQUS finite element solver. With the use of validated models, it is shown that faster cooling rates and high veneer thickness results in higher subsurface tensile stresses due to lack of structural relaxation. Slow cooling rates and lower veneer thickness result in desired compressive stresses in the subsurface. This work shows that structural relaxation in veneer can be used for tailoring the desired stress for the extending lifespan of veneered 3Y-TZP dental restorations.

Keywords

Dental materials, 3Y-TZP, bilayer, porcelain, structural relaxation, viscoelastic, finite element analysis, user material subroutine (UEXPAN, UTRS)

Summary for Lay Audience

Zirconia-based dental materials are widely used for dental restorations due to their excellent aesthetics, bio-functionality, biocompatibility, and affordability compared to other dental materials. Zirconia material is veneered with glassy porcelain to achieve a suitable aesthetic appearance. Unfortunately, clinically such veneered glassy porcelain suffers premature failures due to subsurface manufacturing defects and undesired stresses. These undesired stresses are induced during the last heat treatment conducted for glazing of the veneering dental porcelains.

Extensive work is performed in understanding and identifying various parameters that can potentially result in such premature failures. Nevertheless, the problem remains unresolved. One objective of this research is to conduct a critical literature review to identify all possible parameters and their effects on this material's performance.

Dental porcelains exhibit glass-like behavior. Evaluation of glass characteristics is important for understanding how glass behaves when subjected to high temperature. Structural relaxation is one of the glass characteristics that is never explored in dental porcelains to evaluate its effect on the stress state. Understanding the effects of structural relaxation on the state of the stress is another objective of this research.

Finite element numerical method is used for analysis in this project. This type of analysis is a technique that uses a software to predict the behavior of varied type of physical problems in defined conditions. Basically, finite element method is a mathematical procedure used to calculate approximate solutions for complicated engineering problems by solving equations with the use of commercial softwares. This finite element analysis have shown that faster cooling rates and higher veneer thicknesses result in undesired subsurface tensile stresses due to lack of structural relaxation. Such undesired tensile stresses may lead to premature failure during clinical applications. It is shown that lower cooling rates and lower veneer thicknesses result in desired compressive stresses, which increases the resistance to surface defect.

By modelling the development of stress state with respect to structural relaxation, this research focuses on a promising way forward to improve the lifespan of dental porcelains veneered on zirconia.

Co-Authorship Statement

1) Chapter 2 of this thesis was reproduced from a research manuscript titled "On the Behavior of Bilayer Zirconia-based Dental Materials – A critical review". The title of manuscript, names of the co-author and the contribution made by each co-author are listed below.

   Title: On the behavior of bilayer zirconia-based dental materials – A critical review

   Submitted To: (To be advised)

   Publication Status: -Not applicable-

   Authors: Prashant Shelar, Hamidreza Abdolvand, Sheila Butler

   Contributions: Prashant Shelar conceptualized the method and conducted literature review. Prof. Sheila Butler and Prof. Hamidreza Abdolvand provided guidance and support in research process. They also reviewed and provided comments for revisions on the draft manuscript.

2) Part of chapter 3 to 6 of this thesis were reproduced from a research manuscript titled "Effect of thermal gradient on structural relaxation and characterization of thermal stresses in dental porcelains – A Finite Element Study". The title of manuscript, names of the co-author and the contribution made by each co-author are listed below.

   Title: Effect of thermal gradient on structural relaxation and characterization of thermal stresses in dental porcelains – A finite element study

   Submitted To: Journal of the Mechanical Behavior of Biomedical Materials

   Publication Status: Under review

   Authors: Prashant Shelar, Sheila Butler

   Contributions: Prashant Shelar identified the knowledge gap and motivation for this research. Accordingly he defined the objectives, roadmap and conducted research. Prof. Sheila Butler provided guidance and support in research process. Prof. Sheila Butler also reviewed and provided comments for revisions on the draft manuscript.

Acknowledgments

I want to thank my family, project supervisors and teachers without whom this project would not have been possible. I would like to have specific mentions below for their support, which has encouraged me during this complete journey.

I would like to thank Dr. Sheila Butler for introducing such a critical concern faced in clinical practice. Also I am thankful to her for complete guidance, support and reviewing complete work. I would like to thank Dr. Hamidreza Abdolvand for providing resources required for this work, basic introduction to computer programming, and his inputs on polishing literature review manuscript. I am highly thankful to my supervisor for guidance, valuable suggestions, and time on this project.

I want to thank Dr. Ayman El Ansary from the Department of Civil and Environmental Engineering to have introduced and taught concepts of finite element analysis in an extremely effective manner.

I am thankful to Natural Sciences and Engineering Research Council (NSERC) of Canada to support this research work by means of providing funding through Western University.

I am grateful to my mother for supporting me with the wisdom to evaluate myself during challenging times. I am thankful to my wife for motivating me to explore this journey. Last but not the least, I want to thank my family and friends in London (Watson, Steph, Linc, Henry, Maple, Ruby, Sophie, Susi, Luna and Steve) for their unconditional support and encouragement to keep me motivated on this path.

Table of Contents

List of Tables

List of Figures

List of Appendices

Chapter 1

1 Introduction

Dental restorations have been an inclusive and significant part of human life. Dental materials have gradually seen development and advancement, which has progressed far in recent years to overcome challenges in performance, durability, and affordability. The advancement in dental material research is explained by Bayne et al. [1], starting with the Journal of Dental Research (JDR) in the 1919 till the possible use of Universal Adhesives in 2020.

In recent years, dental materials selection has migrated from traditional and expensive materials like Gold, Silver, or Porcelain Fused to Metal (PFM) to all-ceramic and composite resins. This shift of choice is justified mainly due to affordability, tooth-like appearance, biocompatibility, and bio-functionality of the composite.

Yttria stabilized Tetragonal Zirconia Polycrystal (3Y-TZP) attracted the overall market due to their superior flexural strength, fracture toughness, biocompatibility, biofunctionality and affordability. As a result, alumina-based dental material almost became obsolete. Although, it is seldom mentioned in the literature that fracture or mechanical instability is one of the causes of implant loss for alumina-based dental material [2].

Zirconia has proximity to color and translucency found in natural teeth as it reflects and absorbs light similar to a natural tooth. However, it is still not suitable for anterior teeth. Hence, it is coated with a thin veneer (dental porcelain) layer for a suitable aesthetic appearance. This requirement of achieving a suitable aesthetic appearance has a drawback that the veneer's fails prematurely [3–6].

Extensive research is performed on bilayer 3Y-TZP dental materials for more than a decade to resolve the chipping and fracture of veneers from the framework. To list a few studies, researchers worked on parameters such as lower elastic modulus and fracture toughness [7–9], veneer thickness [9–11], inadequate bond strength [8,12–18], design parameters like the anatomical design of frameworks or poor support to veneer [19–21], heat treatment

variables like heating rates [22,23], furnace atmospheres [24], soaking time / extended cooling mechanism [25,26], firing cycles [27,28], soaking temperature [29,30], sensitivity to cooling protocols [9,22,31–40].

Unfortunately, optimum solutions are not yet found. There is no single source of literature available to the best knowledge of author highlighting the effect of the various parameters affecting the material behavior and conducting effective root cause analysis. This situation demands a consolidated research review performed on the parameters that affect the material behavior and understand their effects.

Such a review facilitates practical future failure analysis, systematic elimination of root causes, and identifying research directions to solve the problem. It further enables the development of guidelines or standard protocols for quality manufacturing, which could guarantee these materials' performance and integrity.

It is also worth noting that the premature chipping of veneers is the most observed clinical type of failure. The failure is limited to porcelain with a thin layer of veneer attached to the zirconia surface [33]. Thermal stresses induced during glazing heat treatment combined with internal subsurface discontinuities are suggested to be the cause of premature chipping [9,35]. Hence, it is expected that defects nucleate within the material and traverse through-thickness.

Swain et al. [9] has described chipping as crack initiation within the veneer and subsequent extension through the thickness, as shown in Figure 1-1. In another study by Benetti et al. [35], a SEM image of clinically chipped porcelain exhibiting fracture initiation within the porcelain is shown in Figure 1-2. Generally, fractures are known to originate from the defects in the veneer [41]. Therefore, the population of flaws in the porcelain in combination with tensile stresses around the flaws may potentially govern the process of crack initiation and propagation.

Fractography studies have shown that the subsurface flaws or discontinuities play a significant role in the failure of cermic materials during strength testing [42]. It is shown that the tensile stresses are developed wihin the material while compressive stresses are

developed at the surface. This stress pattern results in initiation and propagation of cracks within the material. An exception to this can be if any manufacturing defect, e.g., notch or grinding marks or microcracks, are formed at the the surface causing fracture initiation from the surface and propagation below the surface.

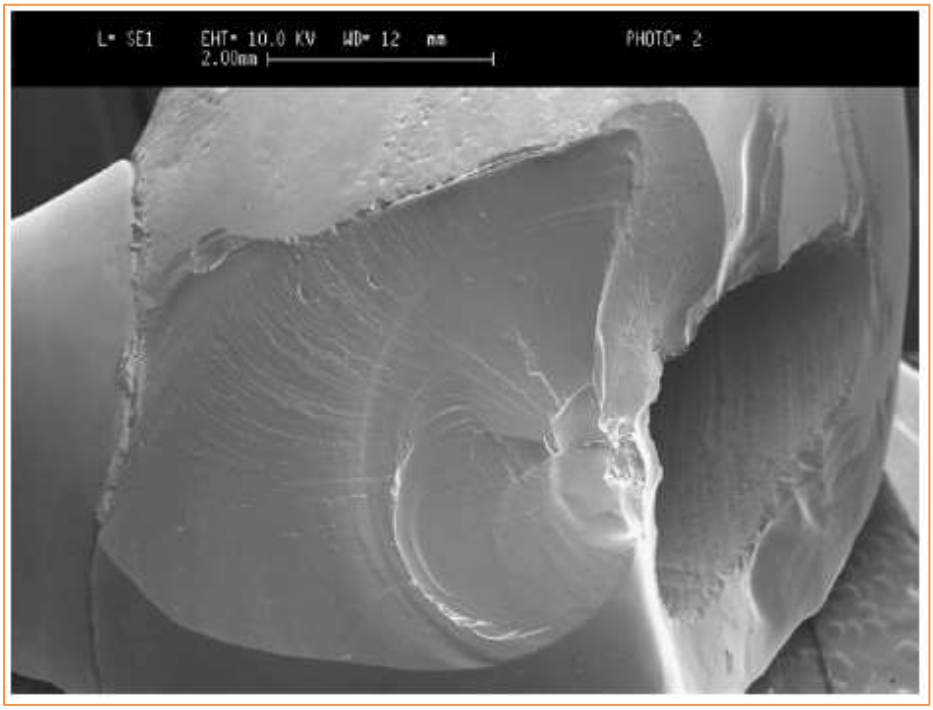

Figure 1-1: SEM image of a chipped porcelain on porcelain fused to zirconia coping abutment (Image Printed from [9])

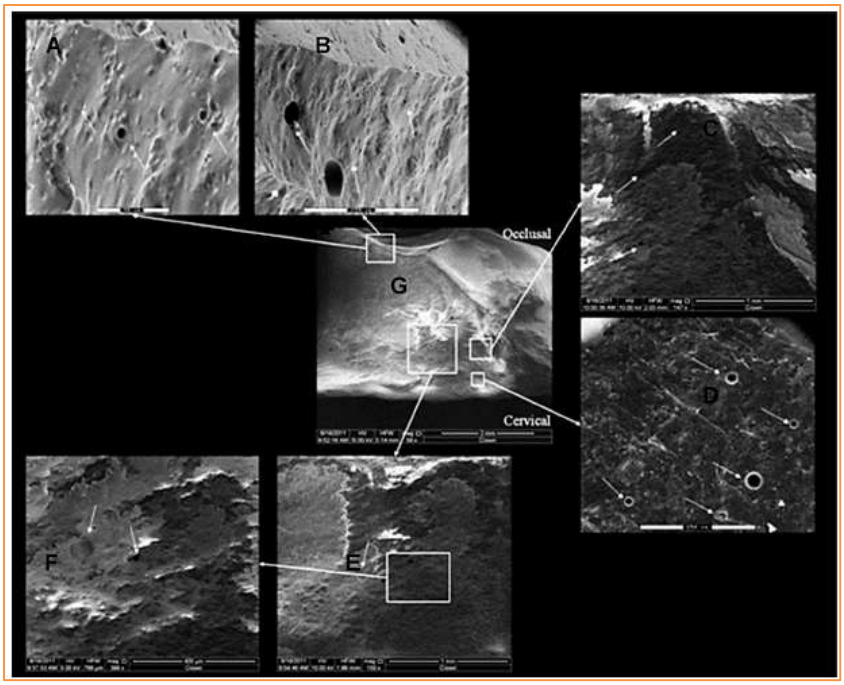

Figure 1-2: SEM images of clinically fractured porcelain.

Images A-F: White arrows show defects and the origin of fracture in porcelain bulk (Image G). Image B shows cracks parallel to the occlusal surface (Image Printed from [35])

Thus, the best possible combinations to induce premature failure of dental systems in the presence of load can be best described in Figure 1-3.

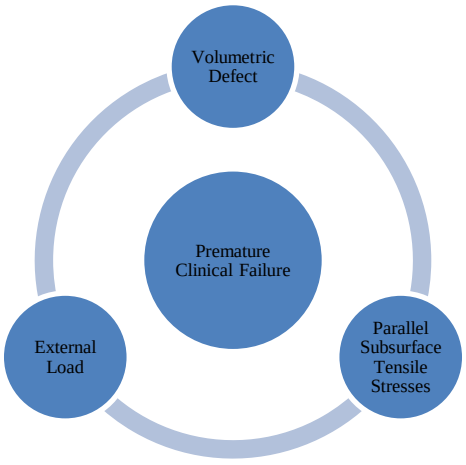

Figure 1-3: Factors facilitating premature clinical failures

Isolated from inherent manufacturing flaws, thermal stresses are the other key factor for the premature failure of veneers. A thermal compatibility study between dental porcelain and zirconia reported a strong dependence between veneer failure and tensile thermal stresses [42]. A continuous evolution of thermal stresses occurs in veneers during cooling, especially at high temperature, that results in transient stresses, i.e. temporary. Higher magnitude of transient stresses are known to cause immediate cracking of the veneers [43].

The difference between the coefficients of thermal contraction (CTC) of zirconia and porcelain is believed to be the significant parameter inducing residual thermal stresses in the veneer [13,14,35,42,44,45]. Many researchers in the field have extensively worked to establish an acceptable CTC difference for ensuring the reliability and thermal compatibility between these materials [43]. However, the issue of premature failure in veneers remains unresolved despite maintaining the acceptable CTC difference. A previous study suggested that the CTC difference is not the only factor to predict the clinical success of dental assemblies [46].

Dependence on the sole CTC difference explains the primary cause that limits progress in improving compatibility of such materials. This necessitates a need to consider additional factors in designing desired stress states in dental porcelains that are veneered on 3Y-TZP frameworks.

Dental porcelains are glass-like viscoelastic material. The principles of glass behavior are applicable to dental porcelains. Within the transition zone range, dental porcelain behaves as viscoelastic material where its properties are dependent on time and temperature in that region. Above transition temperature, any force applied to the structure results in immediate creep, and hence no residual stresses are accumulated in the material. When dental porcelains behave as elastic solids below the transition temperature, any stress applied results in proportional instantaneous elastic strain [9,35,47].

If the system is purely elastic, the thermal stresses are either compressive or tensile due to CTC mismatch only. When one of the materials is viscoelastic, the stresses vary based on the thermal gradient through the transition region [35,45]. It means altering the cooling

within the transition range can alter the stress state within the dental porcelains for the same CTC values and heat treatment temperatures.

There have been studies that tried to take advantage of the viscoelastic nature of dental porcelains to induce a desirable stress pattern during the glazing heat treatment [45]. It is well-known in glass literature that the stress patterns in glasses can be altered or tailored depending on the thermal gradients that develop during cooling processes at high temperature when glass is in viscoelastic state [35,45]. Moynihan et al. [48] showed that higher cooling rates increase the thermal gradients which affects the overall evolution of the thermal stress states in the glass material. Hence, it is known that the effect of thermal gradients on high temperature viscoelastic behaviors of glass materials play a significant role in controlling the overall stresses.

For more than five decades, the effect of thermal gradients on viscoelastic behavior of glasses have been used for improving the performance of tempered glasses. Viscoelasticity in glass like materials exhibits the two behaviors: stress relaxation and structural relaxation. Stress relaxation refers to mechanical response to applied strain. On the other hand, structural relaxation refers to the approach of glass structure towards its equilibrium state. Structural relaxation is the time-dependent response of volume change of glasses with respect to temperature. Structural relaxation is known to cause changes in the physical properties of glasses such as density which has been investigated for decades [49–55]. In a study by Rekhson et al. [55], it is suggested that structural relaxation shall always be considered the intrinsic part of the evolution of thermal stresses in glass materials.

The significance of structural relaxation to control thermal stresses in tempered glasses has been studied over the past decades for its desired performance. On the other hand, to the best of author's knowledge, the characterization of thermal stresses from the perspective of structural relaxation in dental porcelains is not evident. Having already been proven for tempered glasses, it is obvious that understanding structural relaxation in dental porcelains shows a strong potential solution for designing the desired stress states in veneers.

Despite the obvious significance of how further research into structural relaxation could revolutionize veneer quality, only one publication has highlighted need to evaluate

structural relaxation in dental porcelains [35]. Thus, evaluating thermal stresses in dental veneers, based on its principle characteristic (structural relaxation) still remains unexplored, and presents a knowledge gap.

Numerical analysis is required to evaluate the evolution of the structural state of dental veneers and their resulting stress states. Very few studies have been performed in dental materials involving viscoelasticity [11,42,45,56–59]. Recent viscoelastic studies on 3Y-TZP dental materials, Kim et al. [56] and Dhital et al. [11], discuss the stress results in veneers for different cooling rates and thicknesses. However, these evaluations do not delve into causation of such stresses based on veneer behavior in the glass transition zones.

Therefore the current study, subsequent to the work conducted by Kim et al. [56] and Dhital et al. [11], aims to evaluate the effect of thermal gradients on the structural relaxation in dental porcelains, and further characterize causation for the resulting thermal stresses. In this way, this study aims to address the significance of structural relaxation in dental porcelains and evaluate its effect on subsurface thermal stresses. Appropriate solutions can be obtained if the root cause for undesired thermal stresses in dental porcelain is known. Further this study will utilize this evaluation to form a suitable explanation for the development of undesired subsurface stresses, which are known as a primary cause of clinical failures.

1.1 Motivation

The solution to any problem can be devised once systematic root cause analysis is conducted. Despite of extensive research to mitigate clinical failure of bilayer 3Y-TZP materials, a literature identifying major parameters and their influence on material performance is not available. Without such information available in a single source and vast database, it becomes difficult to refer to adequate information. This inadequacy of information in a single literature limits the progress to conduct an effective root cause analysis and devise a mitigation plan. This situation has motivated to conduct a meta-narrative literature review by referring a high number of published manuscripts, to identify critical parameters and discuss their influence on material performance. This report will

facilitate future investigations by considering effect of all parameters that can influence material performance.

Another knowledge gap identified in Introduction of Chapter 1 is related to high temperature behavior of dental porcelains. Dental porcelain is a glass like material. Glasses are developed successfully since several decades by evaluating their thermal stress states with respect to their basic characteristics i.e. structural relaxation. Structural relaxation is known to cause changes in glass properties and hence it is widely used to tailor the desired stress states in tempered glasses. To the best of author's knowledge, in case of dental porcelains which are glass-like materials, structural relaxation has been never evaluated. Considering the success in field of tempered glasses, understanding structural relaxation in dental porcelains and further using it to tailor the desired stress state may revolutionize the product development and eventually the integrity of materials. As a result, this fact sets out the motivation to understand structural relaxation in dental porcelain and characterize the thermal stresses accordingly. It facilitates conceptual understanding of the root cause of thermal stresses and further assists in designing heat treatment protocols accordingly for tailoring desired stress states.

1.2 Objectives

The following are the objectives of this research:

- To conduct a comprehensive meta-narrative literature review to identify all significant parameters that affect the performance of bilayer zirconia dental systems.

- To conduct a numerical analysis by development of user material subroutines, UEXPAN and UTRS, their validation and integration in ABAQUS finite element solver to evaluate the effect of thermal gradient on structural relaxation in dental porcelains.

- To utilize this numerical analysis to understand how undesired subsurface stresses developed are responsible as primary cause of clinical failures of dental porcelains.

1.3 Thesis Structure

Following the introduction, motivation and objectives of Chapter 1, the thesis structure is defined as follows:

- Chapter 2: This chapter contains an evidence-based meta-narrative critical review of a high number of publications to identify parameters affecting the integrity of veneered zirconia dental structures.

- Chapter 3: This chapter forms the theoretical foundation for numerical study to evaluate effect of thermal gradient on structural relaxation in glass materials, their high temperature behavior and evolution of thermal stresses.

- Chapter 4: This chapter contains details of finite element modeling for evaluating structural relaxation. This section includes definition of material properties, geometry, boundary conditions, sensitivity analysis, development and validation of user material subroutines.

- Chapter 5: This chapter contains results and discussion from the finite element analysis, as conducted in Chapter 4.

- Chapter 6: This chapter contains a conclusion, recommendations and future scope of investigations.

Chapter 2

2 On the Behavior of Bilayer Zirconia-based Dental Materials – A critical review

This literature review focuses on identifying various parameters and understanding their effects on material behavior based on a high number of research manuscripts. Considering the amount of information that exists, a meticulous approach was utilized to conduct a qualitative review to relate all parameters. “Evidenced-based meta-narrative analysis” method was followed throughout this literature review. This is an emerging technique of qualitative literature review, and required knowledge was acquired from RAMESES (Realist And Meta-narrative Evidence Syntheses: Evolving Standards) publication standard. The methods and techniques were customized to suit this review exercise’s purpose, as suggested in [60–62].

A customized combination of two techniques, mainly semi-systematic [61] and supported by the integrative approach [62], was used. Such a customized approach facilitates the synthesis of knowledge about effect of various parameters on material performance [60].

The following steps were used for conducting this literature review.

2.1 Step I: Design

This review seeks to identify and understand relevant research on distinct variables/parameters that affect zirconia-based dental materials’ performance and evaluate effect of individual parameters using the meta-narrative technique. It constitutes the primary rationale and objective of this literature review exercise.

This comprehensive review focuses on the manuscipts published in ScienceDirect, PubMed and SAGE databases to identiy relevant manuscripts.

2.2 Step II: Conduct

The search process for identifying the relevant literature for veneered 3Y-TZP dental structures was conducted as per Figure 2-1. An iterative search strategy was used to identify

a large sample size from the database resources. The process of keyword search, resource search details, and shortlisting criteria are as described in Figure 2-1. The overall search strategy's effectiveness was verified using iterative search methodology where many of the manuscripts published over the last two decades were studies, and this includes 3170 manuscripts obtained from the three resources.

Two-step screening was used to filter documents to ensure that documents meet the set objectives. It resulted in 657 manuscripts after the first screening and was further shortlisted to the final 261 manuscripts, which were primarily categorized into four groups depending on the naturer of research conducted.

- Literature review (27 manuscripts, ~11% of final shortlisted manuscripts)
- Experimentation (200 manuscripts, ~75% of final shortlisted manuscripts)
- Finite element analysis (07 manuscripts, ~3% of final shortlisted manuscripts)
- Experimentation and finite element analysis (27 manuscripts, ~11% of final shortlisted manuscripts).

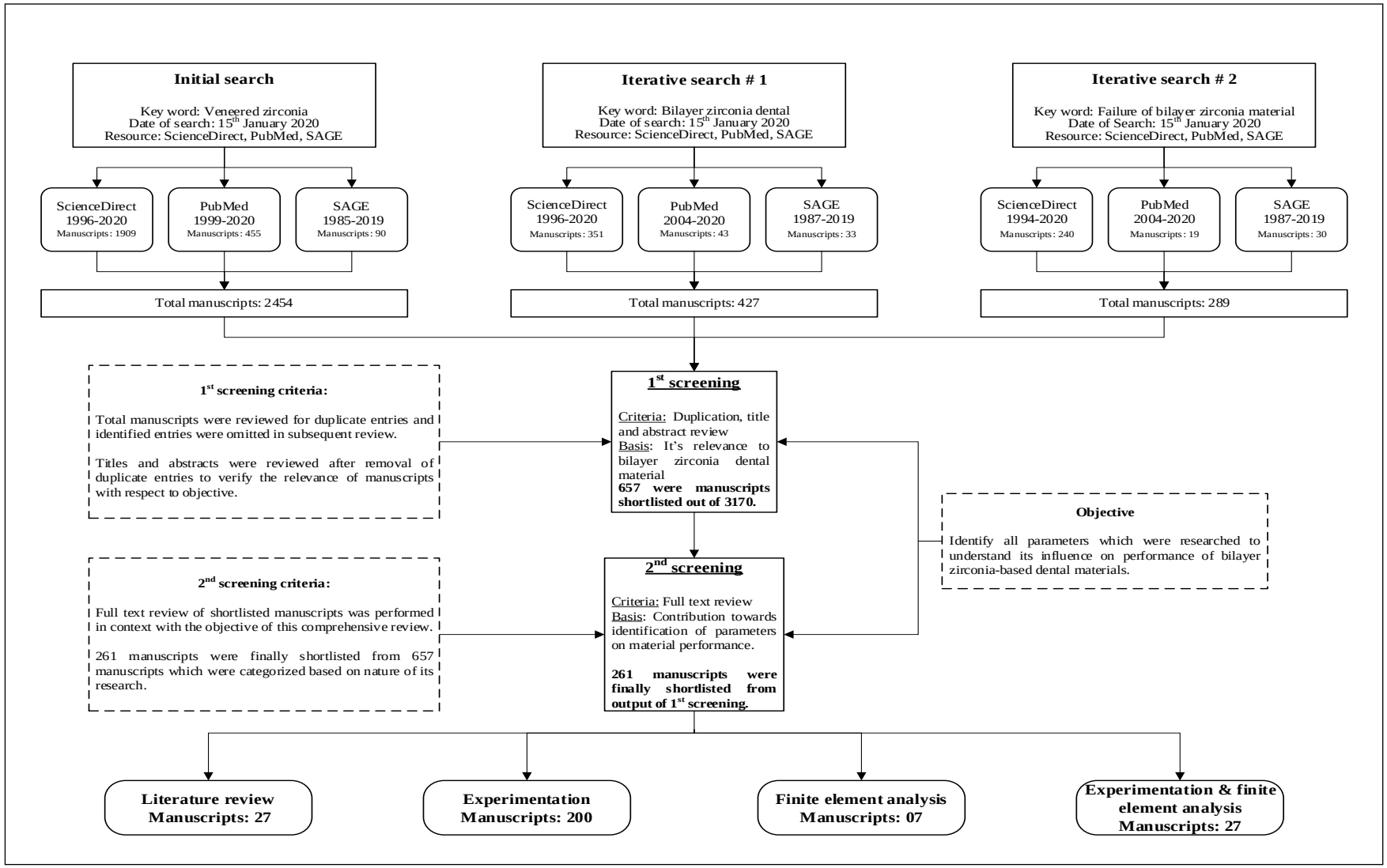

Figure 2-1: Process flow for identification of relevant research manuscripts

2.3 Step III: Analysis

This phase focused on a macro-analysis of shortlisted manuscripts to identify the relevant parameters as per their broad categories. Parameters were categorized according to:

a. Material and thermocycling: any parameter which was directly relevant to the material properties and thermocycling effect.
b. Manufacturing procedures: any parameter which was directly or indirectly relevant to one of the manufacturing process parameters.
c. Geometry: parameters relevant to dimension, shape, configuration, and tolerances.
d. Novel methods/developments: this category was only introduced to identify a few novel methods/improvements related to material, surface treatment, and veneering techniques to enhance material performance.

Using (a)-(d), all identified parameters are grouped into four major categories, as shown in Figure 2-2.

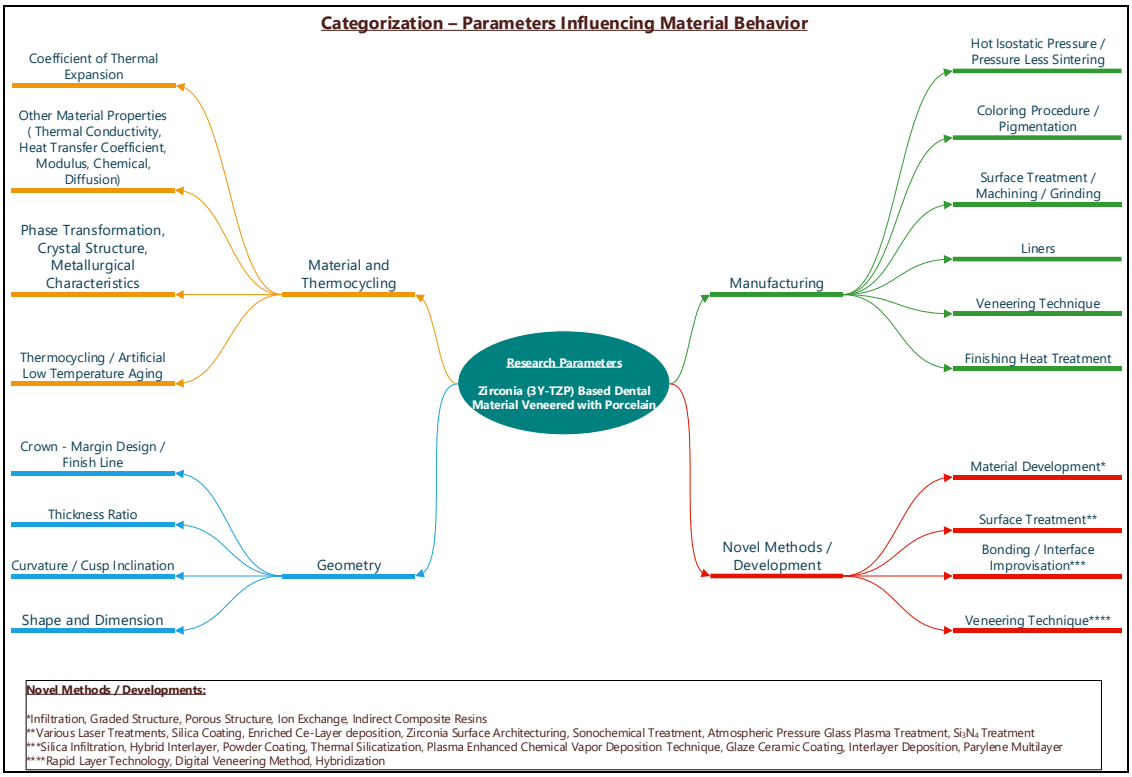

Figure 2-2: Categorization of parameters influencing material behavior

Bilayer zirconia-based dental materials mainly consist of two components: i.e., framework (3Y-TZP) and veneering material (dental porcelain over framework) for suitable esthetic appearance. These two materials are joined through sequential mechanical and thermal operations, which eventually affects overall material behavior based on its material properties, manufacturing procedures, geometry, and thermocycling steps. Accordingly, parameters are directly or indirectly interconnected and affect the material behavior and contribute to the material's failure.

This information was translated into a customized "Cause and Effect Diagram," where zirconia-based dental materials' premature failure was linked to several potential factors. Figure 2-3 shows the customized "Cause and Effect Diagram" linking various parameters that may influence the material performance.

Relevant shortlisted research manuscripts for the respective parameter are summarized in Table 2-1. The information presented in in Figure 2-2, Figure 2-3, and Table 2-1 presents the inputs for the literature systematic meta-narrative analysis. Appendix A exhibits relevant references listing a few novel developments which are explored to improve the material performance. Novel practices were not discussed in this study.

In this analysis, each parameter was reviewed based on the relevant shortlisted research manuscript. Primary mechanism of this review focused on the effects caused by each respective parameter, using a meta-narrative analysis.

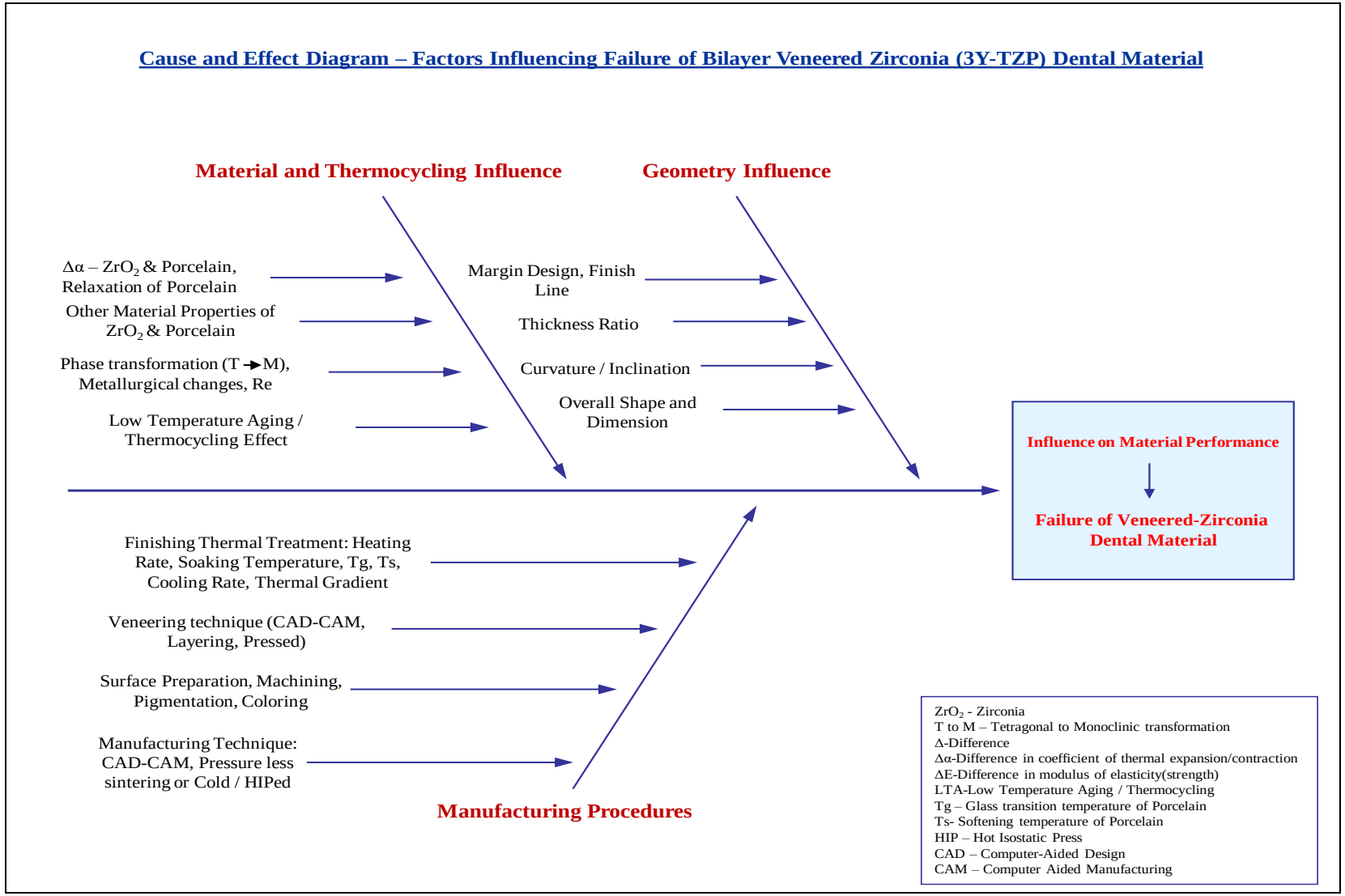

Figure 2-3: Cause and Effect Diagram (Parameters influencing material performance)

Table 2-1: Parameters and References

Sr. No.	Categorization	Parameters	Total Nos. of Ref. Cited	References	Effect On
1	**Material and Thermocycling (Artificial Low Temperature Aging)**	Coefficient of Thermal Expansion	029	[8,9,11,12,15,17,27,31,35,38–40,42–45,56,58,59,63–80]	Thermal Residual Stress, Interface Bonding, Fracture Toughness and Fatigue
		Material Elastic Constants	011	[8,9,18,56,81–87]	Anisotropy of Zirconia Poly-crystal, Interface Modulus, Shear Bond Strength, Nature of Location of Maximum Tensile Stress
		Microstructure / Phase Transformation	024	[27,82,86,88–108]	Microstructure of core, veneer and brief about interface
		Thermocycling	038	[18,21,26,29,64,82,109–140]	Phase Transformation (Core Material), Shear Bond Strength, Fracture Resistance, Hydrolysis, Standardization of performing artificial aging tests
2	**Manufacturing**	Framework Material Manufacturing (Hot Isostatic Pressing, Pressure-less Sintering)	009	[2,88,103,104,107,108,141–143]	Quality of Core Material
		Coloring Procedure / Pigmentation of Core Material	010	[67,70,127,144–150]	Bond Strength, Phase Transformation
		Surface Treatment (Airborne Particle Abrasion, Machining, Grinding, Liners,)	077	[6,15,24,29,30,85,113,118,119,121,125,126,136,138,145,146,151–211]	Surface Roughness, Phase Transformation, Wettability, Flexural Strength, Interfacial Bond Strength, Interfacial Toughness, Residual Stress, Flaw population
		Veneering Technique (Layered, Pressed, CAD/CAM)	040	[9,13,15,41,115,120,121,123,124,129–131,134,139,161,177,212–235]	Phase Transformation, Flaw Population, Interfacial Bond Strength, Fracture Resistance / Toughness, Flexural Strength, Aging, Fatigue Performance
		Finishing Heat Treatment	053	[9,11,17,22–41,56,65,66,68,74–76,126,127,129,130,172,177,223,225,236–250]	Residual Stress State, Phase Transformation in Veneer, Fracture Strength / Toughness, Shear Bond Strength, Fatigue Strength, Standardization, Non-Destructive Testing
3	**Geometry**	Thickness Ratio and Other Geometrical Factors (Shape, Core Design, Finish Line,)	044	[9–11,19,21,22,25,32,34,35,37,38,74,76,83,87,129,131,133,135,161,171,184,216,218,221,228,238–240,242,244,248,251–261]	Residual Stress, Fracture Load, Fracture Resistance, Interface Toughness, Fatigue Behavior, Interface bond strength, Failure, Standardization

2.4 Step IV: Result and Discussion

261 out of 3170 manuscripts were reviewed between 1985 and 2020. A total of 10 parameters were identified and classified into the material, manufacturing, and geometrical aspects.

The effect of every parameter was reviewed on the performance of the bilayer zirconia-based dental material.

2.4.1 Coefficient of Thermal Expansion (CTE)

A framework consisting of metastable zirconia and veneering dental porcelain have different CTE values depending on their material characteristics. The difference between the CTE's of the two materials ($\Delta\alpha = \alpha_{Zr} - \alpha_{Ve}$) degrades the lifetime of bilayer material by affecting their overall quality due to the generation of undesirable tensile stresses from thermal treatment [15,17,31,38,39,44,63,64,66–68,72,73,75,76]. This difference in thermal expansion has deteriorating effects on the fatigue performance and fracture toughness of the material [12,38,63,73,74]. For this reason, the CTE is one of the critical parameters that affect the behavior and performance of bilayer dental materials.

Many studies focus mainly on obtaining a conclusive guideline to derive an acceptable difference in CTE values. However, the ideal solution and clear consensus are not yet established [8,76]. Studies have focused on developing a veneer material, i.e., porcelain, which can have a suitable $\Delta\alpha$ with respect to framework material, i.e., zirconia.

It is reported by Swain et al. [9] that the origin of stresses in porcelain is $\Delta\alpha$ along with the cooling process followed during manufacturing of the bilayer dental material. These stresses are mainly tensile at the porcelain surface; however, they can be compressive and high at the interface. Considering a constant CTE for the framework and variable CTE for dental porcelain, there are three possibilities which are continuously explored in the studies conducted on this bilayer dental material, when $\Delta\alpha>0$, $\Delta\alpha=0$-or $\Delta\alpha<0$. These studies focused on the effects of $\Delta\alpha$ on the state of the residual thermal stresses, interfacial bonding

strength, fracture toughness, and fatigue performance, as schematically shown in Figure 2-4 [8,9,12,17,31,38–40,44,56,63–77].

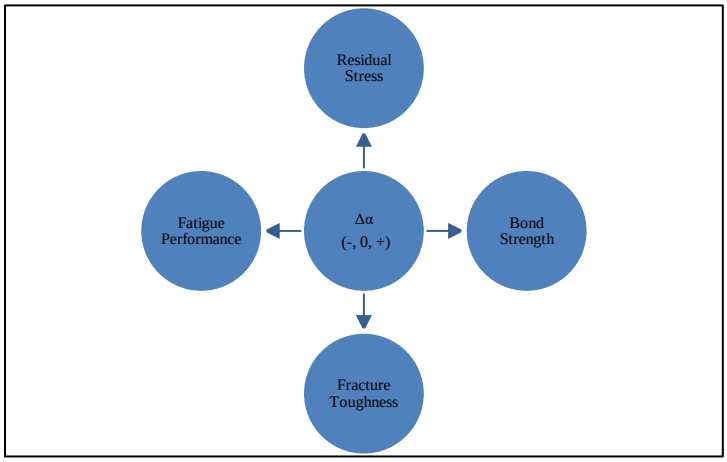

Figure 2-4: Influence of difference in CTE

Positive Δα:

Traditionally the concept of using a veneer material with slightly lower CTE comparing to the framework material, i.e., $\Delta\alpha>0$, is widely accepted for the manufacturing of bilayer dental materials. This concept of $\Delta\alpha>0$ is based on the understanding derived from metal-ceramic systems, which generates compressive residual stresses in the veneering porcelain, and it further facilitates higher resistance to crack propagation or chipping failures [8,78,79]. However, all-ceramic systems do not demonstrate the same behavior during cooling compared to metal-ceramic systems.

There is no consensus derived on having a desired performance for the bilayer dental material when $\Delta\alpha>0$. Some studies have indicated that increasing $\Delta\alpha$ towards more positive values would result in a significant increase in the residual thermal stresses [38,39,63,74,76], along with a shift of stress states from compressive to tensile, as well as when $\Delta\alpha$ increases are as much as $+1x10^{-6}$ 1/°C [9].

.

Interface bond integrity, fracture toughness, and fatigue performance are influenced by the state of the residual stresses, which are a function of Δα [8,12,31,38,40,67,69,72,73,75]. On the other hand, few studies [17,44] suggested that the CTE mismatch does not influence interface bond integrity. Besides, disagreements are seen in the literature for the optimum positive value of Δα. . The CTE of 3Y-TZP is 10.5 x 10^{-6} 1/°C. In these studies, the dental veneer porcelain Vita VM9 (CTE = 9.3 x 10^{-6} 1/°C) is preferred option over Lava Ceram (CTE = 10.2 x 10^{-6} 1/°C) and in some studies it is recommended vice-a-versa [31,38,56,66]. Larger CTE mismatch, including positive Δα, would result in a 4-5 folds increase in the state of residual stresses causing preferential sites for crack nucleation and propagation.

It was reported by Zhang et al. [63] that when Δα reaches +5 x 10^{-6} 1/°C, lateral tensile stresses above 150 MPa were observed in the framework, causing cracking of the framework during indentation. Additionally, it was reported by Juntavee et al. [11] that Δα of +2.93 and +2.94 x 10^{-6} 1/°C resulted in the formation of tangential cracks perpendicular to veneering ceramic, leading to bond strength reduction. Higher Δα would result in undesirable residual stresses that lead to the fracture of veneers [38,65].

Zero Δα:

A veneer material with the same CTE as the framework is not yet commercially available. Although, the production of novel porcelain material has been explored. Finite element analysis [76] has revealed that a desirable stress field was developed when Δα is zero. Experimental results by Aboushelib et al. [69] suggested that bilayer dental systems with zero Δα exhibited higher failure load (i.e. 64 N) compared to those with positive Δα (42 N, 50 N). The latter failed due to delamination with a crack nucleation at the interface while the former cracked below the veneer surface. Numerical analysis has provided a fair way forward to explore possibilities of using framework and veneer with matching CTE.

Negative Δα:

This situation is never desired as it generates tensile residual stress fields in the veneer, which facilitates immediate chipping or brittle failure by forming microcracks when subjected to any shock, impact, or load [31,44,64,65,69,70,75,76].

The above studies indicate significance of CTE values in overall performance of the material. Positive Δα has proven to result in compressive stresses within dental porcelain. If it is optimum, it possibly tends to cause tetragonal to monoclinic phase transformation at the framework interface increasing resistance to crack formation and propagation [64–66,77]. It eventually enhances the integrity of the bond interface, fracture toughness and fatigue behavior of the bilayer dental system.

Another significant consideration:

Another significant aspect altering the stress state in dental porcelain is its high-temperature properties. Being a glass-like material, dental porcelains exhibit viscoelastic behavior at higher temperatures. CTE values significantly becomes 4-5 times higher compared to its room temperature values. This situation is not desired as it induces stress fields, facilitating the propagation of flaws [68]. Viscoelastic behavior is a strong function of the thermal gradient within dental porcelains, and thus cooling rate plays a significant role in controlling the stress states [35,45]. CTE magnitude, especially in transition zone, is strongly dependent on the viscoelastic relaxation, which depends on the kinetics of the cooling process.

It is worth noting that very few studies focused on the viscoelastic behavior of dental porcelains [11,42,56,58,59,80]. Previous work by Taskonak et.al. [45] suggested that the desired stress state within dental porcelain can be tailored through appropriate use of viscoelastic behavior and thermal gradient. Despite such importance of viscoelastic behavior of dental porcelains, this field remains not much explored in veneered 3Y-TZP dental restorations.

2.4.2 Material Elastic Constants

Elastic constants are used to describe the constitutive behavior of materials and they depend on the crystal structure of crystalline materials. Isotropic elastic materials are represented by 2 elastic constants namely, modulus of elasticity (E) and Poisson's ratio (μ) whereas anisotropic materials, such as zirconia, have more than two elastic constants [86].

The stress in bilayer dental materials is a function of each layer elastic properties; hence, the precise determination of elastic constants is of significant importance for accurate analytical solutions [87]. All studies of all-ceramic dental materials consider that framework is an isotropic elastic material and use E and μ for analysis. However, tetragonal zirconia is an anisotropic material that requires six elastic constants to describe its behavior [86].

There is a lack of studies evaluating the effects of anisotropy of zirconia on the behavior of the bilayer zirconia-based dental material. In contrast, several studies [8,9,56,82–85] considered zirconia exhibiting isotropic behavior which provided certain understanding of stress fields in the material. In these studies, the elastic constant of zirconia is generally assumed to be 200 GPa which is three times higher than that of veneer porcelain (~70 GPa).

Finite element studies by Kim et al. [56] have shown that the difference in the magnitudes of elastic modulus (ΔE) of the two layers results in the variation of the location of maximum tensile stress, i.e. maxima being at the porcelain interface with lower stiffness and at central fossa surface of the porcelain with higher stiffness. Therefore, porcelains with lower modulus of elasticity are believed to provide more desirable stress patterns. Previous study by Swain et al. [9] showed that the magnitude of residual stress in veneer porcelain does not dependent on the stiffness of the veneer. Thus, there is no consensus established on the desired level of the difference of modulus of elasticity between the framework and dental porcelains.

It has been suggested that ΔE can significantly affect the crack propagation within the bilayer dental material [83,84]. It is generally observed that usually a crack nucleates at the subsurface of veneer, and as soon as it reaches near interface it deviates causing the veneer delamination. This either indicates that 3Y-TZP has superior crack resistance, or the quality of the bond is inadequate. Considering that ΔE is generally high, it was suggested a thick zirconia layer under a thin layer of veneer [83].

2.4.3 Microstructure and Phase Transformation

The microstructure of bilayer zirconia-based dental materials can affect its performance

and hence it is investigated in three (3) categories as follows.

Microstructure and phase transformation in the 3Y-TZP framework:

At ambient pressure, zirconia polycrystal in its pure form, i.e. free from stabilizing compounds, consists of three types of crystal structure: cubic (c), tetragonal (t), and monoclinic (m). The presence of each crystal depends on the temperature. The monoclinic phase ($P2_1/c$) has the lowest symmetry and is stable from room temperature to 1127°C. The tetragonal phase ($P4_2/nmc$) is present from 1127°C to 2293°C, and the high temperature cubic phase (Fm3m) is present from 2293°C to the melting point of zirconia, 2707°C [86,103]. Unalloyed zirconia exhibits large volume expansion (4 to 5%) when transforms from/to tetragonal to/from monoclinic phase, and hence cannot be used in structural applications [103,104]. On the other hand, the tetragonal phase becomes metastable at room temperature when alloyed with 3% Yttrium Oxide.

Under stress, a martensitic transformation occurs from tetragonal to monoclinic phase (T to M). This phase transformation occurs at the surface and is a function of residual and applied stresses. This phase transformation induces compressive stress field at the material surface, arresting the propagation of any existing cracks while increasing the toughness and flexural strength of the bilayer material. This phenomenon is known as "Transformation Toughening" which has enabled the use of 3Y-TZP material as one of choices for framework material in dental applications [103–105].

The sintering process and zirconia's grain size affects transformation toughening since it is a martensitic transformation that depends on the critical grain size. It is observed that above a critical grain size, the tetragonal phase is less stable, resulting in spontaneous phase transformation. Moderate transformation rate is observed for grain sizes less than 1μm while no transformation toughening is observed for grain sizes below 0.2 μm [88,103,107,108]. Figure 2-5 shows the relationship between the grain size of zirconia and sintering temperature [89].

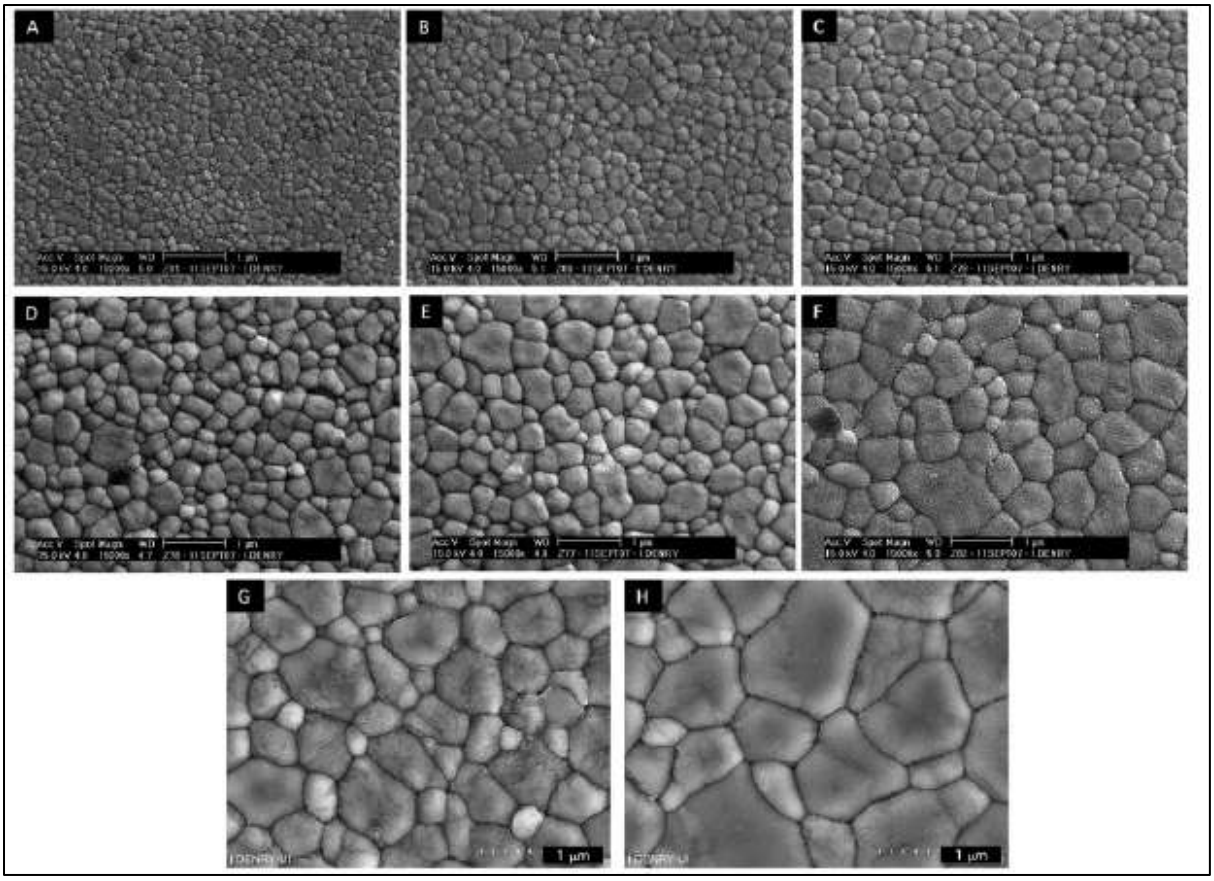

Figure 2-5: 3Y-TZP grain size as a function of sintering temperature. Sintering was done for 2 hours (image reprinted from [89]).

Image Label: (A) 1,300°C; (B) 1,350°C; (C) 1,400°C; (D) 1,450°C; (E) 1,500°C; (F) 1,550°C; (G) 1,600°C; and (H) 1,650°C]

The presence of the cubic phase restored at the room temperature could also be deleterious to the performance of metastable zirconia. In the presence of the cubic phase, the tetragonal phase becomes unstable and transforms to the monoclinic phase. As a consequence, cubic-phase is not desirable in the metastable zirconia [90,103].

Microstructure and phase transformation in veneering dental porcelain:

Layers of veneer are applied on framework for suitable aesthetic appearance. Generally, leucite and non-leucite based feldspathic porcelains are used as veneering dental porcelain for the 3Y-TZP framework. These porcelains, depending on their chemical composition,

mainly comprise of both glassy and crystalline phases. Depending on the ratio of glassy and crystalline phases, bilayer all-ceramics can be classified into the four categories [91] as follows:

- Category 1: fully glass-based system (mainly alumino silicates with low CTE values)
- Category 2: glass based + crystalline system (feldspathic porcelain, high leucite glass ceramic, lithium disilicate)
- Category 3: crystalline + glass filler system (e.g., alumina)
- Category 4: polycrystalline (framework material, e.g., 3Y-TZP)

Leucite-based feldspathic dental porcelains contain crystalline phase i.e. leucite, which is known to undergo phase transformation upon heat treatment.

Leucite, i.e., Potassium alumino-silicate, forms the crystalline part of feldspathic porcelain. The CTE, flexural strength, and fracture resistance of the porcelain are significantly affected by presence of leucite. Leucite undergoes transformation from cubic to tetragonal upon cooling which results in volume contraction of 1.2%, the formation of microcracks, and tangential compressive stresses around crystals. This volume contraction results in two contradicting scenarios, i.e., microcracks which are not desired and compressive stresses around crystals which are always desirable. As a result, the extent to which such volume contraction occurs, i.e., whether in excess or minor extent can affect overall performance of veneer [27,92,93,102].

Interface:

Based on the shortlisted manuscripts, it is observed that there is a lack of data for evaluating phase transformation at the interface of the veneered 3Y-TZP dental restorations. The interface between 3Y-TZP framework and veneer porcelain is considered as the zone of mismatch. Microscale inter-diffusion between both materials was observed using Raman analysis [94]. It is also shown that the expansion of interface into framework material results in lower elastic modulus at the interface [82] which eventually affect the bond

strength.

2.4.4 Thermocycling / Low Temperature Degradation (LTD)

Thermocycling is performed to expose the dental materials to change in temperature, usually 5°C-55°C, in an environment that resembles the oral environment to understand the performance of the material in "real condition". Low temperature degradation (LTD) is performed in an autoclave at certain temperature, pressure and time to evaluate changes in properties of dental materials. It is evident that this artificial oral environment or aging in an autoclave can induce specific changes in the material behavior and may contribute in deteriorating the bilayer dental material.

Thermocycling and LTD can affect framework, interface, and veneer as discussed below.

Framework:

Certain studies [82,109,110,112,113,137–140] have thermocycling or LTD as part of their analysis to evaluate its effects on the framework, especially near the interface. These studies have focused on investigating the effects of thermocycling on tetragonal to monoclinic phase transformation, grain size alterations, and the development of stress fields. With increasing thermocycling cycles, the concentration of Yttria or tetragonal phase stabilizer decreases, grain size as well as the monoclinic phase increases which eventually results in extensive formation of microcracks [82,109,110,112,113,137–140]. There are some studies, though, that report no significant change in strength of framework due to monoclinic transformation [111]. It was reported by Peng et al. [82] that 5% monoclinic phase transformation due to LTD is the optimum and favorable fraction for biomedical applications.

Zirconia-Veneer Interface:

Results of the investigations conducted on the interface have generally demonstrated the insignificant effects of thermocycling/LTD on the fracture resistance, especially at the interface [18,115–121]. Nevertheless, in presence of residual stresses and internal material flaws, thermocycling may act as a catalyst to poor material performance [26,122,125].

Veneer:

Except for silicate or glass-based ceramics, adequate information on the effect of thermocycling on veneer porcelain is not available. Previous evaluations by Peng et al. [82] have reported that mechanical properties of veneer porcelain are not affected by LTD.

It is now known that aging can influence overall material behavior. However, some other parameters such as manufacturing techniques, the CTE values, heat treatment, and geometrical aspects shall also be taken into consideration to predict the effects of thermocycling on the material behavior [18]. Hence, considering that non-standardized procedures are generally followed, the results obtained in the mentioned studies are hardly comparable [21]. As such, it is not possible to extract predictive models to simulate the sole effects of thermocycling or LTD on materials behavior.

2.4.5 Manufacturing of Framework

Parameters such as impurities content, grain size and phase stabilizers play a significant role in governing the performance of framework with respect to strength, corrosion resistance and its behavior during aging. Studies are conducted to improve the quality of framework for better in-service performance [2,143]. Hot Isostatic Pressing (HIP) and CAD/CAM technologies are useful sources to produce dense zirconia framework by eliminating pores and achieving desired density. Table 2-2 provides the properties of zirconia achieved after pressure-less sintering and HIP technique.

Table 2-2: Comparison of mechanical properties of Y-TZP for pressure-less sintering and HIPed samples [2,110]

Property	Pressure-less sintered Y-TZP	HIPed Y-TZP
Density (g/cm^3)	6	6.1
Average grain size (µm)	Less than 1	Less than 0.5
Microhardness (Vickers)	1000-1200	1000-1300
Young's Modulus (GPa)	200	200
Bending Strength (MPa)	800	1200
Toughness KIC ($MPam^{0.5}$)	9-10	9-10

As shown in Table 2-2, both average grain size and bending strength of the materials produced by the two techniques are different. Critical grain size is an important factor affecting the transformation toughening mechanism. Materials with a grain size less than 1μm have shown lower transformation rates, while those with the size below 0.2 μm have shown no transformation toughening mechanism [88,103,107,108]. Both methods produce grain sizes which are optimum for transformation toughening with lower transformation rate for tetragonal to monoclinic phases. The bending strength of HIPed material is higher as shown in Table 2-2 [141].

There have been some attempts to reduce the defects which are introduced during the HIPing process. It is shown that post-sinter HIP is ineffective in closing large subsurface volumetric defects in the range of 10-60 μm. Hence this process would not help increase the density of the product [142].

2.4.6 Coloring Procedure and Pigmentation

The framework is veneered with glassy dental porcelain for suitable aesthetic appearance, especially for its anterior application. Depending on the translucency of 3Y-TZP framework, the thickness of porcelain may vary. Generally, as the contrast ratio in framework decreases, the thickness of the required porcelain reduces [144].

Two techniques are mainly used to adjust the contrast ratio of zirconia framework material. The first technique consists in adding color pigments to zirconia powder before or after pressing blocks and the second is to dip zirconia blocks in dissolved coloring agents [70,144,147]. Liners are also used to maintain optical properties.

Studies were conducted to understand the effects of the coloring procedure on the interface (framework-veneer) bond strength and fracture resistance of the framework. Some studies have shown that coloring has no or insignificant effects on the bond strength [67,145,148]. However, others have shown that coloring or pigmentation of framework affects the overall interface bond quality between framework and veneering dental porcelain [127,144,149,150].

It is shown by Aboushelib et al. [144] that coloring alters the characteristics of both surface and bulk structure. This research reported that adding color pigments provides homogeneous and uniform distribution of pigments in matrix, resulting in better interface bond quality. On the other hand, dipping of the framework block in liquid results in higher concentration of pigments on outer surface compared to the framework interior. This further crystallizes on surface during sintering resulting in the reduction of interface bond strength [127,144,146].

Also, it is estimated that low melting point coloring agents have can be located at the grain boundaries of the framework and facilitates depletion of stabilizer [144]. This may facilitate spontaneous transformation from tetragonal to monoclinic phase resulting in excessive volumetric expansion followed by formation of microcracks. This may also reduce the bond strength, irrespective of the coloring technique used.

Therefore, coloring technique and ingredients are essential parameters exhibiting potentials to hamper the properties of the framework.

2.4.7 Surface Treatment

Surface treatment is generally a combination of manual, mechanical, chemical, or thermal process performed on the framework. It is accomplished to achieve a suitable surface to facilitate an effective bond with the dental porcelain without deteriorating the quality of the framework. Surface treatment is one of the main parameters affecting the quality of bonding, which further determines the reliability and lifespan of the bilayer dental material.

Surface treatment is known to affect quality of bonding between framework and veneer. The stage at which surface treatment should be carried out has been the broad subject of research and clear guidelines are not yet established. Previous studies recommended surface treatment such as sandblasting or polishing followed by grinding and re-polishing after sintering. Reduction in mean strength or flexural strength was observed if sintering was conducted after surface treatment [118,177,185]. In contrast, other studies showed improvement in strength when surface treatments such as airborne particle abrasion were performed on partially sintered material or before sintering heat treatment. Also,

subsequent sintering heat treatment has shown transformation of monoclinic to tetragonal phases [173,178,180,188,193,194].

The effects of surface treatment can be broadly classified into the categories shown in Figure 2-6. These effects were mainly evaluated with respect to the type of surface treatment methods used in the experiments or clinical practices. The main methods used for surface treatment are classified in Figure 2-7.

Methods used for surface treatments of dental materials and the testing methods used to ensure bond integrity are not well-established and are non-standardized. As such, it is hardly possible to compare the results obtained from different studies [126,136,145,164–166,173,186].

In addition, there is no specific guideline in selecting most suitable surface treatment. It is known that manufacturer suggest various methods of surface treatment for e.g. airborne particle abrasion with fine particle size while others may suggest with coarse particles prior or after sintering. Essential variables are known to induce damage on the material surface such as time, distance from nozzle, pressure and material flow are not adequately addressed in laboratory or manufacturer guidelines [173]. This has resulted in non-standardized surface treatments on framework materials. Hence results obtained in one study do not generally hold in another. Nevertheless, the methods used and their impacts are briefly described.

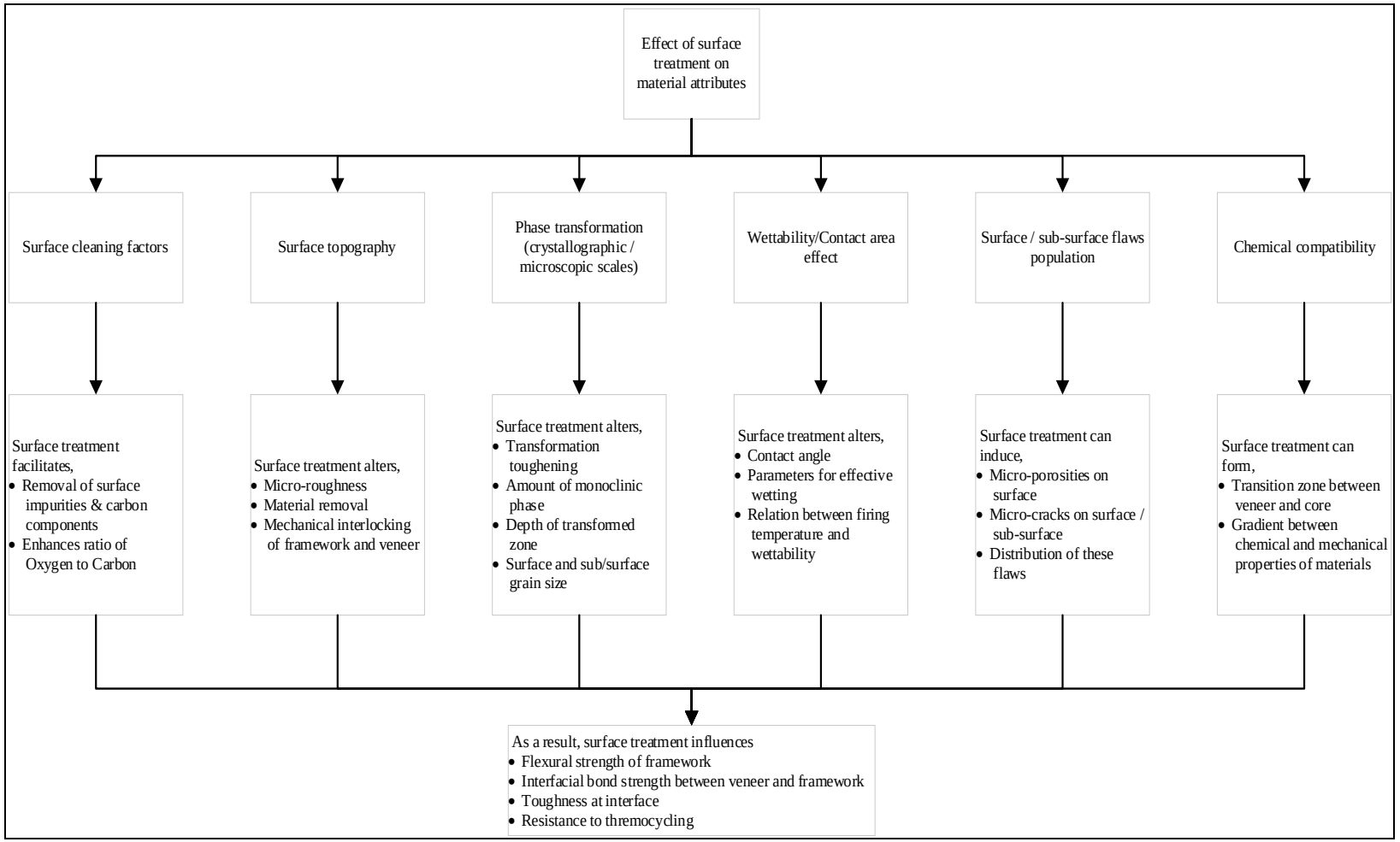

Figure 2-6: Broad classification for effect of surface treatment

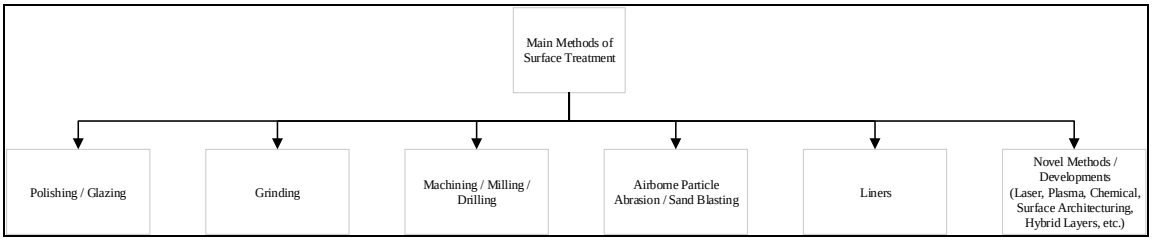

Figure 2-7: Methods of surface treatment

Polishing, grinding, milling, and drilling:

Polishing is mainly known to remove CAD/CAM milling lines [166,179]. This removal process may yield the removal of the compressive stress layer from the framework, lowering flexural strength [177]. On the contrary, polishing may facilitate the damage of the restoration surface which improves the flexural strength of the framework material [179] and also results in optimum surface roughness generating better wettability with the veneer compared to other surface treatment method such as sandblasting [24]. It was observed that the difference between the bond strength by polishing and other techniques, e.g., sandblasting, laser polishing, was insignificant [164,166,170]. Also it was suggested that polishing or glazing cannot restore the original fracture resistance of the adjusted veneered zirconia crowns [125]. In contrast, any milled framework surface without any subsequent surface treatment showed inferior wettability with dental porcelain [30].

Coarse bur drilling (e.g. 150 μm) results in reduced amount of monoclinic phase transformation due to the higher temperatures generated in the process. This fact facilitates reverse transformation toughening resulting in higher damage depth (~9 μm) [172]. Whenever performed on pre-sintered core material, milling results in rough surface with cracks which demands polishing of the milled surface to achieve optimum defect free surface [193].

Grinding may produce unevenly distributed large defects (e.g. microcracks) on material surface, inducing higher stresses and monoclinic phase transformation which will negatively affect flexural and bond strength [145,169,178,189]. The reduction in biaxial flexural strength due to grinding can be restored by airborne particle abrasion [195].

Although, previous investigations [179,190,194–198] suggested that grinding with proper parameters (e.g. using diamond burs instead of tungsten carbide, using slow speed grinding, with coolant) may increase or has no negative effects on the flexural strength of the framework. The use of proper coolant reduces defects and enhances transformation toughening reducing the risk of degrading the mechanical properties of the framework material [194,196]. Heat treatment after grinding was reported in some evaluations [180,193] as it leads to reverse phase transformation from monoclinic to tetragonal and restores toughness.

Airborne Particle Abrasion (APA) / Sand Blasting:

This surface treatment technique has certain controlling parameters that generally affect the surface morphology, micro-roughness, mechanical interlocking, and eventually affecting flexural strength, wettability, and interfacial bond strength. These parameters are shown in Figure 2-8.

Generally, the abrasive methods and instructions are provided by zirconia framework manufacturers specifically to each brand, and if used on others, they may negatively affect flexural strength and material reliability [164]. It is understood that following the manufacturer's recommendations results in better surface compatibility and hence enhancing bond strength [164]. Nevertheless, general guidelines for selecting suitable surface treatment methods are not yet established and are not addressed adequately by manufacturers [171,173].

Superior surface quality can be achieved by sandblasting which removes machining lines, resulting in improved surface roughness with increased effective surface area that enhances wettability and bond strength [166,168]. Particle size is considered as one of the critical factors where using low particle size results in better quality [85,121,173,185,191]. Using bigger particle sizes increase surface roughness and the depth of damage within the monoclinic phase. For example, the use of 50 µm and 125 µm particle sizes respectively resulted in 11% and 14 % monoclinic phase with surface roughness of 0.759 Ra and 1.028 Ra. The use of 35 µm and 105 µm particle size respectively resulted in 4 µm and 11 µm damage depth [85,121,170,172,174,185,192].

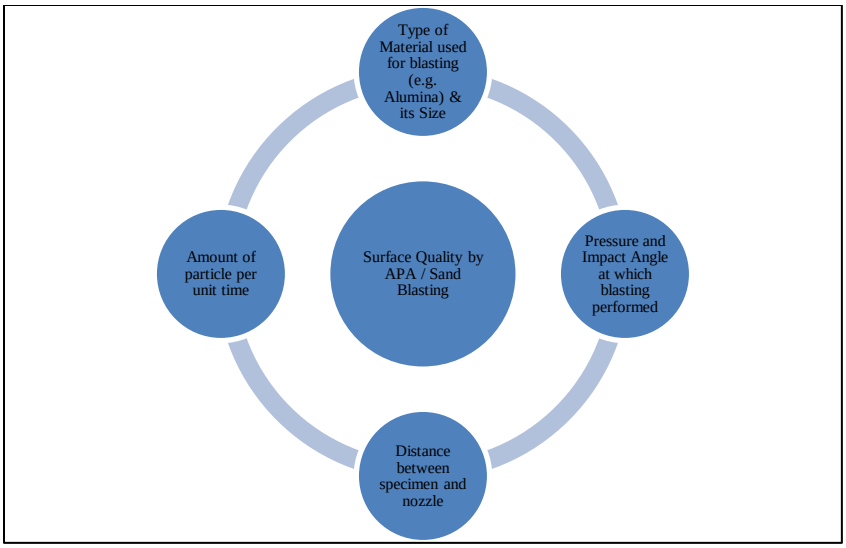

Figure 2-8: Process parameters of Airborne Particle Abrasion (APA) / Sandblasting technique

Surface treatment using 120 µm particles resulted in 7% monoclinic phase which is believed to cause significant reduction in flexural strength of zirconia framework compared to sandblasting using 50 µm particles [173]. Whenever framework is subjected to high temperature sintering after surface treatment, it resulted in reverse transformation toughening that caused volumetric changes. This protocol further decreases strength of the framework. Hence subsequent sintering shall be avoided after surface treatment [173,185,186]. Sandblasting may induce critical surface flaws or voids with certain damage depth; these flaws may act as the preferred sites for crack formation and propagation reducing interfacial toughness [171].

The pressure used during the sandblasting technique serves as another critical factor for controlling surface roughness. At higher pressures, surface roughness increases facilitating superior interfacial bonding [175], but result in widespread surface flaws, high depth of damage, plastically deformed grains, and the presence of martensitic plates [113,182,185,187,188].

At lower pressures, the kinetic energy of particles will be lower and the plastic deformation zone will be limited to around the impact zone. Depending on the pressure and particle size, the resulting compressive stresses will vary, which will accordingly affect the strength

of the material [85].

On the contrary, it was reported in some studies that sandblasting parameters do not affect flexural strength or bond quality [119,136]. It was also reported that sandblasting always improves the flexural strength of the framework, regardless of the parameters used [181].

Sandblasting with suitable parameters produces an optimum transformation toughening without excessive monoclinic phase which subsequently increases fracture strength framework, wettability, and effective bond strength. As a consequence, the material is more reliable without any negative effects of surface treatment [30,138,167,169,182,183].

It is evident from the above information that there are no generic guideline in adopting sandblasting parameters for surface treatment. If an absolute pressure is considered to achieve desired results in one study, it may produce poor results in another study [175,191].

Liners:

The basic physical application of liners in bilayer dental materials is to mask the white color of zirconia. It also acts as an agent to provide chemical compatibility and to create a smooth transition zone between veneer and framework material which will enhance the bond strength [209]. Intermediate layers are said to enhance mutual diffusion and provide resistance to thermal residual stress fields created due to difference in the coefficients of thermal expansion [136]. Liners are recommended to be used with layering veneer [176,209], as delamination was reported when they are used with pressed veneer.

The selection of liner material is important for material reliability. Liner materials, e.g. lithium disilicate, possessing both chemical composition and coefficient of thermal expansion in between veneer and framework will lead to a more stable behavior. Such linear materials will also provide optimum shear bond strength [165]. At appropriately high firing temperatures, it results in homogeneous glassy matrix enhancing wettability with framework and increasing shear bond strength [29].

The application of a liner is critically important. Poor application results in low quality liner material, e.g. by brush-like pasting technique producing air bubbles, inefficient

wettability with framework material resulting in decrease in bond strength, interfacial toughness and reliability [171,174,184,209]. The use of glass ball to apply mixed liner results in uniform well condensed layer [209].

The effects of thermocycling should always be considered while selecting glass liner materials.

2.4.8 Veneering Technique

Veneering process is the series of activities performed to overlay dental porcelain over the framework material to achieve the desired thickness of aesthetic porcelain. The technique used for veneering is important in controlling the overall quality of bilayer dental ceramics. Any shortcoming in veneering will reduce the longevity of the material. Veneering is broadly classified into three (3) categories, as shown in Figure 2-9.

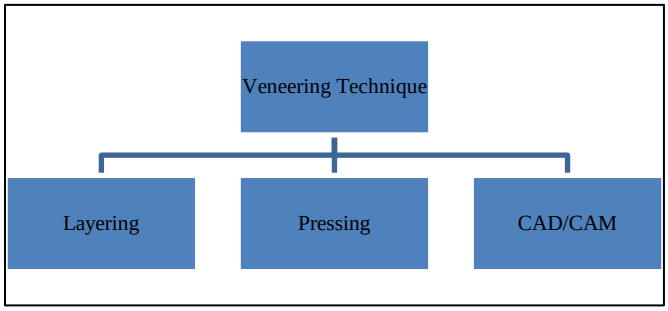

Figure 2-9: Major veneering techniques

Layering: It is the manual application of porcelain layers, followed by heat treatment for each layer.

Pressed: Applying a bulk veneer using pressure which is followed by a single heat treatment cycle. It is also referred by different names such as press-on, hot pressed, heat-press, press-over, and over pressed in literature.

CAD/CAM: Readymade framework matching high strength veneer prepared using CAD/CAM technology. It is also referred to as CAD-on / File Splitting Technique in literatures.

The performance of the veneer layer depends on the technique and materials used [129,130,212–215]. There is indirect evidence of strong interface bond between veneer and zirconia resulting in complete cohesive failure demonstrating the effectiveness of layering technique [115]. The fracture risk is reduced using leucite or lithium disilicate reinforced veneer material [216] or leucite containing pressable veneer has shown to develop superior bond with zirconia, compared to non-leucite based veneers [130,213]. Also, layering and pressed technique have shown similar crystalline phase with insignificant difference [41]. Water based veneers have shown to trigger low temperature degradation due to thermocycling [13,217].

Regarding manufacturing methods, studies have described that layering and pressed-on techniques are exhibiting insignificant difference in characteristics such as bond strength, fracture strength, and fracture toughness of the final product [41,120,130,134,215,218–223]. For that reason, the products of different veneering techniques possess similar quality, irrespective of the manufacturing route. However, there are evaluations indicating a significant difference in the quality and reliability of the material used [13,15,41,121,123,124,129,131,161,217,224–232].

Since the approaches used in manufacturing are non-standardized, such variation in studies is expected. Hence it is important to understand the material behavior that affects the performance of the product. The overall effect of various techniques and manufacturing variables in veneering techniques can be summarized as follows:

Manual Method (Layering): The performance mainly depends on dental laboratories, technician skills and established work procedures. These variables largely control the structural homogeneity, flaw population (size, number, distribution) and wettability with the framework. When experienced dental technicians use appropriate established work procedures, it results in a less flawed population, effective wettability with framework, less probability for nucleating sites for microcracks, and eventually good quality veneer. In turn, good quality veneer influences overall material behavior.

Machine / Controlled Processes (Pressed-on or CAD/CAM): Prefabricated ingots are melted and over-pressed in a mold cavity which is a highly controlled process with

minimum manual intervention. When these controls are rightly managed then it results in the high- quality product. However, product quality is affected due to the learning curve in handling the automation and new materials.

Examples of studies conducted to understand the effects of layered and pressed veneer techniques on material behavior are provided in Table 2-3. The studies listed in the table indicate that material behavior is mostly affected by flaw distribution.

Table 2-3: Examples of studies conducted to understand the effects of layered and pressed veneer techniques on the behavior of the material

Characteristic	Exhibited Behavior	Compared to	Cause (Determined or Potential)	Reference
Fracture / Bond Strength	Layered is inferior	Pressed	Surface lift due to tetragonal to monoclinic transformation.	[224]
	Layered is superior	Pressed	Higher Sintering Temperature and veneer material used in the technique.	[121]
	Pressed is superior	Layered	Fewer Faults due to controlled production.	[216]
	Pressed is superior	Layered	Sound framework-Veneer Interface due to external pressure.	[224]
Flexural Strength	Layered is superior	Pressed	Release of residual stresses due to multiple firing cycles for each layer.	[225]
	Pressed is superior	Layered	Fewer Faults due to controlled production and homogeneity.	[131]
Fracture Toughness	Layered is superior	Pressed	A durable interfacial bond was due to using the first layer of the same veneering material instead of a liner.	[226]
	Pressed is inferior	Layered	Porosities, along with the interface, localized stresses revealed insufficient bonding, weak strength with the possibility of ineffective wettability.	[227]
	Pressed is superior	Layered	Less void on the fracture surface indicates material with less flaw density.	[230]
Fatigue Performance	Layered is superior	Pressed	Release of residual stresses due to multiple firing cycles for each layer.	[228]
	Pressed is inferior	Layered	Ineffective handling and inexperience with the new ceramic system.	[228]
Aging / Thermocycling	Layered is inferior	Pressed	Significant exposure of framework to moisture and multiple firing cycles to trigger low-temperature degradation is not the Pressed Technique case.	[124,139,177]
	Pressed is superior	Layered	It is not associated with any exposure to moisture and reduced firing cycles, causing a reduction in residual thermal stress.	[9,124]

Fractures are known to originate from defects in porcelain, where cracks are initiated within porcelain [41]. As a result, the population of flaws can directly or indirectly govern the process of crack initiation and propagation. The SEM images shown in Figure 2-10 [41] indicate that the fracture originated from a defect.

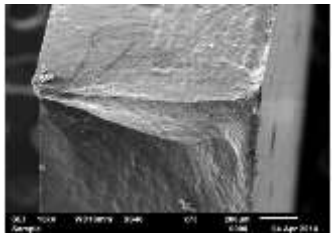	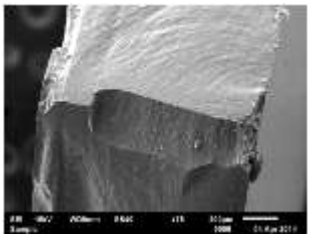
An SEM image is showing a fracture of a VM9 bilayer. Fracture started from an internal defect close to the interface and propagated to the surface. The layered technique was used in manufacturing the specimen.	An SEM image of a broken PM9 bilayer showing that fracture originated from a defect at the interface and within the porcelain layer. The pressed technique was used in manufacturing the specimen.

Figure 2-10: SEM images showing crack nucleation from preexisting defects in the porcelain layer (image reprinted from [41])

The CAD/CAM veneering technique has shown mixed results compared to the other two conventional techniques (layering and pressed). Products are proved to be less sensitive to aging, but possess lower fracture resistance than those fabricated by the layering technique [123]. CAD/CAM technique has demonstrated superior fracture strength due to lower flaw population resulting in superior quality of veneer material [215]. CAD/CAM has proven to be a cost effective process reducing dependency on subjective and technique sensitivity [232]. It is evident from these studies that further research is necessary to address the suitability of this technique.

The combination of the mentioned techniques has revealed promising results. For example using the CAD/CAM method and the pressed technique has shown insignificant effect of thermocycling on veneer performance [124]. Also, the use of “double veneer technique” has revealed a high bond strength and a superior interface [15]. Such high quality can be attributed to the fact that employing the pressed technique for reducing the flaw density within veneer and employing the layering technique for superior aesthetics without sacrificing the strength of material. In conclusion, further studies are required to predict the performance of bilayer dental ceramics [228].

2.4.9 Finishing Heat Treatment

Heat treatment is known to affect material properties from Macro to Nano- scales, and the parameter used in heat treatment are critical in determining the properties of the final product.

Parameters:

Major heat treatment parameters are described in Figure 2-11. Various studies are performed to understand the effects of heating rates [22,23], the atmosphere of the furnace [24], soaking time and cooling rate [25,26], firing cycles [27,28], soaking temperature [29,30], and the sensitivity to cooling cycles [9,22,31–40]. Several evaluation were focused on understanding the effects of cooling rates. A few investigations indicated that other variables may also have significant effects on the behavior of material.

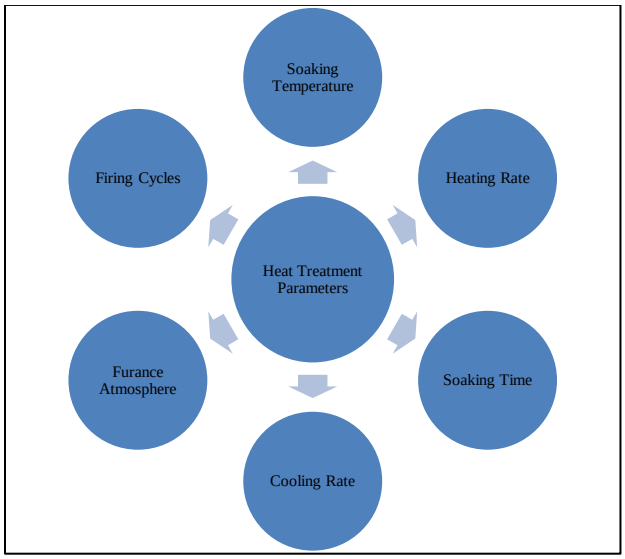

Figure 2-11: Heat treatment parameters

Effects:

Heat transfer coefficients, CTE, veneer to zirconia thickness ratio, chemical composition, the glass transition temperature of porcelain, and overall geometry of compoenent are all relevant during heat treatment.

The effect of cooling cycle were analyzed extensively along with the effects of the phase transformations that occur during the heat treatment. On the other hand, there are some studies that indicate cooling cycle has no or minimal effects on material behavior [66,126,223]. Table 2-4 summarizes the studies done on the effects of heat treatment parameters.

Table 2-4: Examples of studies conducted to investigate the effects of heat treatment on the material behavior

Heat Treatment Parameter	Effects	References
Cooling cycle	Stress state, fracture resistance, fatigue strength, bond strength, flexural strength, fracture toughness	[9,11,22,23,25,26,31–41,56,68,74,76,127,236–243,245–247]
Firing Temperature, Firing Cycles	Phase transformation, leucite transformation, distribution and its refinement	[27–29,237,247]

Based on the mentioned studies, the following provides a review on the probable effects of cooling rate and phase transformation on the overall state of the stress:

Slow Cooling Rate: Generates low thermal gradient within dental porcelain resulting a uniform cooling throughout the material volume. Appropriate time is available for viscoelastic relaxation. It induces lower magnitude stress states compared to fast cooling.

Fast Cooling Rate: Generates higher thermal gradient within dental porcelains. It creates non-uniform cooling throughout the volume. Adequate time is not available for viscoelastic relaxation. Hence, higher stresses are induced in the veneers. The presence of higher magnitude transient stresses is also noticed for fast cooling rates.

Phase transformation in dental porcelains: Leucite-based veneers has shown recrystallization on extremely slow cooling. It resulted in cubic to the tetragonal transformation of leucite inducing undesired tensile stresses and exhibits significant potential to affect the quality of bilayer dental material. Non-leucite-based dental material has shown to induce higher transient stresses on faster cooling but is suitable at slow cooling.

It is evident that heat treatment cycles are non-standardized, making the results of one study not comparable to another [40,223]. In addition, some findings contradict others [127,245]. Table 2-5 summarizes the protocols followed in various studies to investigate the effects of cooling cycles.

Table 2-5: The protocols followed in different studies to investigate the effects of cooling cycles

Reference	Definition
Fast cooling, and bench cooling	
[11,22,38,56,66,68]	Cooled at a certain cooling rate as recorded in the experiments or as simulated in finite element modeling (e.g., 200°C/min, 300°C/min, 500°C/min, 600°C, 900°C, 2700°C/min, 6000°C/min).
[22,35,40,65,74,240,243,246,247]	Furnace doors immediately opened upon reaching soaking temperature.
[23,25,33,41,127,239,242]	Samples immediately removed from the furnace upon reaching soaking temperature and subject to open air or removing the specimen from the muffle as soon as the muffle was fully descended.
[37,241,245]	Samples were removed from the furnace immediately after the holding time and blasted by compressed air, or the furnace was opened to blow cold on the sample.
[223]	Furnace remains completely closed from 900°C-800°C and then was opened till the ambient temperature was reached.
Slow cooling	
[11,22,25,38,56,66,68,238,240,243,250]	Cooled at a certain rate from soaking temperature to room temperature, recorded in the experiments or simulated using finite element modeling (e.g., 30°C/min, 32°C/min, 20°C, 10°C/min, 2°C/min).
[33,76,242,246,247]	Cooled to a certain temperature in furnace (e.g., Tg, 200°C, 500°C) and then subjected to open air or door opened. Finite element analysis used.
[23,127]	Samples kept in the oven with the door open 30% till temperature reached 500°C and then removed from the oven.
[41,245]	After the end of firing, the oven was switched off and kept closed with the specimens inside until room temperature.
[22,35,250]	Maintaining the chamber closed until the temperature reached 50°C below Tg. Then the furnace door was opened.
[74]	Door of the oven opened only 10%, following a complete opening as soon as the temperature inside the oven reached 200°C. The cooling rate of 30°C/min was recorded between 900°C to 500°C.
[238]	Door closed until 450°C was reached (i.e., below Tg). Then samples were subjected to ambient temperature.
[40]	Cooling of the specimens from the sintering temperature to Tg within 5 minutes inside the furnace.
[241]	Specimens removed from the furnace when the temperature reduces to 100°C
[239]	Samples were cooled at 20°C/min until 400°C, held for extra 5 minutes in a furnace before bench cooling.
[223]	Samples cooled with the door closed till 600°C, and the door was opened.
Cooling Rates with incomplete description	
[17,27–29,34,36,75,126,129,130,172,177,225,240]	Heat treatment parameters not determined (e.g., manufacturer's recommendation used or no information regarding cooling rate exist).
Other Terminologies used for Cooling Rates	
[238]	Extremely slow cooling: Specimens were cooled at 2°C/min to room temperature.
[241,245]	Normal cooling: 500°C was reached inside the furnace, samples were removed and cooled to room temperature.
[23]	Moderate Cooling: Specimen to be left in the fully open muffle for 7.5 minutes until a muffle temperature of 500°C was reached.
[243]	Modified Cooling – Cooling from 900°C to 600°C while the furnace door was closed

Complying veneer manufacturer's instructions is essential for achieving the desired quality [34,248]. However, there is no clear definition of slow cooling or desired cooling rate [238,245]. In contrast, sufficient clarity on heat treatment is not yet established and results in a product with unpredictable properties [38]. After heat treatment, the product's quality cannot be tested using visual examination of the shade color, as suggested by manufacturers and requires validated procedures.

2.4.10 Thickness Ratio and Other Geometrical Factors

Thickness Ratio:

It is proven that geometrical factors have a significant role in affecting the characteristics of the product. Thickness serves as the critical geometrical factor that affects the magnitude, nature, and distribution of residual stresses in bilayer zirconia-based products [9,32,248].

Thickness ratio is referred as the ratio of the framework thickness to that of veneering dental porcelain. For a given total thickness, as the thickness of veneer decreases, and thickness ratio increases, it results in decrease in magnitude of thermal stresses. Decrease in stresses results in further improvement of the performance of the bilayer dental material [10,11,34,37,256]. Finite element analysis has shown 50% reduction in residual stresses when thickness ratio was changed from 1:2 to 2:1 [11]. Also, higher thickness ratios have shown higher phase angle - ratio between sliding and opening modes at an interfacial crack tip. This results in higher interfacial toughness and maximum resistance to crack propagation [171,184]. On the contrary, Zhang et al. [257] have indicated that a desired stress pattern can be achieved for thicker veneers.

The porcelain veneered on zirconia framework has low thermal diffusivity, high heat capacity and low thermal conductivity [10,34,35,218,242]. Additionally, during cooling, a thick porcelain will have a solidified outer surface and a viscous internal surface that restricts viscous-liquid content. This results in a differential thermal contraction and high

thermal gradient due to poor heat transfer that induces higher residual thermal stresses in the veneer layers, enough to induce microcracks [10,11,35,218]. Fast cooling has shown to induce higher thermal gradients compared to slow cooling and hence cooling rate becomes significant as it governs the stresses in veneer [22,37,239].

In conventional designs, cusp region has higher and uneven thickness of veneer compared to other regions. Higher and uneven thicknesses in such regions raise concerns such as becoming susceptible to higher undesired thermal residual stresses from final heat treatments or decreasing flexural strength or steep cusp inclination. Consequently, frequent failure are observed in such areas [34,76,133,257,260]. Also, curved areas with small radius are preferential sites for stress concentration [74]. Modified crown design with anatomic structures facilitates achieving uniform thinner veneer creating lower residual stresses and mitigates the risks of premature veneer failures [25,135,228,254].

Generally, increasing the framework thickness improves the strength of the product. The extent to which thickness of framework can be increased is constrained by other parameters such as aesthetic appearance [87] and thermal gradients [83,258]. Veneer thickness should be maintained minimum for achieving the desired aesthetic properties [251], resistance to thermocycling effects and wear [10]. In summary, the use of appropriate thickness ratios is highly recommended [244].

Other Geometrical Factors:

Overall geometry of veneered 3Y-TZP dental restorations has significant effects on the thermal stress pattern within the material [21,74]. The shape of the material can potentially change the location of maximum tensile stresses, favoring crack propagation from the top of veneer surface in flat specimens to the interface in crown shaped specimens [76]. Hence, results obtained from flat samples may not be extrapolated to complex crown designs [76]. Nevertheless, Tanaka et al. [238] used same thickness combinations as in [76], different specimen shapes exhibited similar stress profiles in a finite element analysis [238]. A stress sign inversion occurs due to phase transformation in zirconia for a certain veneer thickness [240].

Framework design is another crucial aspect which is known to affect the load bearing capacity of the structure [129]. A design with additional cervical collar in slice preparation has shown improvement in the fracture strength with improved technical and biological suitability [129,252]. Modified crown design with high thickness ratio has advantage of uniform veneer thickness in all areas. This kind of design has shown to provide anatomical support upon loading. Also uniform low veneer thickness mitigates the risk of having higher thermal stresses during cooling steps, improving overall performance of the material [25,83,135,216,218,228,251,252,254,261].

In a study, other geometrical aspects such as finish line design have presented no effects on the short term fatigue or fracture resistance [255]. Shoulder height may act as a stress absorber and it has been shown to improve fracture resistance [259]. However, the porcelain shoulder may not have any effects on the fracture load [221].

2.5 Step V: Recommendations

A comprehensive literature review on the effects of various parameters on veneer and zirconia performance was provided. It was shown that although some parameters are studied in detail, there exist discrepancy and variation between various findings. The most possible cause for such variation is the absence of a common methodology for manufacturing bilayer zirconia-based dental materials. As such the following points are suggested for establishing an optimum solution:

- Failures are mainly known in veneers which is affecting the integrity of dental restorations. Thermal stresses consititutes primary factor in premature chipping of dental porcelains. It is recommended to evaluate behavior of dental porcelains at higher temperatures especially in the transition zone. Such studies may provide significant insight into the material response to high temperature heat treatments and delve into the causation of undesired thermal stresses.

- It is recommended to plan research improvements in the field of veneered 3Y-TZP dental structures by considering effects of every parameter on their overall performances. It is evident now that these variables and their effects on material performance are

interconnected and do not act in isolation.

- More finite element studies should explore the use of accurate material behavioral aspects by including detailed viscoelastic relaxation in veneers, anisotropic behavior of the framework, and phase transformations.

- Studies are required to drive the direction towards standardization of parameters in dental laboratories. Standardization is the key to achieve the desired performance of bilayer zirconia-based dental material.

Chapter 3

3 Theoretial background

This chapter describes the basic material nature of dental porcelain, their classification and characteristic behavior. In this way, the intention of this chapter is to form the theoretical foundation for numerical analysis.

3.1 Dental Porcelain and Characteristic Behavior

Generally, porcelains are hard, shiny, white substance which is made by heating a special type of clay material to a high temperature. Clay materials are mainly consisting of silica. There are various types and applications of porcelains such as cups, plates, decorations, etc. The porcelains which are used in dental restoration materials are known as dental porcelains.

Layers of dental porcelains are applied to the zirconia framework material for a suitable aesthetic appearance. These dental porcelains mainly consist of glassy and crystalline phases in their microstructure based on their chemical composition. Dental porcelains are classified in two main categories as per [81], which are shown in Figure 3-1.

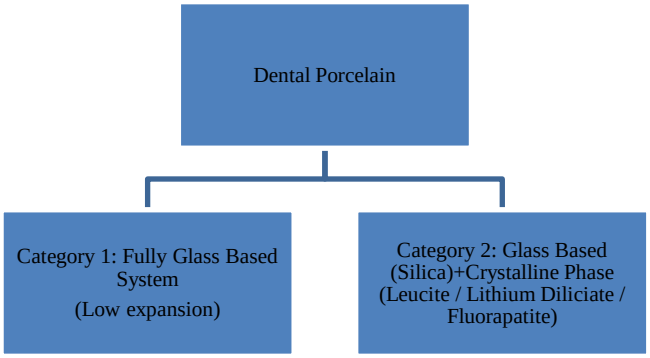

Figure 3-1: Classification of veneering dental porcelain

Based on this classification, it is evident that veneering dental porcelains consist of mainly glassy matrix and tend to behave as a glass material at a higher temperature. Hence, it is crucial to understand glasses' behavior at higher temperatures and the evolution of stresses that occurs upon cooling from softening temperatures. Accordingly, it assists in a better

understanding of the evaluation of residual thermal stresses in dental porcelains.

Therefore, in this report, wherever glass is mentioned, it shall be considered equivalent to dental porcelains.

Following sections are dedicated to understanding the glass materials and how it behaves at high temperatures.

3.1.1 Characteristics of glass material

Glass is an amorphous material that exhibits a glass transition when heated towards the liquid temperature or cooled from that temperature range [262]. As an amorphous material, glass material lacks long-range periodicity of structure and possesses a high degree of short-range order of arrangement of atoms due to its chemical nature.

When the glass is heated at high temperatures and rapid cooling relative to its characteristic crystallization time, its crystallization is obstructed. Such rapid cooling generates solid-state of glass with disordered short-range atomic configuration of that of super-cooled liquid.

Molecules in glasses are arranged similar as those in liquids but are more tightly packed. The resulting final structure determines the kind of stress state and properties achieved in the glass materials. Due to the nature of glass, it is essential to know where and why the liquid ends and glass begins [263].

3.1.2 Glass Transition

The thermomechanical behavior of the glass is highly dependent on the temperature. Scherer has explained the process of the glass transition [264]. As shown in Figure 3-2, three different regions are identified when the glass is subjected to heat treatment. The glassy region is evident below the transition temperature, the transition region within the transition temperature range, and the liquid region above the transition temperature's upper limit.

Glasses tend to behave as elastic solid at a temperature below the lower limit of transition temperature (i.e., in the glassy region below T_L). At higher temperatures (i.e., in the liquid region above T_U and below melting temperature T_M), glasses behave as the viscous liquid or supercooled liquid. Glasses exhibit the behavior of viscoelastic solid with the bound of the upper (T_U) and lower temperature (T_L) region (i.e., in transition range). Viscoelastic mechanical behavior of the glass in the glass transition zone ($T_L < T < T_U$) is exhibited around the limit of 50-100°C from glass transition temperature (T_g). Glass transition temperature is generally the midpoint of the glass transition range [49,264].

The glass transition is a kinetic transition driven phenomenon. As the liquid state is cooled, continuous evolution in the properties and structure of glass occurs between the supercooled liquid and the solid states is strongly dependent on temperature. As a result, the glass' structure and properties can be altered mainly by modifying the cooling mechanism's kinetics and not by the thermodynamics of the process. Glass transition occurs due to diverging differences between internal and external timescales of the cooling liquid [262].

Differences in crystals and glasses' behavior can be explained mainly due to processes with and without dependency on thermodynamics.

Crystals:

In crystal structure of metals, the liquid crystallizes to a thermodynamically stable state crystalline phase, as presented in Figure 3-2, and it represents a type of thermodynamic transition. The structures are governed by the chemical potentials of the material phases. There exists a fixed value of melting and transformation temperature. The crystalline phase has a smaller volume than the liquid state, and it further shrinks with the reduction in temperature. The slope of the cooling curve (i.e., change in volume to temperature) is the coefficient of thermal expansion/contraction (α) where α_{liquid} is very high compared to α_{solid}.

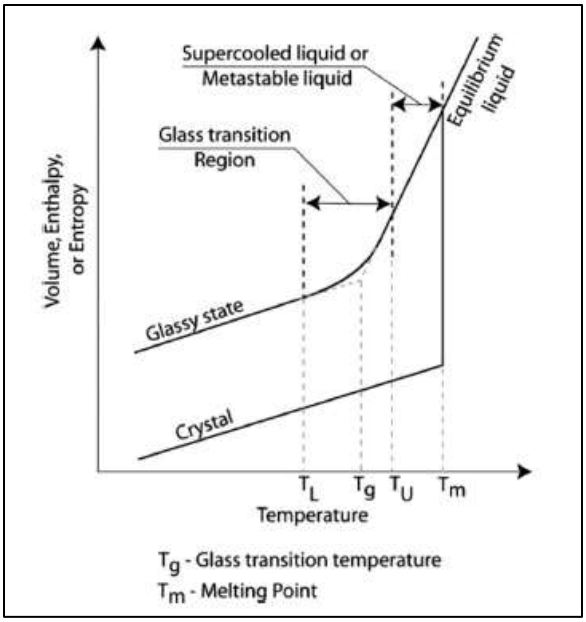

Figure 3-2: Volume change comparison in glass and crystalline materials (e.g., metals) (Image reprinted from [264])

Glasses:

The glass transition is a kinetic transition phenomenon, i.e., the structural transformation takes place from the liquid state only if sufficient time is provided for that change to occur. Figure 3-2 shows the region of "Supercooled Liquid," which indicates glass-forming liquids that bypass melting point (T_m). In this region, liquid possesses high viscosity reducing the diffusion of atoms in the structure. Liquids, whenever subjected to high cooling rates, do not facilitate enough time for crystallization.

Considering above explanation, there are two timescales in case of the glasses, i.e., external time scale (Δt) controlled by the external factors (e.g., cooling rate) and internal time scale (τ) governed by the viscosity of the liquid (e.g., bonding). The internal time scale (τ) is governed mainly by bonding between atoms/ions. It shows that the stronger the bonding is, the higher is the τ required for structural transformation and vice versa.

At higher temperature $\tau < \Delta t$ due to the weaker bonding (i.e., structural changes are instantaneous as the equilibrium can be reached instantaneously). $\tau \sim \Delta t$ or $\tau > \Delta t$ in the viscous region (supercooled / transition range) where glass exhibits a viscous or very

viscous state (i.e., glass structure and properties are history-dependent). At low tempeatures, τ is very high compared to Δt where liquid cannot achieve equilibrium as bonds are very strong (i.e., all mechanical and thermal effects only affect atomic vibrations). For that reason, at low temperature, τ is very large compared to time step Δt. This fact indicates the dependency of glass properties on both time and temperature.

3.1.3 Viscoelastic Relaxation - Stress Relaxation

Viscoelasticity, in its simplest form, can be defined as the time-dependent strain response of viscoelastic material to constant stress or vice versa. In other words, it is the isotropic rate-dependent material behavior for materials in which the dissipative losses are primarily due to internal damping effects. Due to a viscoelastic material's time-domain effects, it is assumed that deviatoric and dilatational behaviors are independent in multiaxial stress states.

Glass is a viscoelastic material and exhibits time-domain viscoelastic behavior, i.e., deviatoric (shear) and dilatational (volumetric) behavior shows viscoelasticity. It shows a time-dependent strain response for a continuously applied stress [264]. As presented in Figure 3-3, the generalized Maxwell model is generally used to fit the viscoelastic behavior of glass. The generalized Maxwell's model is a rheological discrete model. It is an association of several Maxwell's models (spring and dashpot in series). The absence of the isolated spring would ensure fluid-type behavior whereas the absence of the isolated dash-pot would ensure an instantaneous response.

Time domain viscoelasticity is available in Abaqus for small-strain applications where the rate-independent elastic response is defined with a linear elastic material model. This is used for defining viscoelasticity of glass in the current work. The constitutive equations for viscoelastic behavior of glass are given as [50,264,265],

$$\boldsymbol{\tau_{ij}(t) = \int_0^t G_R(t-s)\frac{\partial \gamma_{ij}(s)}{\partial s}\,ds} \tag{3-1}$$

$$\boldsymbol{\bar{\sigma}(t) = \int_0^t -K_R(t-s)\frac{\partial \bar{\varepsilon}(s)}{\partial s}\,ds} \tag{3-2}$$

Where $\boldsymbol{\tau_{ij}}$ and $\boldsymbol{\bar{\sigma}}$ are the shear and volumetric stress, respectively, Shear and volumetric strains are described by $\boldsymbol{\gamma_{ij}}$ and $\boldsymbol{\bar{\varepsilon}}$. $G_R(t)$ and $K_R(t)$ are the time-dependent shear and bulk relaxation moduli; t and s are the current and past time, respectively.

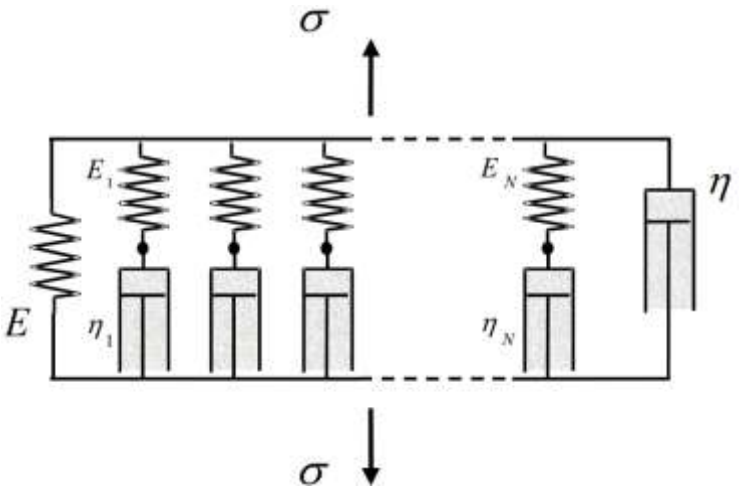

Figure 3-3: Generalized Maxwell Model

The relaxation moduli are expressed further in terms of Prony series parameters. In Abaqus [265], the time-dependent shear relaxation moduli is expressed using a dimensionless normalized shear relaxation modulus form $g_R(t)$ as,

$$\mathbf{g_R(t)} = \frac{\mathbf{G_R(t)}}{\mathbf{G_0}} \tag{3-3}$$

Where $G_0 = G_R(0)$, which is the instantaneous shear modulus. Dimensionless shear relaxation function has a limiting value of 1 at time t=0 and G_∞/G_0 at $t=\infty$. 4-term Prony series expansion was used to calculate the dimensionless form of shear relaxation moduli. The relaxation properties, as defined in Table 4-4 of Chapter 4, were used to define the 4-term Prony series. Prony series expansion was used to calculate the dimensionless form of shear relaxation moduli.

$$\mathbf{g_R(t)} = \mathbf{1} - \sum_{\mathbf{i=1}}^{\mathbf{n}} \bar{\mathbf{g}}_{\mathbf{i}}^{\mathbf{p}} \left(\mathbf{1} - \mathbf{e}^{\frac{-\mathbf{t}}{\tau_{\mathbf{i}}^{\mathbf{G}}}}\right) \tag{3-4}$$

where $\bar{g}_i^p$ and $\bar{\tau}_i^G$ were the material constants of the 4-term Prony series, as defined in

Chapter 4. Similar relationship can be defined for bulk modulus; however, studies have outlined that there is negligible effect of bulk modulus on viscoelastic relaxation [56,58,264]. Thus, volumetric behavior was assumed to be elastic, where instantaneous bulk modulus ($\mathbf{K_0}$) represents the time-dependent bulk modulus ($\mathbf{K_R}$).

The main driving force for stress relaxation is the residual stress in the viscoelastic material. An equilibrium state in such response can only be achieved with the zero stress-state in the material.

3.1.4 Stress Relaxation – Thermorheologically Simple (TRS) Behavior

TRS behavior of a material is referred to the state of material when the structure is stabilized. Accordingly, when the structure of glass is stabilized, it can be considered as TRS material. In other words, glass exhibits the same mechanical behavior at different temperatures, but only microstructural changes evolve [50].

Scherer et al. [264] has explained the process of TRS behavior exhibited by glassy material. TRS behavior captures the temperature effect on the relaxation moduli. Considering TRS's definition, the relaxation function can be known at any temperature if the value of the relaxation function is known at a reference temperature. It consists of the relaxation function shift on a logarithmic time scale using the "Shift Function – A(T)." It is exhibited in Figure 3-4 from [264]. As shown in this figure, the respective relaxation function on the logarithmic time scale maintains the same shape.

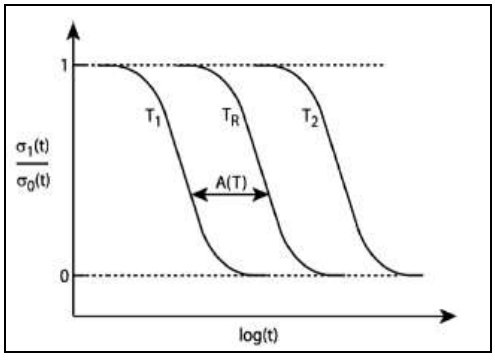

Figure 3-4: Thermo-rheological Simple Behavior of glass (Image reprinted from [264])

The temperature effect on the relaxation moduli is introduced through the concept of reduced time concept. As the viscoelasticity of glass is a function of internal time scale, the concept of reduced time plays an important role. In reduced time, time itself is a function of variables (e.g., temperature). The internal time scale in glasses is time-dependent. For any relaxation function (e.g., τ), the effect of temperature is known through reduced time (ξ) as,

$$\boldsymbol{\tau_{iT}(t) = \tau_{iT_{ref}}(\xi)} \tag{3-5}$$

Where i=1,2,3,….n is the number of terms in the Prony series used to determine the material constants.

The accurate time-temperature dependence of any relaxation function while considering stress relaxation in glasses is described using Arrhenius relation [54,266] which is as,

$$\boldsymbol{\xi(t,T) = \int_0^t \frac{\tau_{ref}}{\tau(T,s)} ds = \int_0^t A\big(T(t)\big) ds} \tag{3-6}$$

where A(T) is the shift function which is calculated as,

$$\boldsymbol{\ln\big(A(T)\big) = -\frac{H}{R}\left[\frac{1}{T_{ref}} - \frac{1}{T}\right]} \tag{3-7}$$

Where H = Activation Energy / Enthalpy of material, R = Universal gas constant, T_{ref} = reference temperature at which relaxation function is identified as a material constant, T=current temperature. In this manner, if the relaxation function is known at a reference temperature, then considering the TRS behavior of glassy material, relaxation functions at any temperature can be recognized with shift function as per Arrhenius form.

3.1.5 Viscoelastic Relaxation – Structural Relaxation

The temperature-time dependence of glass properties (e.g., coefficient of thermal expansion/contraction, specific heat, refractive index, density, viscosity, and enthalpy) is defined as structural relaxation. E.g., the coefficient of thermal expansion/contraction has instantaneous values in the glassy and liquid state; and it is a function of time-dependent glass response in the transition region [264].

In other words, it corresponds to temperature history-dependent thermal expansion/contraction, which occurs within the glass transition temperature region, as shown in Figure 3-5. How glass is cooled in the transition zone determines the thermal expansion coefficient, which is different at each material point [49].

Figure 3-5 presents the instantaneous and time-dependent response of volume change in glass in the transition region. The instantaneous response is characterized by slope along the glass line (α_{VG}), whereas the time-dependent response is characterized in the vertical direction towards the equilibrium liquid line having slope (α_{VL}). Hence, it can be said that as the cooling rate (i.e., external time scale) decreases, the equilibrium value of the volume decreases.

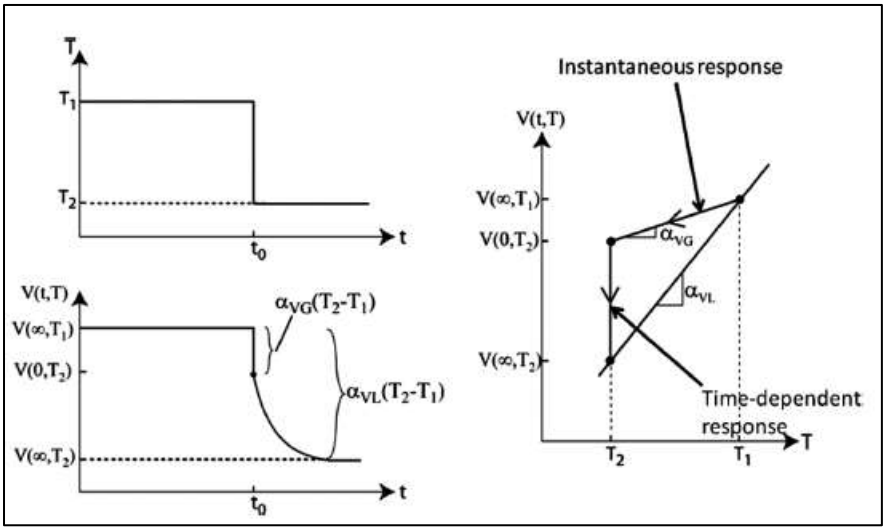

Figure 3-5: Effect of volume change in the glass when subjected to a sudden change in the glass transition region (Image reprinted from [264])

3.1.6 Structural Relaxation – Fictive Temperature Theory

We have seen that there are two-time scales during cooling for the glass volume (i.e., internal and external) to reach equilibrium. Depending on the kinetics of the cooling process, the cooled glass state may not be in equilibrium, which shows the sensitivity of glass towards time scales. This sensistivity of glass equilibrium towards time scales is explained through the Narayaswamy model of structural relaxation in glasses [52–54].

Narayanaswamy's model of the structural state concerning the change in a specific glass volume depending on the thermal loading kinetics is explained by Daudeville in [50] as exhibited in Figure 3-6.

Figure 3-5 and Figure 3-6 complement each other to understand the changes in the glass' volume upon heat treatment. Glasses are in a stable equilibrium state in their liquid state. Point A in Figure 3-6 indicates when a glass is heated at temperature T_1 below the transition range, the glass structure reaches a stable state at point B. When the temperature is far below the lower transition temperature, such a state is difficult to observe, which corresponds to a higher difference between internal and external time scales of material. At this point, the internal time scale required is very high compared to the external time scale. This phenomenon is described as direct structural relaxation.

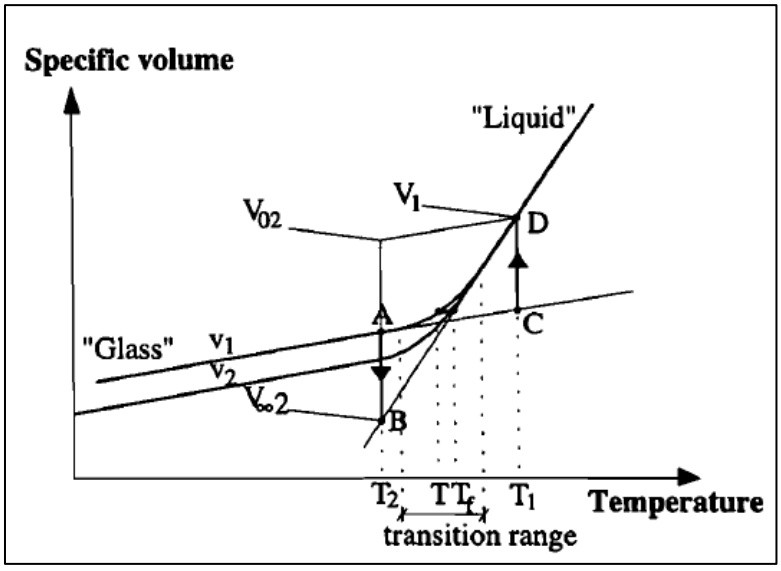

Figure 3-6: Change in specific volume for 2 cooling rates (Image reprinted from [50])

When the glass is heated directly above the transition temperature range (Point C), representing unstable structural configuration, glass reaches a stable state at point D. This phenomenon is described as reverse structural relaxation. Cooling of glass exhibits similar behavior as heating of glass. This structural relaxation process to achieve a stable state structure shows multiple possibilities of the glass states at different temperatures.

The concept of fictive temperature was introduced by Tool [267] to account for the structural changes during heat treatment in the glass. Tool has explained fictive temperature in [267] as,

"The physiochemical condition or state of a glass is reasonably well known only when both the actual temperature and that other temperature at which the glass would be in equilibrium, if heated or cooled very rapidly to it, are known. This latter temperature has been termed the 'equilibrium or fictive temperature' of the glass.''

As exhibited in Figure 3-5 and Figure 3-6, variations in the specific volumes describe the equilibrium temperature (i.e., fictive temperature). In other words, the fictive temperature is a mathematical concept that can quantify the structural changes in the glass and represent the theoretical temperature indicating glass equilibrium. There is the existence of three-wide possibilities [50,51] to understand the relationship between the actual temperature (T) and the fictive temperature (T_f). The difference in actual and fictive temperature provides the extent to which the glass has deviated from equilibrium [51].

a. Possibility 1: When T > Upper transition temperature: $T_f = T$

b. Possibility 2: When T = Glass transition range: T_f = Intersection between the straight liquid line and parallel to glass straight line in the glass transition zone as shown in Figure 3-6. In this situation, the fictive temperature starts lagging behind the actual physical temperature ($T_f \geq T$) which describes the beginning of a departure from the equilibrium.

c. Possibility 3: When T < Lower transition temperature: T_f = Intersection between straight liquid line and straight glass line below the glass transition zone as presented in Figure 3-6. This is the case where the fictive temperature at low temperatures is frozen at some value above the physical temperature ($T_f > T$).

To establish a relationship between the responses of specific volume change to temperature, a response function $M_v(t)$ is defined as,

$$\mathbf{M_v(t)} = \frac{\mathbf{V(t) - V_{\infty,T_2}}}{\mathbf{V_{0,T_2} - V_{\infty,T_2}}} = \frac{\mathbf{T_f - T_2}}{\mathbf{T_1 - T_2}} \tag{3-8}$$

Reference to Figure 3-5 and Figure 3-6: Volume $V(t)$ has the instantaneous value (i.e. $t = 0$) of $V(0)$ and equilibrium value (i.e. $t = \infty$) of $V(\infty)$ at temperature T_2. T_1-T_2 is the temperature increment in the glass transition zone, and T_f is the fictive temperature at T_2.

The variations in the fictive temperature can be defined through the relaxation function $M_v(t)$, which can be considered the structural / volume relaxation function. The dependence of the response function is defined through reduced time ξ.

As the structural state of glass is a function of the internal time scale, reduced time plays an important role. In reduced time, time itself is a function of variables (e.g., temperature). The internal time scale in glasses is time-dependent. A unifying parameter regulates the internal time scale (e.g., free volume change). Any changes in the free volume alter the internal time scale. Variations in the fictive temperature are defined through,

$$\mathbf{T_f(t)} = \mathbf{T(t)} - \int_0^t \mathbf{M_v[\xi(t) - \xi(s)]} \frac{\mathbf{dT(s)}}{\mathbf{ds}} \mathbf{ds} \tag{3-9}$$

As indicated in Figure 3-5, it can be observed that instantaneous change of volume occurs immediately at the glassy area (slope α_{VG}), and the time-dependent response of volume change takes place on the vertical line (slope α_{VL}). This internal time-scale-dependent behavior referred to as structural relaxation is analogous to the stress relaxation mechanism discussed earlier, where the behavior of strain response is seen with a sudden change in stress or vice versa. The structural relaxation in the transition range is mainly dependent on the cooling rate, which is similar to stress relaxation, where strain response is dependent on the change of stress rate.

This analogy between stress relaxation and structural relaxation describes the response function to calculate the fictive temperature for structural relaxation, which is jointly contributed by Tool [267] and Narayanaswamy [53]. It is defined as through Prony series as,

$$\mathbf{M_v(\xi)} = \sum_{\mathbf{i=1}}^{\mathbf{n}} \mathbf{C_i exp}\left(-\frac{\boldsymbol{\xi}}{\boldsymbol{\omega_i}}\right) \tag{3-10}$$

M_v is the relaxation function in structural relaxation similar to the relaxation function in stress relaxation defined in equations 1 and 2. Weight functions of the Prony series are defined by (Ci), ω is the structural relaxation time.

It is observed that structural relaxation times are proportional to stress relaxation time with a ratio within the range of 9 to 10 [50,56,58]. Scherer et al. [264] reported that structural relaxation for glasses is 4 to 20 times slower than stress relaxation. Minor or negligible changes in the stress state are observed in the material by changing structural relaxation times in range of $1/4^{th}$ to $1/20^{th}$ of shear relaxation times [58]. Refer Appendix-B for senstitivity analysis of stress change due to change in structural relaxation times.

Very few studies were performed to determine the high temperature shear relaxation properties. Data on the structural relaxation times are not available for dental porcelains. Hence, structural relaxation times are considered $1/10^{th}$ of the shear relaxation times for this study's modeling purpose.

3.1.7 Computation of Fictive Temperature

The fictive temperature allows to accomodate the glassy material' structural state by incorporating the internal and external time scales. Therefore, the structural state of glass, especially in the transition range, is dependent on the actual physical temperature and fictive temperature. Markovsky and Soules [268] determined a stable algorithm to calculate the glass material's fictive temperature.

It is determined by,

$$\mathbf{T_{f_i}(t) = \frac{T_{f_i}(t-\Delta t)+T(t)\frac{\Delta t}{\omega_i}}{1+\frac{\Delta t}{\omega_i}}} \tag{3-11}$$

T_{f_i} represents the partial fictive temperature, i=1,2,3,4 are the terms in the 4 term Prony series. Structural relaxation time ω at various time step is calculated using the expression,

$$\mathbf{\omega_i = \omega_{i,ref}\, exp\{ -\frac{H}{R}\left[\frac{1}{T_{ref}} - \frac{x}{T(t)} - \frac{1-x}{T_f(t-\Delta t)}\right]\}} \tag{3-12}$$

where H is the activation energy, R is the universal gas constant. Tref is the reference temperature used to measure the glass material constants (relaxation times) and x ($0 \leq x \leq 1$) is the material constant determined using experiments that represent the nonlinearity parameter. Properties from Table 4-4 were used.

Finally, the fictive temperature is calculated using the expression,

$$\mathbf{T_f(t) = \sum_{i=1}^{n} C_i T_{f_i}(t)} \tag{3-13}$$

T_f is the fictive temperature at time t. At higher temperature (i.e., above the upper limit of the glass transition temperature or when the glass is in the super-cooled metastable state), fictive temperature value is equal to the value of the actual physical temperature glass.

3.1.8 Structural Relaxation – Thermorheologically Simple (TRS) Behavior

It is already observed how glass behaves as TRS material and how the effect of reduced time concept are used to determine the relaxation functions that incorporate temperature, as described in equations 6 and 7. Based on these expressions, it is evident that the shift function is decided based actual physical temperature (T) in case there is only stress relaxation.

In the case of structural relaxation, the shift function (A) is defined using Tool-Narayanaswamy [53,267] as,

$$\mathbf{\xi(t, T, T_f) = \int_0^t \frac{\tau_{ref}}{\tau(T,s)} ds = \int_0^t A\big(T(t), T_f(t)\big) ds} \tag{3-14}$$

where,

$$\mathbf{\ln\big(A(T, T_f)\big) = -\frac{H}{R}\left[\frac{1}{T_{ref}} - \frac{x}{T} - \frac{1-x}{T_f}\right]} \tag{3-15}$$

The above equations are similar to the TRS of glass materials when only stress relaxation is considered in the model. However, in these above expressions, the inclusion of fictive temperature indicates the inclusion of the glass materials' structural state and the viscous

state. The parameter ‘x’ in the above equation is a non-linearity parameter that is determined experimentally. Properties from Table 4-4 were used.

3.1.9 Free Strain Concept

Free strain $[\varepsilon^f]$ is a strain generated in an unconstrained region of the material due to changes in the temperature. Any distribution of temperature in glass material leads to the generation of free strains. It shall be noted that change in temperature is not the only source of the free strains, and significant sources of free strains are written in a general form as [55],

$$\left[\boldsymbol{\varepsilon^f}\right] = \int_{\mathbf{P_i}}^{\mathbf{P_f}}[\aleph] + \int_{\mathbf{C_i}}^{\mathbf{C_f}}[\boldsymbol{\beta}] + \int_{\mathbf{T_i}}^{\mathbf{T_f}}[\boldsymbol{\alpha}] \qquad (3\text{-}16)$$

$[\aleph], [\beta], \text{and } [\alpha]$ are the expansivity matrices responsible for the generation of free strains in a glass material as a response to change in pressure (P), concentration (C), and temperature (T), respectively.

This current study on the evaluation of thermal stresses is only based on temperature-induced free strains in the material. For that reason, the first two terms in equation 16 are not included as part of this study.

The free strain increment for 3Y-TZP framework was computed using,

$$\mathbf{d\varepsilon^f(T)} = \boldsymbol{\alpha_g(T)dT} \qquad (3\text{-}17)$$

The free strain increment for dental porcelains was calculated as explained below:

It is described in a review by Rekhson et al. [55] that residual thermal stresses in the glass materials are formed through the non-uniform irreversible dissipation of thermal strains. Especially when the temperature distributions are non-uniform, the generated free strains $[\varepsilon^f]$ become incompatible.

For the system to be compatible, additional strain $[\varepsilon^{th}]$ needs to be applied. Therefore, the total strain $[\varepsilon]$ in the material can be expressed as [55],

$$\boldsymbol{\varepsilon}(\mathbf{t}) = \boldsymbol{\varepsilon}^{\mathbf{f}}(\mathbf{x}, \mathbf{t}) + \boldsymbol{\varepsilon}^{\mathbf{th}}(\mathbf{x}, \mathbf{t}) \tag{3-18}$$

This additional strain [ε^{th}] applied for compatibility, calculated by Abaqus solver from compatibility equations, determines the magnitude of the irreversible free strain at every material point, which results in residual thermal stresses. Consequently, the residual thermal stress generated at any material point and time is proportional to the applied thermal strain [ε^{th}]. Therefore, determination of free strain [ε^{f}] facilitates to calculate residual thermal stresses in glasses.

The free strains are generated from thermal contraction of a mechanically unconstrained material. Evaluation of free strain based on the theory of structural relaxation phenomenon shall constitute an essential part of the residual thermal stress analysis in glasses [55].

Indenbom and Vidro [269] have explained the calculation of free strain by ensuring the incorporation of structural relaxation. It focussed on the difference in the thermal history of various regions of the materials [55]. As per their description, it is quoted,

"The difference in the nature of thermoplastic and structural stresses in amorphous materials can be illustrated by a comparison of mean interatomic distances in different parts of the specimen.

In the case of the thermoplastic stresses, the density in compressed regions is greater than in regions under tension. After division of the specimen, a process which leads to the removal of internal stresses, the density becomes identical everywhere.

In the case of the structural stresses, the density in the stressed specimen is everywhere identical, but after division the density in the formerly compressed parts turns out to be less than in the parts formally under tension."

The thermoplastic stresses refer to the stress state variation related to instantaneous volume response and structural stress due to structural relaxation. Based on this understanding of the free strain, the free strain increment is calculated using,

$$\mathrm{d}\varepsilon^{\mathrm{f}}(\mathrm{T}, \mathrm{T_f}) = \alpha_{\mathrm{g}}(\mathrm{T})\mathrm{dT} + \left\{\alpha_{\mathrm{l}}(\mathrm{T_f}) - \alpha_{\mathrm{g}}(\mathrm{T_f})\right\}\mathrm{dT_f} \tag{3-19}$$

which can be further expressed as,

$$\mathbf{d\varepsilon^f(T, T_f) = \alpha_g(T)dT + \alpha_s(T_f)dT_f} \quad (3\text{-}20)$$

where α_g is the coefficient of thermal contraction in a glassy state, α_l is the coefficient of thermal contraction in the liquid state, T_f is the fictive temperature, and T is the actual temperature. Coefficient of thermal contraction is calculated using values as defined in Table 4-3.

α_s represents coefficient of thermal contraction due to structural relaxation. The first term in right side of equation 20 represents the strain responsible for thermoplastic stresses due to instantaneous material response, and second term containing α_s represents the strain due to structural relaxation responsible for structural stresses. The free strain calculated using this expression provides an understanding for the dependency of structural relaxation on the fictive temperature, i.e., free volume change based on the transition region's fictive temperatures.

Tool-Narayanaswamy [53,267] model for calculation of free strain is similar to the one discussed in equation 19. In Tool-Narayanaswamy model, the liquid coefficient of thermal expansion, i.e., α_l is assumed to be constant and is not a function of fictive temperature. Another consideration in Tool-Narayanaswamy model is the dependence of glassy coefficient of thermal contraction, i.e. α_g on actual physical temperature and not on fictive temperature.

In the current study, the calculation of free strain considers the dependency of structural stresses on the fictive temperatures, as shown in the above equation 19. The free strain is calculated using this expression, as it provides a clear understanding of the dependency of the structural relaxation on the fictive temperature i.e., free volume change based on the fictive temperatures in the transition region. Free strain as calculated above is applied through UEXPAN subroutine for estimation of residual thermal stresses which are determined using ABAQUS internal time-dependent material response to applied strain for small strain application.

Chapter 4

4 Finite Element Model

Finite element modeling was performed by developing a rectangular geometry model in commercial finite element software (Abaqus).

4.1 Material definitions

3% Yttria stabilized Tetragonal Zirconia Polycrystal (3Y-TZP) was used as the framework material with one layer of a dental porcelain on the framework. The characteristic property parameters used in the model were obtained from different reports due to the lack of information from one unique source. Anisotropy of 3Y-TZP is discussed in section 2.4.2. Effect of anisotropy of 3Y-TZP on thermal stresses in dental structures is not evaluated.

4.1.1 Properties of 3Y-TZP

3Y-TZP was considered a linear elastic material with isotropic properties. The room temperature and high-temperature properties are described in Table 4-1 and Figure 4-1.

Table 4-1: Room temperature (25°C) properties of 3Y-TZP (zirconia)

Material	Young's Modulus, E (MPa)	Poisson's Ratio, μ	Density, ρ (kg/mm^3)	Thermal Conductivity, k (W/mm °C)	Specific Heat, c (J/kg °C)
3Y-TZP [42,56]	206,500	0.30	6.1e-06	2.92e-03	466

4.1.2 Properties of Dental Porcelains

Dental porcelains are generally glassy amorphous materials. Dental porcelains were considered a linear viscoelastic material with isotropic properties. The room temperature and high temperature-dependent elastic properties are presented in Table 4-2 and Figure 4-1.

Table 4-2: Room temperature (25°C) properties of Vita VM9 and IPS Empress 2

Material	Young's Modulus, E (MPa)	Poisson's Ratio, μ	Density, ρ (kg/mm^3)	Thermal Conductivity, k (W/mm °C)	Specific Heat, c (J/kg °C)
VM9 [42,56]	66,500	0.21	2.400e-06	1.370e-03	734
Empress 2 [58]	65,000	0.26	2.531e-06	10.12e-03	734

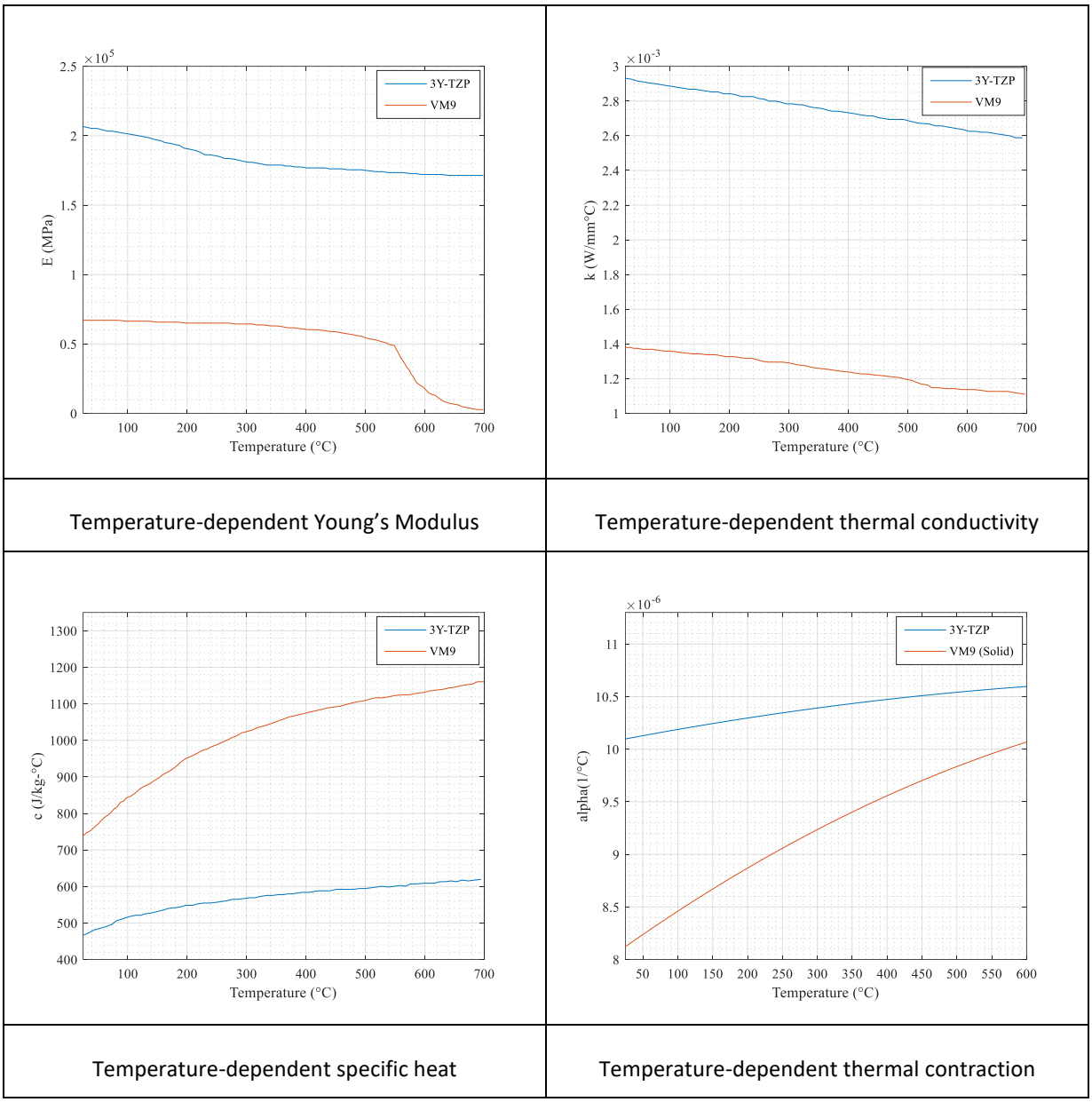

Figure 4-1: Temperature-dependent properties of 3Y-TZP and dental porcelain

4.1.3 Coefficient of Thermal Contraction (CTC)

CTC for 3Y-TZP framework was used in a second-degree polynomial form with the constants as shown in Table 4-3. CTC for dental porcelains were used in a second-degree polynomial form for solid CTC (α_g) and linear polynomial form for liquid CTC (α_l) as presented in Table 4-3.

The polynomials are given by,

$$\alpha_g(T) = a + bT + CT^2 \quad (4\text{-}1)$$

$$\alpha_l(T) = d + eT \quad (4\text{-}2)$$

Table 4-3: Thermal contraction coefficient constant of the dental ceramics used in this study

Material	a (1/°C) 10^{-6}	b $(1/°C)^2$ 10^{-9}	c $(1/°C)^3$ 10^{-12}	d (1/°C) 10^{-5}	e $(1/°C)^2$ 10^{-7}
3Y-TZP [11]	10.0660	1.2856	-0.6697	-	-
Vita VM9 [56]	8.0052	4.7623	-2.2062	-27.7820	5.0500
IPS Empress 2 [58]	10.7510	-24.2080	57.2670	-3.91180	1.1526

4.1.4 Viscoelastic Properties of Dental Porcelains

Few investigations experimentally determined the high-temperature relaxation properties of dental porcelains. Dehoff and Anusavice et al. [42,43,58,59] are the only reports determining the viscoelastic properties of dental porcelains. Hence, in this study, two dental porcelains (Vita VM9 and IPS Empress 2) were used for this analysis. The viscoelastic properties used in this study are listed in Table 4-4. It has been shown that viscoelastic relaxation function for dental porcelains can be characterized by four-term Prony series [42,43,58,59]. Accordingly, four-term Prony series data is used in this analysis from published literature.

Table 4-4: Viscoelastic properties at the high-temperature range for the veneering dental ceramics

Material	x	ΔH (kJ/mole)	T_{ref} (°C)	C_1 or g_1	C_2 or g_2	C_3 or g_3	C_4 or g_4	τ_1	τ_2	τ_3	τ_4
Vita VM9 / VMK68 [42]	0.27	379	700	0.9960	0.0030	0.0006	0.0004	1.316e-2	1.000e-1	5.000e-3	3.000e-3
IPS Empress 2 [58]	0.30	385	700	0.9833	0.0123	0.0012	0.0032	1.390e-3	9.030e-3	9.770e-3	8.820e-3
			600	0.9969	0.0014	0.0017	0.0000	0.18000	14.4000	22.0000	2269.00
			575	0.9721	0.0230	0.0045	0.0004	0.67000	11.0000	47.0000	548.000
			550	0.8548	0.1112	0.0298	0.0042	2.70000	17.1000	67.0000	323.000
			525	0.4745	0.4125	0.0077	0.1053	4.16000	31.5000	118.000	299.000

4.2 Geometry and Boundary Conditions

Rectangular geometry was used in this study [56]. For symmetry, a quarter of the sample (5 mm width x 5 mm depth x different thickness combinations as below) were simulated in this finite element model, as shown in Figure 4-2.

Thickness ratios used for this study:

- 3Y-TZP (0.7 mm) + veneering dental porcelain (1.5 mm) [56] – Used for validation and analysis.
- 3Y-TZP (0.5 mm) + veneering dental porcelain (0.7 mm) – Used for analysis. This thickness ratio is generally observed in clinical situations, and hence it was considered in this study for the required analysis.
- In addition to the above, higher dental porcelain thicknesses (i.e., 1.4 mm and 2.1 mm) on a 0.5 mm framework was used to analyze the effect of thickness.

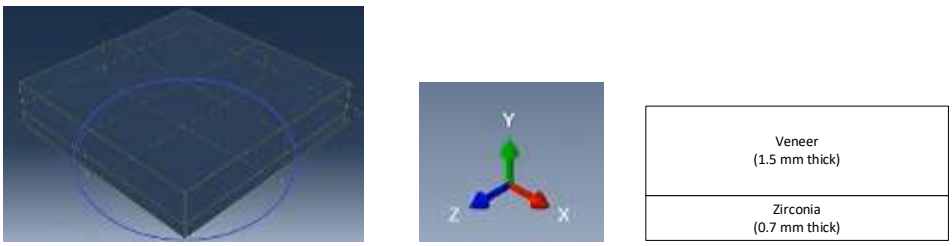

Figure 4-2: Symmetry of rectangular samples used in this finite element model

Mechanical Boundary Conditions:

Symmetry boundary conditions were applied for x- and z-symmetry, as shown in Figure 4-3. A node in y-direction restricted at intersection of x- and z-direction [56,238]. X-Symmetry BC (U_1=UR_2=UR_3=0), Z-Symmetry BC (U_3=UR_1=UR_2=0), Displacement in y (U_2=0).

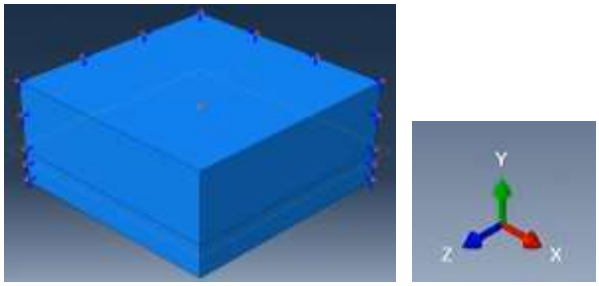

Figure 4-3: Mechanical boundary conditions

Temperature Boundary Condition:

The stress generated in the firing cycle of each layer of the veneer porcelain is not considered as a significant factor for the contraction of dental porcelain due to the heating of the subsequent firing process, which relieve the residual stress of the previous layer. The residual stress related to premature failure of veneering porcelain is associated to the residual thermal stresses generated in the last firing cycling (i.e. glazing heat treatment), especially during cooling of structure from soaking temperature. This specifies the importance of cooling conducted during last firing cycle.

The bilayer zirconia-based dental material temperature was assumed to be uniform at the beginning of computation (at a temperature at and above 700°C). Therefore, the predefined temperature of 700°C was applied at the beginning of the computation. This temperature was selected at the start of the simulation since it is above the glass transition temperature where dental porcelain is in a super-cooled / metastable state [56]. Temperature above 700°C is expected to creep the dental porcelain as it is nearing its melting temperature.

Heat Exchange Boundary Condition:

The dental material cooling was modeled using a convective heat transfer mechanism on the material's face. It was characterized by the heat transfer coefficient (h) and air (25°C sink) temperature. Thermal transfer coefficients were assumed to be constant during the cooling of dental materials. The effect of radiation was not taken in consideration in this simulation.

The convective heat transfer coefficient used are listed as follows [11,42,56]:

Cooling Rate	Convective heat transfer coefficient (h)
3°C/min	1.7E-6 W/mm^2 °C
30°C/min	1.7E-5 W/mm^2 °C
200°C/min	0.6E-4 W/mm^2 °C
300°C/min	1.7E-4 W/mm^2 °C
3000°C/min	1.7E-3 W/mm^2 °C

4.3 Abaqus Implementation – Free Strain

Commercial finite element software (Abaqus) was used to perform the numerical analysis. Abaqus standard / implicit method was used for the finite element modeling.

3Y-TZP framework was assumed to be a linear elastic material, and hence its properties were established through material definitions in Abaqus except for the coefficient of thermal contraction defined through UEXPAN subroutine as shown in Figure 4-4.

Abaqus material definitions were used to input the elastic and viscoelastic properties of dental porcelains. User material subroutines (UEXPAN and UTRS) were developed and used to input thermal strains and temperature dependence of the relaxation functions, respectively.

The following process was used to implement stress and structural relaxation:

Stress Relaxation:

Time dependence of the relaxation function was defined through Prony series parameters (n=4 terms) as defined in Table 4-4 using Abaqus input. Free strain is applied through UEXPAN subroutine by defining the strains as per equations 19 and 20. Temperature dependence of relaxation function was defined through the UTRS subroutine.

Structural Relaxation:

The structural strain component of free strain was applied through the UEXPAN subroutine by defining strains as per equations 19 and 20. The temperature dependence of the structural relaxation function was defined through the UTRS subroutine. UEXPAN subroutine defines the algorithm to calculate the fictive temperature, and its temperature

dependence was defined through the Shift function in the UTRS subroutine. Data on the structural relaxation times are not available for dental porcelains. Thus, structural relaxation times (ω) were considered $1/10^{th}$ of the shear relaxation times (τ) for this study's modeling purpose [56,58,264]. Refer appendix B for sensitivity analysis of stress with changes in structural relaxation times.

Relaxation functions in structural relaxation are both the actual temperature and the corresponding fictive temperature determined using the reduced time effect. Hence, the relaxation function's temperature dependence, in this case, is updated and returned through the user-defined UTRS subroutine.

UEXPAN subroutine flowchart is described in Figure 4-4.

Development of UEXPAN was performed diligently with continuous verification and validation of predictions with the Abaqus internal results. This type of internal verification and validation was used during the initial development of subroutines. The user-subroutine results were then appropriately matched with the results obtained through Abaqus internal analysis. Once the viscoelastic properties (structural relaxation) were introduced in the subroutine, the subroutine was validated through qualitative and quantitative means as discussed in Section 4.5.

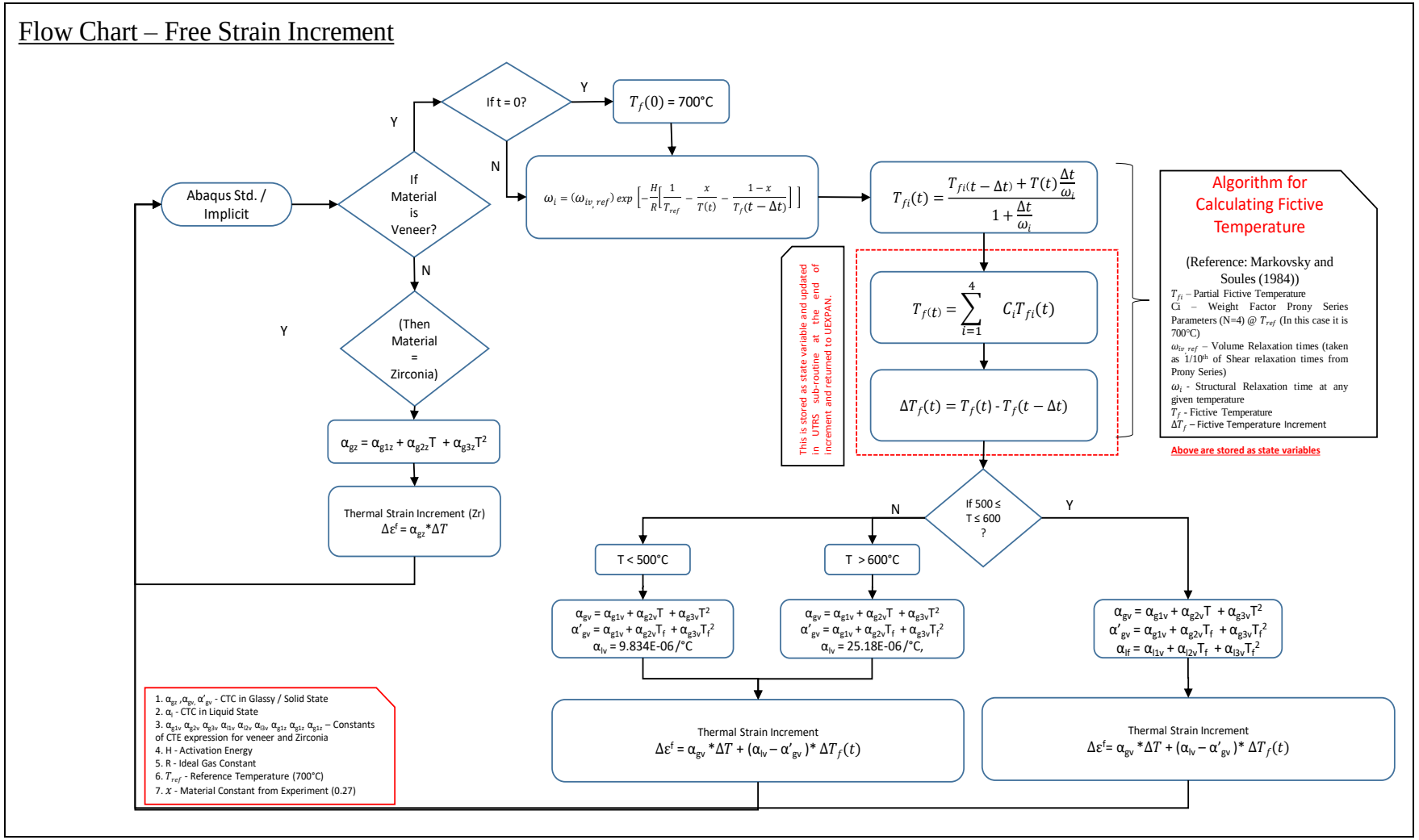

Figure 4-4: UEXPAN subroutine

4.4 Meshing

A fully coupled temperature-displacement type of analysis was used in this finite element model. In this method, mechanical and thermal solutions affect each other intensely. For that reason, they were obtained simultaneously. Stress analysis is mostly dependent on the temperature distribution. Therefore, a fully coupled temperature-displacement type was most suitable for this kind of analysis.

The fully coupled temperature-displacement analysis provides a provision to include the creep / viscoelastic behavior of the material. Strain tolerance was assumed to be 1E-05 due to the viscoelastic behavior. The interface between veneer and framework is assumed to be continuous connected with nodes.

Element Type:

In this analysis, the C3D8T element was used. It is a first-order continuum element with an 8-node trilinear displacement and temperature element (i.e., 8-node brick element). In addition, Abaqus default element controls were used.

Using first-order trilinear elements (2x2x2 integration points) instead of quadrilateral elements has allowed modeling the simulations with full integration and appropriate computation times. Using full integration has mitigated the risk of the hour-glass effect, which is prone while using elements with reduced integration. In this manner, risk of hour-glass effect was mitigated with the use of appropriate computation times.

These elements are prone to “locking” behavior, i.e., both shear and volumetric locking. Shear locking occurs in the elements when subjected to bending. Shear locking is also known as parasite-shear, where numerical calculations increase shear strains that do not exist. In such case, elements become too stiff in bending, especially when each element size is equal to the material thickness. Such locking is only evident in the mechanical bending problems. Thus, shear locking is not anticipated in the current study as the focus is on thermal stress analysis [265].

Volumetric locking occurs when the behavior of the material is almost considered incompressible. It results in developing the false pressure stresses at the integration points. In this situation, the element behaves too stiffly for any deformations preventing volume changes. Pressure stresses were verified at all integration points of elements, and it showed the same values of stresses at all 8-integration points without any signs of checkerboard patterns [265]. Thus, volumetric locking was not evident in this study.

Meshing and Sensitivity Analysis:

Mesh density was fixed based on a sensitivity analysis indicated in Figure 4-5 for convergence of the stress results in 2.2 mm thickness (0.7 mm 3Y-TZP + 1.5 mm Veneer). Acceptance criteria of 10% difference in the stress values were used to fix the mesh density. Total 78,500 elements (i.e., 0.1 mm thickness = 3636 elements) were used to achieve mesh density in this analysis.

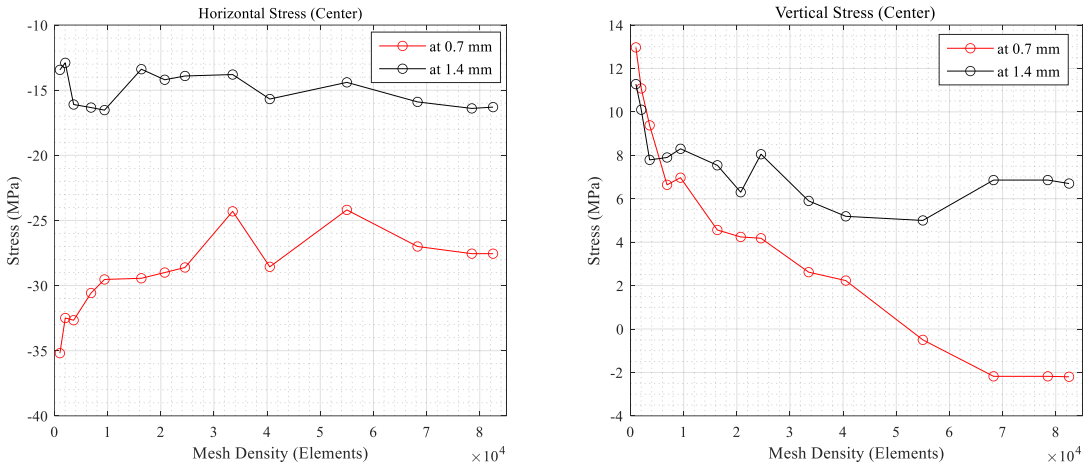

Figure 4-5: Sensitivity analysis for mesh density

4.5 Validation

This model consists of two user subroutine systems, UEXPAN and UTRS, where the input to calculate thermal stresses is computed through only one subroutine i.e. UEXPAN. This system of model is relatively simple and free from involvement of multiple sub-systems. This type of system demands a simpler validation since the model predictions are only

from one system. A good validation agreement, in such cases, represents strong confidence and acceptable quality of model for its intended use.

Despite of the fact above, a rigorous verification and validation multi-checks were performed. These checks cover aspects related to conception, mathematics, computational coding, simulation outcomes, acceptable agreements and demonstration of expected material behaviors.

The performed checks are described as follows:

4.5.1 Verification

As the subroutine was being developed from its conception and mathematical model, confidence was established through the collection of evidences that the mathematical model and solution algorithms were working correctly. This was performed to establish error free coding for thermal expansion behavior and the generated thermal stresses.

Verification was performed to verify accuracy of thermal stress calculations through UEXPAN for various combinations i.e. when property values are constant and when properties are function of temperature. At this stage, the results of user subroutine outcomes were verified with Abaqus internal analysis. Model predictions showed complete agreement with Abaqus internal results. This finding confirmed the accuracy of calculation of thermal strain using UEXPAN subroutine.

4.5.2 Quantitative validation with physical reality

The goal was to quantify acceptable confidence in the capability of the model, by comparison with experimental data. Upon completion of the coding, the predictive capability of the model with physical reality was validated. This assessment was made by comparing the predictive results of the model with previously determined validation experiments.

The finite element model was computed for validation purposes using the dental porcelain Vita VM9 [56]. Thickness combination of 0.7 mm 3Y-TZP + 1.5 mm dental porcelain was used and the cooling rate was 30°C/min. Properties of the materials were defined in the

previous material section. User subroutines were used to input thermal free strains. Experimental results from Kim et al. [56] were compared to the finite element prediction obtained in this study, as shown in Figure 4-6.

The variations of the traction $S22\ (\sigma yy)$ and $S11(\sigma xx)$ in the dental porcelain were compared to the experimental residual thermal stress through Vickers indentation [56]. The model predictions have exhibited excellent agreement with the experimental stress results.

These comparisons were satisfactory and the model was deemed validated for its intended use. In this way, the expected outcome of the model validation process has demonstrated a quantified level of agreement between experimental data and the model prediction, as well as the predictive accuracy of the model.

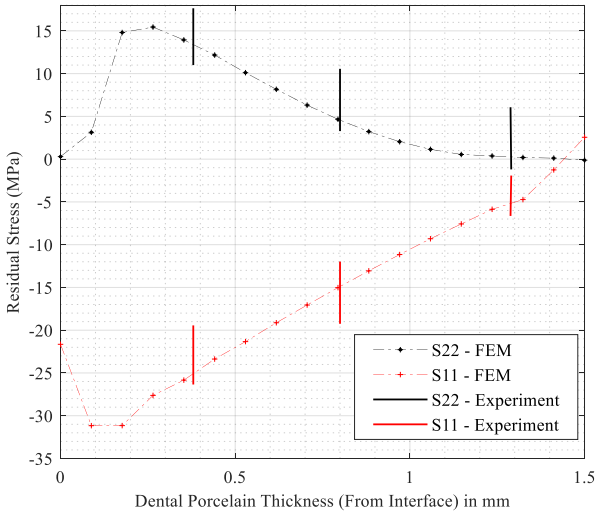

Figure 4-6: Validation with experimental results

4.5.3 Qualitative validation

Qualitative validations were conducted to ascertain acceptable predictive behavior of the model and confirm the absence of any illogical outcomes. It was performed by confirming the Thermo-Rheologically Simple (TRS) behavior of dental porcelain. Qualitative validation of the model was conducted where the predictions demonstrated the expected TRS material behavior at high temperature [58].

To validate the theoretical aspect of TRS behavior exhibited by dental porcelains, experimentally determined viscoelastic properties of IPS Empress2 (a dental veneering porcelain) at various reference temperatures were used in the current model. Properties of IPS Empress2 used for validation purpose are as listed in Table 4-2, Table 4-3, and Table 4-4 . In this finite element model, viscoelastic properties experimentally determined from four different reference temperatures were used for a specific cooling rate (30°C/min) and thickness combination (0.7 mm 3Y-TZP + 1.5 mm Veneer).

The fictive temperature evolution describing the structural state and corresponding stress evolution describing the mechanical state are presented in Figure 4-7 and Figure 4-8, respectively.

As shown in Figure 4-7, the evolution of fictive temperature within the glass transition range follows the same behavior for all four combinations of viscoelastic properties experimentally determined. This finding demonstrates that the structural state follows the same pattern for all combinations of viscoelastic properties and is a precise measure of the TRS behavior exhibited by dental porcelains. The corresponding stress evolution in the transition zone is indicated in Figure 4-8. The evolution of stress also followed the same pattern for all four combinations of viscoelastic properties.

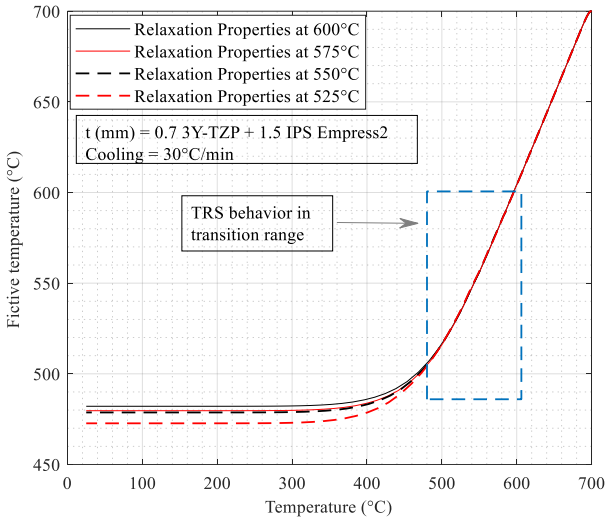

Figure 4-7: TRS behavior of IPS Empress2 for relaxation properties at various temperatures

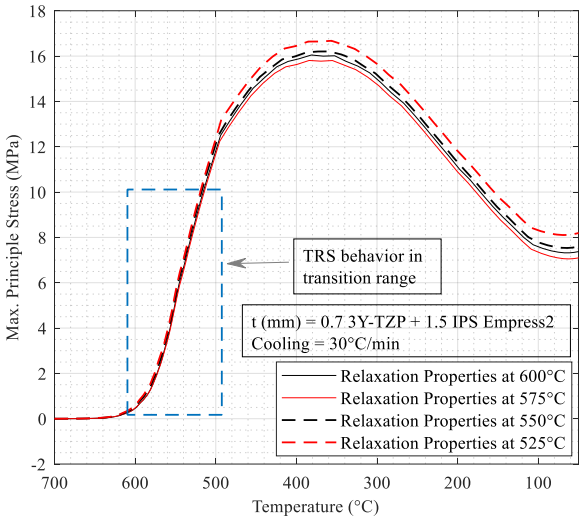

Figure 4-8: Stress evolution for IPS Empress2 exhibiting TRS behavior

The model predictions validated TRS behavior theory which was confirmed by previous investigation [58].

4.5.4 Sensitivity analysis

Sensitivity analysis is another means of achieving qualitative validation of computational models. A sensibility analysis was carried out by varying the mechanical and thermal properties of the dental porcelain Vita VM9 as shown in Figure 4-9. Characteristic parameters were modified +20%, +10%, -10%, and -20% from the values used in the quantitative validation model to evaluate its effect on residual thermal stresses. The tractions $S22 - \sigma yy\ (side\ face)$ and $S11 - \sigma xx\ (top, middle\ and\ side\ face)$ were measured for dental porcelains, as indicated in Figure 4-9.

In this current evaluation, the parameters of the five characteristic properties of veneers were changed to evaluate their effect on thermal stresses. The first three charateristic properties: Poisson's ratio, specific heat (c) and thermal conductivity (k) cause very insignificant changes in thermal stresses. The fourth property, Young's Modulus (E), have only a moderate effect on thermal stresses. However, the fifth property, coefficient of thermal contraction (CTC), significantly influenced thermal stresses. Thus, model validation of these five chracteristic properties did show the expected effect on the thermal stresses and they are also described in previous reports [50,56].

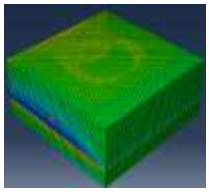

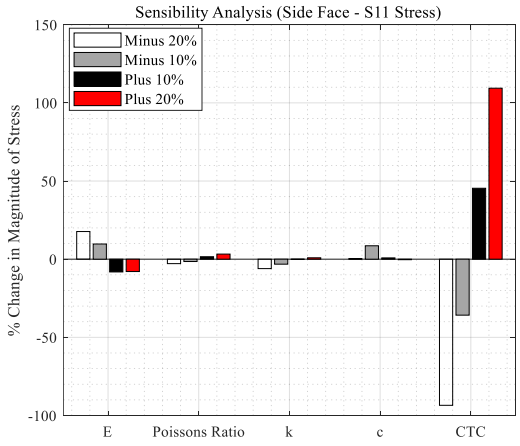

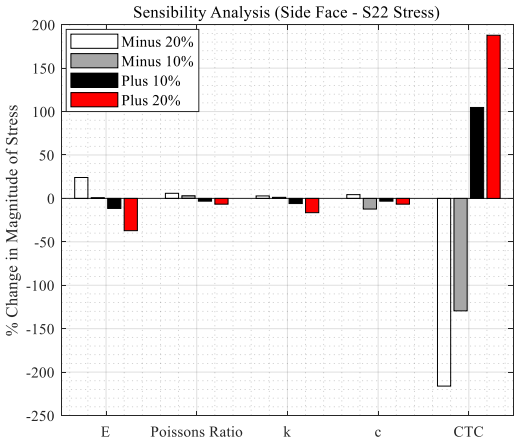

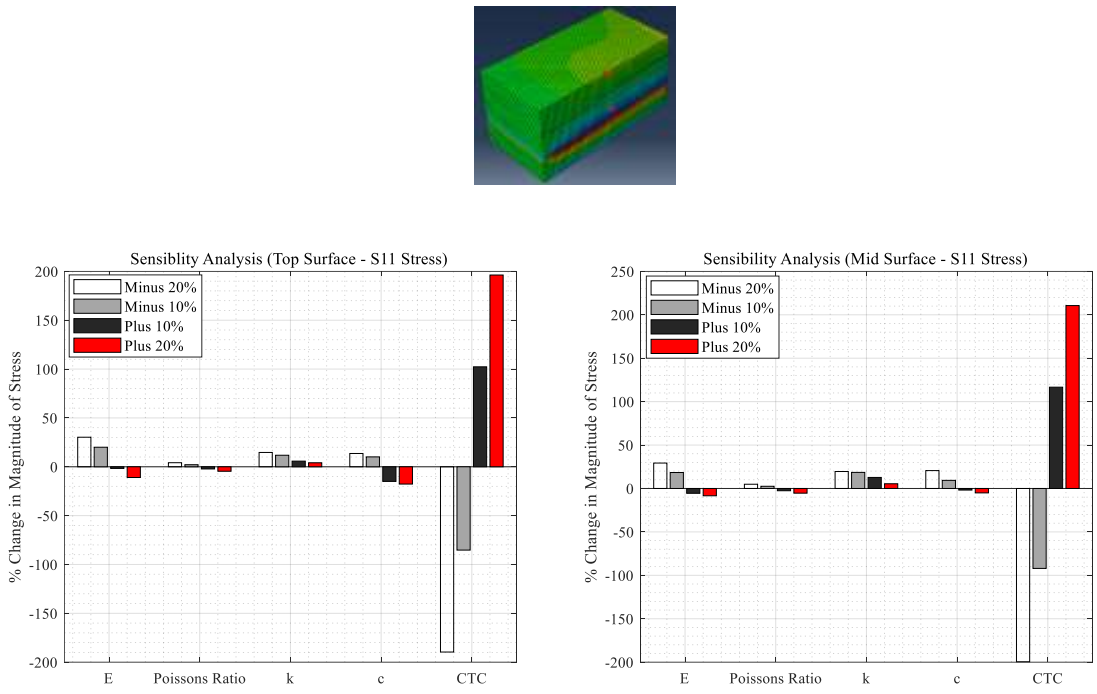

Figure 4-9: Sensibility analysis for residual thermal stress in dental porcelain

Structural relaxation plays a significant role in altering the evolution of CTC of dental material. The time-dependent response of volume change is based on the fictive temperature evolution affecting the structural state, significantly influencing thermal stress state in dental porcelain. This sensitivity analysis provides a strong foundation for the evaluating structural relaxation and its corresponding effect on residual thermal stresses in dental porcelains [55].

4.5.5 Exhibiting known behaviors

From glass literature, it is well known that the faster the rate of cooling, the more glass will deviate from structural equilibrium which is characterized through fictive temperatures [51]. This known behavior for various cooling rates was demonstrated through model predictions as presented in Figure 4-10.

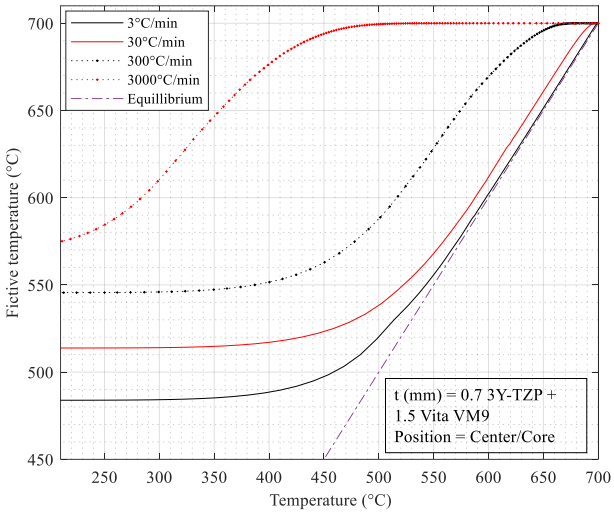

Figure 4-10: Fictive temperature evolution for different cooling rates

To summarize, the qualitative and quantitative validations demonstrated satisfactory confirmation of the desired expected material behavior. Hence, this model has demonstrated the expected behaviours of dental porcelains, since it is in line with known material behaviour. This model has adequately predicted related instances of the intended use and demonstrated excellent agreements with physical reality. Therefore, this model is validated to generate predictions for the intended use.

Chapter 5

5 Results and Discussions

As the subsurface tensile stresses are an important cause of clinical failures, significant consideration was given to the center core of dental porcelain in the evolution and evaluation of tensile stresses. It was further used to form a suitable explanation for the development of subsurface tensile stresses causing clinical failures of dental porcelains.

Fastest heat exchange is at the edge of dental porcelain and slowest cooling occurs within its center core. In order to evaluate effect of these extreme conditions from fastest and slowest cooling on structural relaxation, results are evaluated at integration point of surface edge and core of the dental porcelains.

Thermal stresses were expressed in terms of maximum principle stress (in MPa) and evaluated based on element integration points. Fictive temperatures (in °C) were evaluated as solution dependent variables also based on element integration points. Temperatures (in °C) were evaluated from nodal outputs.

5.1 Thermal Gradient

It was observed that with an increase in the cooling rate from 30°C/min to 300°C/min, the difference in the temperature between surface and center of material increases significantly, especially in the transition zone as presented in Figure 5-1. The highest temperature difference of more than 120°C was observed in the transition zone which indicates that viscoelastic region exhibits maximum thermal gradient [48].

Tensile stresses that facilitate premature failure of dental porcelains must be minimized, and this will only be possible after a better understanding of the evolution of such stresses [59]. Also, thermal gradients induced from varying cooling rates have significantly contributed to the evolution and nature of stresses in dental porcelains [35,45]. Hence, evaluating the effect of thermal gradient on structural relaxation, which is an integral part of the viscoelasticity of dental porcelains, shall establish a suitable reason for developing tensile stresses within dental porcelain.

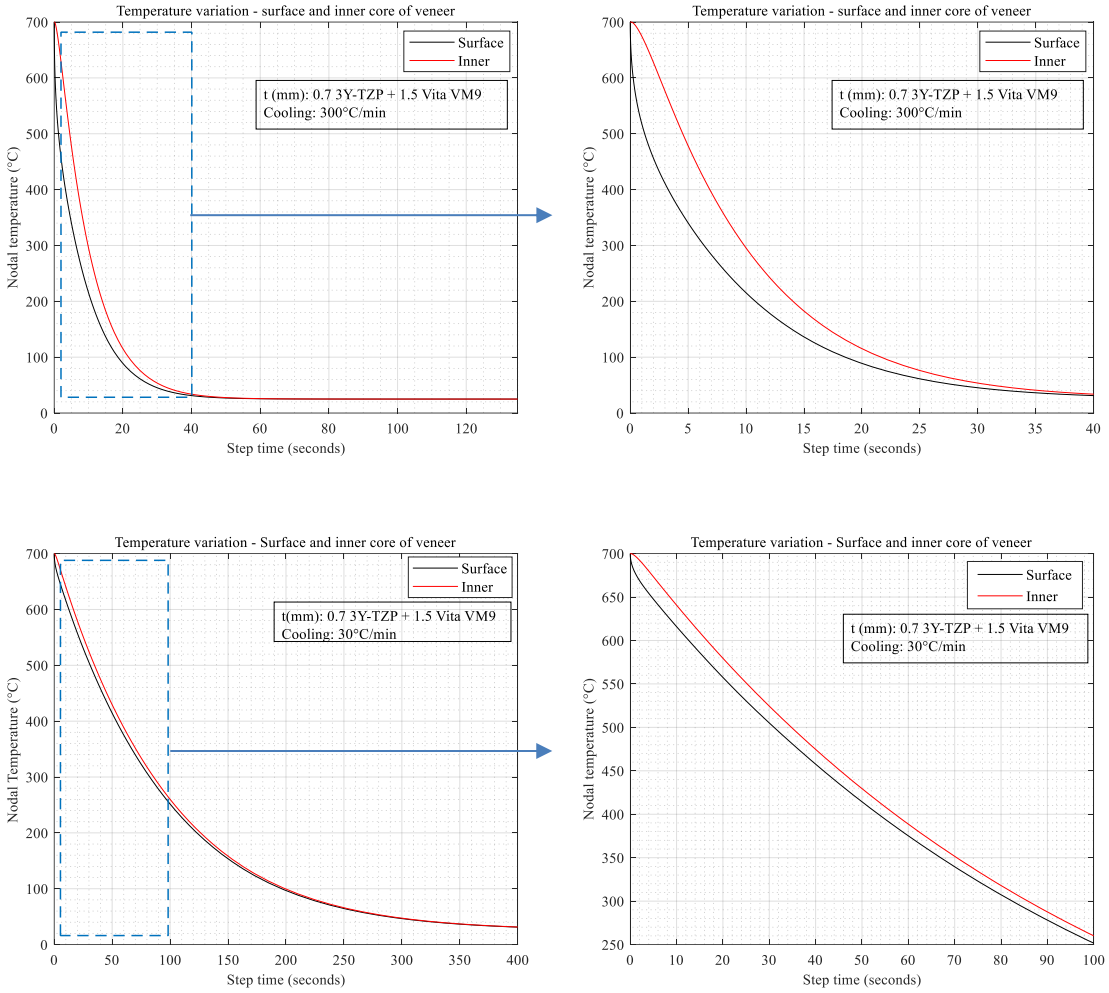

Figure 5-1: Temperature variation / gradient between the surface and inner core (center) of dental porcelain

5.2 Relaxation Models v/s Linear Model

The linear numerical model ignores viscoelastic relaxation of dental porcelains. The stress relaxation model ignores structural relaxation. The structural relaxation model includes the stress relaxation and time-dependent response of volumetric changes in the transition region of dental porcelains.

The difference on the results at a cooling rate of 30°C/min and 300°/min in these three model predictions are shown in Figure 5-2.

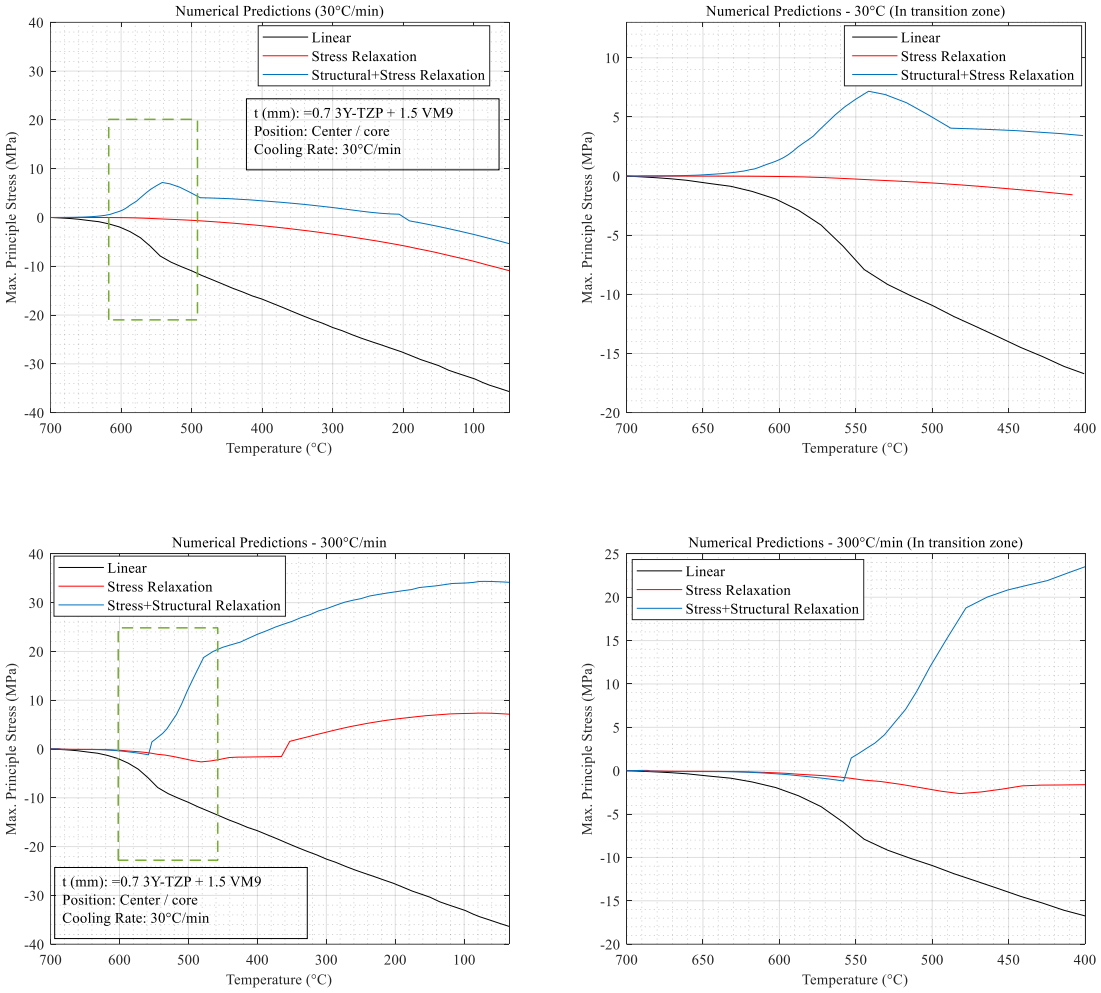

Figure 5-2: Maximum principle stress evolution (Relaxation and Linear models)

The resultant residual stress in the linear model was very high as it ignores the viscoelastic relaxation. The linear model evolution and magnitude were not altered due to change in cooling rate from 30°C/min to 300°C/min, indicating its insensitivity to cooling rate. Such model accounts purely on thermoplastic residual stresses, which has a higher magnitude due to only instantaneous volume changes.

The difference between stress and the structural relaxation is evident for higher cooling rates (300°C/min). The stress relaxation model has significantly lower residual thermal stresses around 8 MPa with the absolute absence of high temperature transient stresses. However, the structural numerical model has shown residual thermal stresses of magnitude

24 MPa with sudden transient stresses of more than 20 MPa in the high-temperature range of 500°C-550°C. The inclusion of structural relaxation in the numerical analysis includes the presence of transient stresses due to structural changes. The evaluation of transient stresses is equally significant as it can induce instantaneous dental porcelain failures upon heat treatments.

5.3 Structural State: Fictive temperature and stress state

The kinetics of the cooling cycle alter the state of glass equilibrium, as explained by Narayanaswamy et al. [52–54]. The cooling rate effect on fictive temperatures which represents structural relaxation is evident for different cooling rates, as presented in Figure 5-3. The ideal equilibrium situation is when the fictive temperature equals the actual temperature. Such equilibrium indicates that the internal time scale governing the structural rearrangements is equal to the solidification external time scale. In this situation, the instantaneous response of volume change is equal to its time-dependent response.

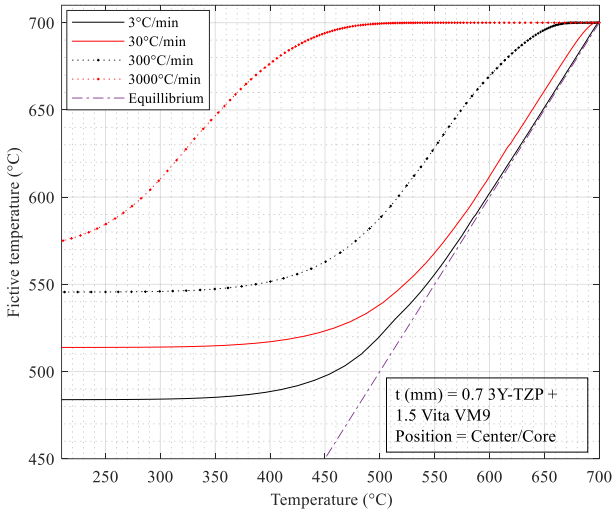

Figure 5-3: Fictive temperature evolution for different cooling rates

The slower cooling rate (e.g., 3°C/min) has shown better agreement with the equilibrium state in the transition zone. On the contrary, as the cooling rate increases, the structural state of dental porcelain deviates from its equilibrium state. In other words, for a hypothetical cooling rate of 3000°C/min, when dental porcelain is in the solid elastic range

(i.e. 450°C), the structural state of the material is at 700°C (i.e., supercooled liquid with higher interatomic distance). In this situation, the instantaneous volume change is exhibited by material resulting in higher thermal strains, whereas the time-dependent volume change response is wholly suppressed. The stress accounts in such cases are referred to as the thermoplastic stresses [55].

Resulting stress patterns from different cooling rates are indicated in Figure 5-4. In reference to higher cooling rates (e.g., 300°C/min and 3000°C/min), it is evident that no relaxation has taken place. Higher tensile residual thermal stresses for this case indicate the pure thermoplastic stress due to the supercooled liquid state locked in a solid-state. Higher thermal gradients in high cooling rates result in higher non-uniform, irreversible thermoplastic strains due to instantaneous volume changes. This mechanism explains the resulting higher thermal tensile stresses in the subsurface of dental porcelains for faster cooling rates.

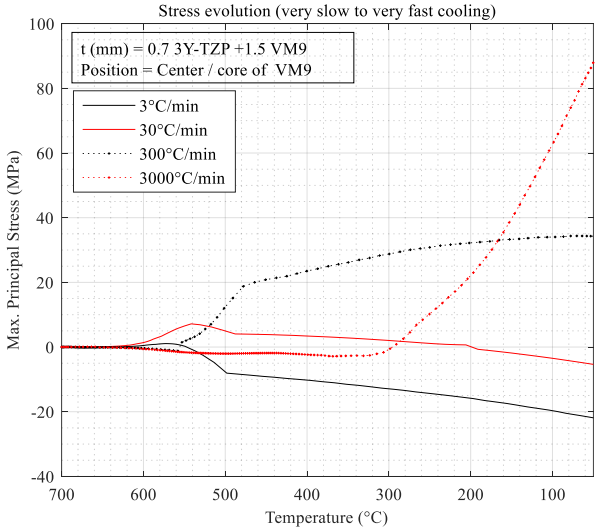

Figure 5-4: Maximum principle stress development in the center of dental porcelain for different cooling rates

On the contrary, slow cooling (e.g., 3°C/min and 30°C/min) induced by structural rearrangement has decreased the magnitude of overall volume change. This fact explains the compressive state of stress, which is possible in the presence of relaxation in the glass

transition zone. The resulting stresses in such cases are the combination of both thermoplastic and structural stresses [55].

Transient stresses of induced tensile nature during cooling may result in immediate cracking of dental porcelains or induce microcracks, resulting in the material premature failure. The maximum principle stresses for fast cooling are in the range of 40 MPa to 90 MPa, that significantly exceeds the tensile strength of dental porcelains. At room temperature, the tensile strength of dental porcelains is around 50-60 MPa; however, it drastically decreases at higher temperatures, increasing risks towards transient stresses. Consequently, the presence of any internal material flaws further drops the strength of the material.

The transient stresses and sudden change in their nature during heat treatment induce instantaneous microcracks within the material [9,11,35]. This process was explained [35] by an example of dilatant fluids such as starch in water and silly putty. These fluids flow without breaking at low strain rates. Nevertheless, they induce instantaneous brittle fracture at higher strain rates. This same concept can be applied in dental porcelains when they are in the viscoelastic region with a sudden appearance of transient stresses.

This kind of behavior for dental porcelains can only be best evaluated by understanding the evolution of transient stresses, especially in its viscoelastic regime (high thermal gradients), through an evaluation of structural relaxation.

5.4 Effect of cooling rates

The finite element predictions of the fictive temperature evolution on the surface edge and center core of dental porcelain and their corresponding stress states are shown in Figure 5-5. The cooling rate influences the structural state of the surface and inner (center/core). A lower cooling rate (e.g., 3°C/min), having a lower thermal gradient, has shown the overlap of fictive temperature at the surface and center of dental porcelains. This fact indicates equal structural relaxation in different regions of the material. Stress evolution demonstrates a similar structural relaxation pattern with an opposite magnitude to maintain

equilibrium. Compressive stresses are observed in the center with the compensating tensile stresses on the surface with almost equal magnitude.

As the cooling rate is increased (e.g., 30°C/min and 300°C/min), the difference between the relaxation is observed in the finite element predictions. Due to the lack of structural arrangement and no stress relaxation for higher cooling rates, transient and residual thermal stresses of tensile are introduced in the center of the dental porcelains.

It can be reasoned that the center portion of materials deals with an undesirable phenomenon such as,

- Deviation of fictive temperatures from equilibrium.
- Locking of supercooled liquid in the solid-state.
- High magnitude instantaneous volume to temperature change.
- Complete suppression of the time-dependent response of volume change.
- Absence of a relaxation mechanism in the transition zone.

Accordingly, transient and thermal tensile stresses at the center of material were induced. There are 2 significant risks based on the results of fast cooling, which are worthwhile to note:

a. Transient tensile stresses at the material surface that reverses its nature to compressive in seconds. Referring to the example of high strain rates, such transient stresses at the surface can induce instantaneous failure on the material surface during cooling itself.

b. Residual thermal stresses in the center region are tensile. In the presence of manufacturing defects, such tensile stresses facilitate microcracks initiation and then the immediate premature failure of dental porcelains.

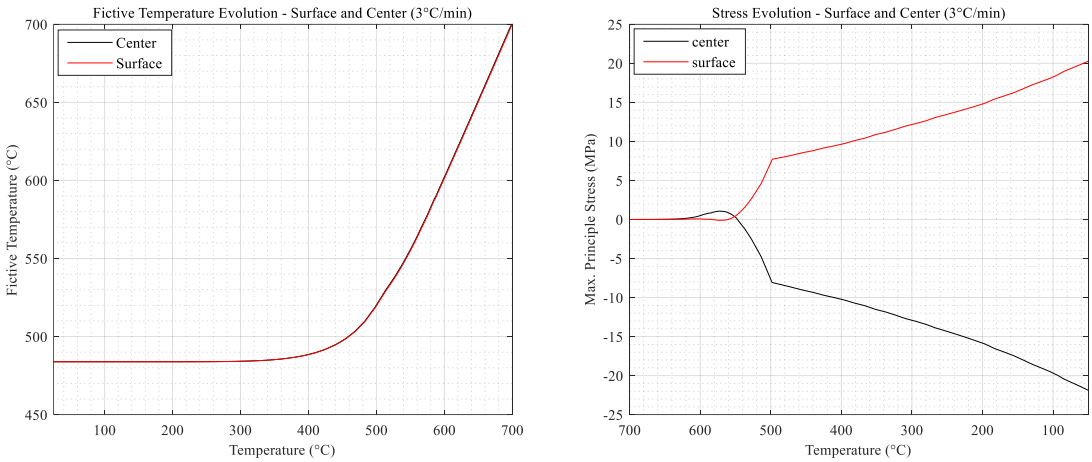

a) Fictive Temperature and Stress – 3°C/min

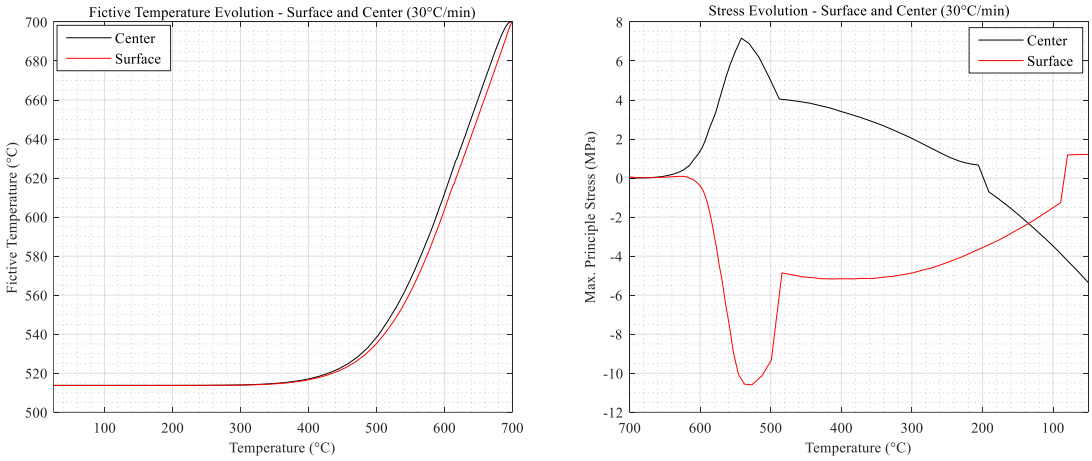

b) Fictive Temperature and Stress – 30°C/min

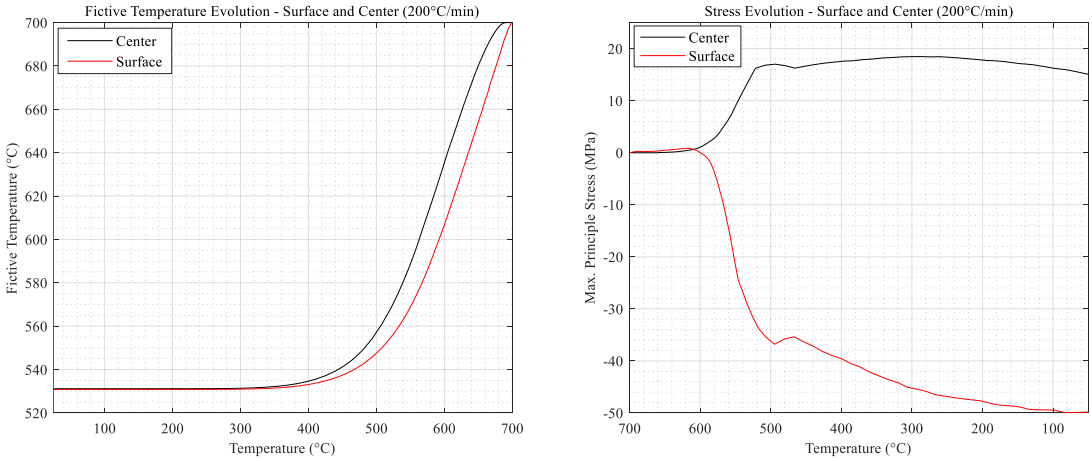

c) Fictive Temperature and Stress – 200°C/min

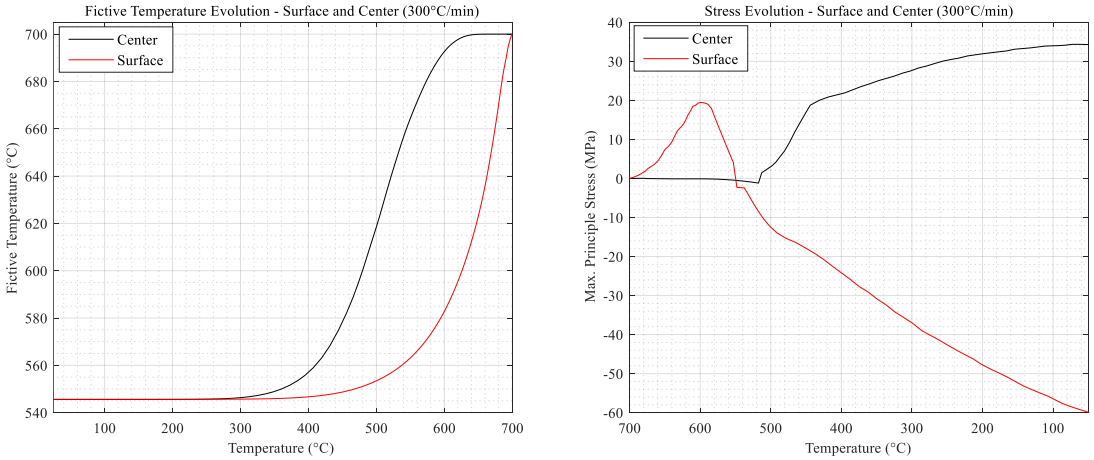

d) Fictive Temperature and Stress – 300°C/min

Figure 5-5: Fictive temperature and stress evolution for 4 cooling rates (Surface Edge and Center)

Surface compressive stresses induced from fast cooling may assist in resisting external load or defect introduction from external point contacts. However, transient stresses from fast cooling can induce instantaneous microcracks from surface to subsurface areas. Also, the presence of any volumetric defects, which is very likely to occur in any manufacturing activity, can facilitate instantaneous failure due to residual tensile stresses induced during fast cooling.

5.5 Effect of dental porcelain thickness

The effect of varying dental porcelain thickness on structural relaxation is exhibited in Figure 5-6. The cooling rate shows a consistent effect on fictive temperature in all cases, with the faster cooling rate having the highest deviation from the equilibrium structural state.

The high thickness of dental porcelain presents a hotter and more viscous area in the subsurface compared to the outer surface. Thus, it constricts the hot viscous-liquid content. Differential thermal contractions may produce transient stresses to generate microcracks or complete solid-state porcelain fractures due to ineffective relaxation. This is due to the poor thermal properties of 3Y-TZP and veneer [35].

The slower cooling rate (30°C/min) with a minimum thickness of dental porcelain (0.7 mm) has presented the greater relaxation than higher thicknesses. Thicknesses of 1.4 mm and 2.1 mm failed to undergo relaxation for 200°C/min cooling rate. On the other hand, a lower thickness of 0.7 mm exhibited relaxation with minimum stresses.

An increase in the veneer thickness certainly poses a risk of a lack of relaxation in subsurface locations, resulting in higher tensile stresses even for slow cooling rates. This risk becomes very specific and predominant with the increase in the faster cooling rate.

Higher veneer thickness subjected to faster cooling induces undesired tensile stresses. It suppresses effective structural relaxation and accounts for only thermoplastic stresses. Additionally, with an increase in the thickness of dental porcelains (e.g., 2.1 mm), the depth of tensile stresses is significantly higher, as shown in Figure 5-6 and Figure 5-7. Surprisinly, for slow cooling (30°C/min), the depth of tensile stress occupies more than 50% of the thickness. It is worst for high cooling rates (300°C/min) where, except for minor compressive stress on the surface, the entire thickness has tensile stresses. In such situations, instantaneous brittle fractures or premature failure of veneers may occur, which is accelerated in the presence of internal manufacturing defects.

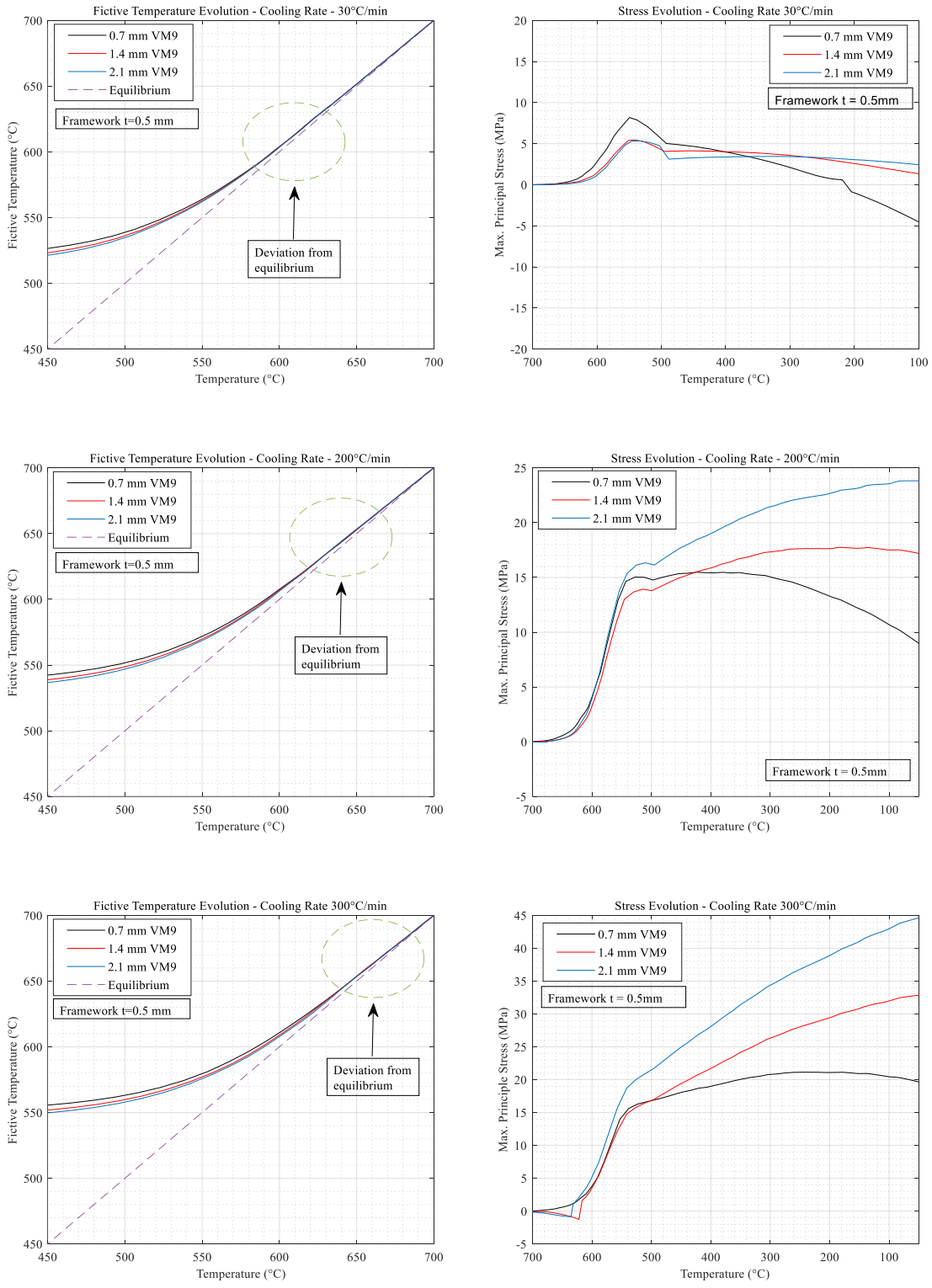

Figure 5-6: Different thickness of dental porcelains - cooling rate and stress states

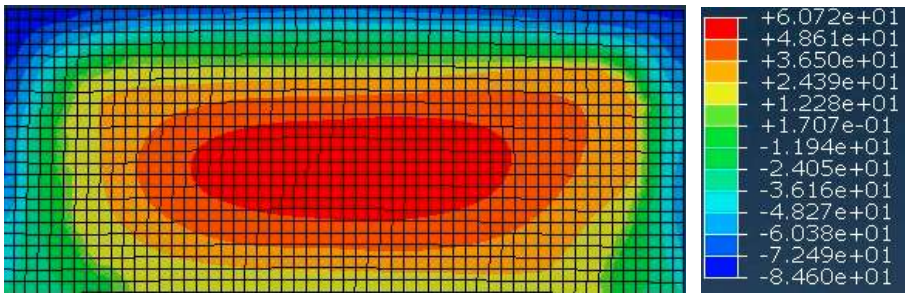

a) t = 2.1 mm VM9 (Cooling Rate 300°C/min)

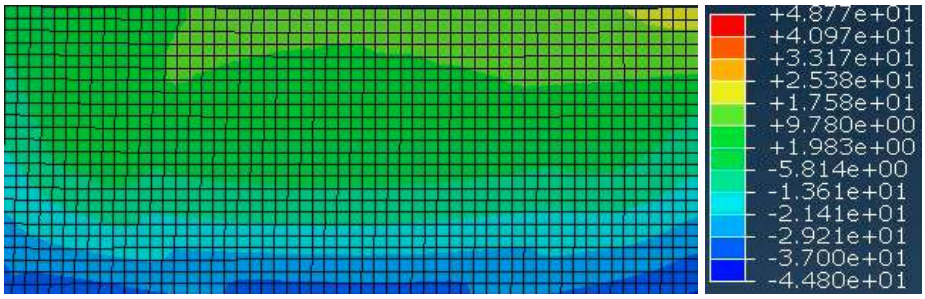

b) t = 2.1 mm VM9 (Cooling Rate 30°C/min)

Figure 5-7: High thickness of dental porcelain – Through thickness stress state (Max. Principle Stress in MPa) for 2 cooling rates

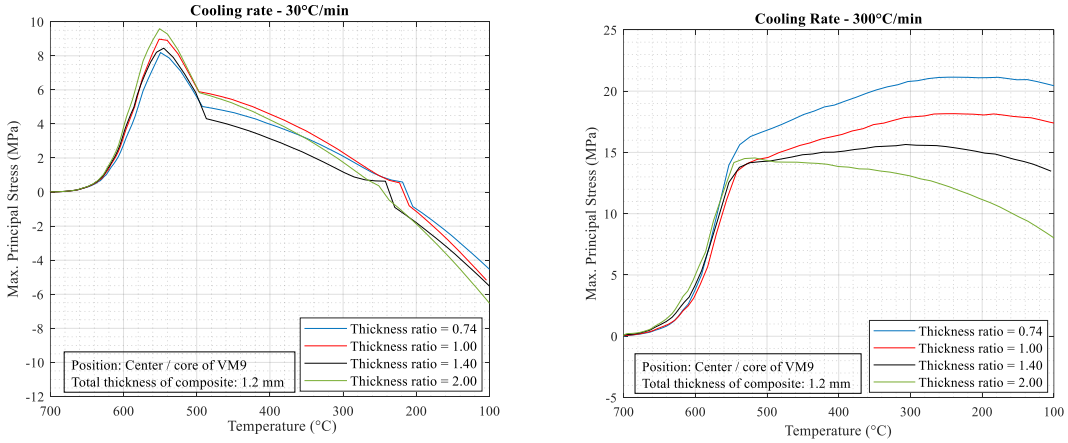

Figure 5-8: Comparison of four thickness ratios on resulting stress states in dental porcelain

Thickness ratio is the ratio of the thickness of the framework to that of the veneering dental porcelain. For a composite with total thickness of 1.2 mm, four different thickness ratios are evaluated for slow (30°C/min) and fast (300°C/min) cooling to demonstrate the

thickness ratio effect as shown in Figure 5-9. It is observed from this figure that as the thickness of veneer decreases, i.e., the thickness ratio increases, lower thermal stress will develop especially for the case of higher cooling rate. These results are in agreement with the observations in the literature [10,11,34,37,256].

5.6 Effect of instantaneous volume change (CTC)

The results of fictive temperature evolution and their stress states for two different dental porcelains (Vita VM9 and IPS Empress 2) are demonstrated in Figure 5-9. In the transition zone, the fictive temperature evolution of Vita VM9 and IPS Empress2 were very similar; but the relaxation patterns were not the same. IPS Empress2 exhibited an absence of relaxation in the transition zone with tensile thermal stresses. However, Vita VM9 indicated visible relaxation in the transition zone, leading to compressive stress in the center.

IPS Empress2 structural state evolution is in better agreement with structural equilibrium compared to Vita VM9. Furthermore, stress states are more desirable in VM9 in contrast to IPS Empress2, which presents a discrepancy in understanding structural relaxation and its effect on stresses.

The role of CTC can explain this discrepancy. The instantaneous CTC difference between a framework and dental porcelain ($\Delta\alpha=\alpha_{Zr}-\alpha_{Ve}$) plays a significant role in deciding the thermal compatibility of the system. Studies have reported that it is always desirable to maintain this difference positively for appropriate thermal compatibility. The CTC difference between Vita VM9 and IPS Empress2 for the glassy state (i.e., 25°C to 600°C) is shown in Figure 5-10. It is evident that Vita VM9 maintains the desired positive difference, and IPS Empress2 follows a highly negative difference.

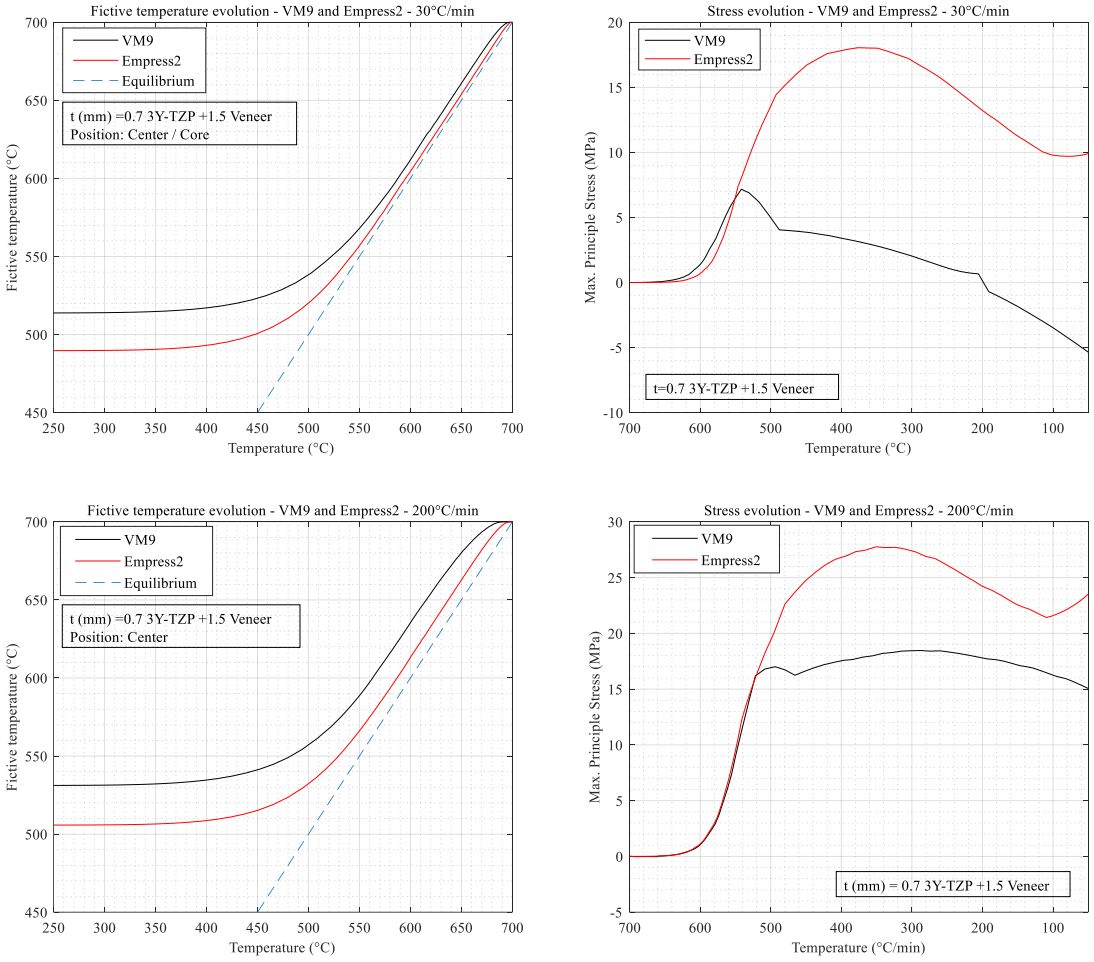

Figure 5-9: Fictive temperature and stress evolution to compare Vita VM9 and IPS Empress2

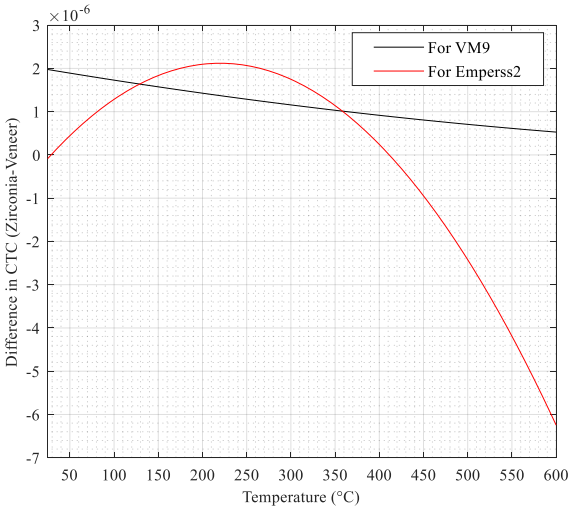

Figure 5-10: Instantaneous CTC difference for Vita VM9 and IPS Empress2

This signifies the importance of the instantaneous CTC values when selecting dental porcelains. Based on this understanding, the first step is to establish an acceptable CTC difference and then evaluate relaxation effect in transition zone for various heat treatments.

Chapter 6

6 Conclusion, Recommendation, and Future Scope

6.1 Conclusion

Subsurface thermal stresses of tensile nature must be minimized, and it is only possible with proper understanding of the origin of such stresses. This study has indicated that structural relaxation can effectively help to evaluate the stresses generated in veneering dental porcelain, especially at higher cooling rates.

The thermal gradient within the dental porcelain increases significantly when the cooling rate changes from 30°C/min to 300°C/min. An increase in the thermal gradient deviates the fictive temperature evolution from equilibrium, suppressing overall structural relaxation. As a result, the subsurface of the veneer is retained with undesired transient and residual thermal tensile stresses, capable of causing instantaneous cracking or subsurface residual tensile stresses. On the other hand, slow cooling has exhibited lower thermal gradients with desired compressive stresses in the subsurface region due to structural relaxation.

An increase in dental porcelain thickness has generated deleterious effects including slower cooling rates with undesired subsurface tensile stresses. Combining the higher thickness of veneers with faster cooling rates has presented a considerable increase in undesired subsurface tensile stress, sufficient to cause immediate failure. Low thickness of dental porcelains subjected to slow cooling rates have shown effective relaxation with more desired subsurface stresses.

In this way, the present work emphasizes and evaluates the thermal gradient effect on structural relaxations in porcelain veneers. This approach can be used to tailor the desired stress state to extend the longevity of dental porcelains veneered on 3Y-TZP frameworks. As a way forward, this study can be enhanced with further analysis performed on clinical crown forms.

Thus, this research was performed in depth of the science behind the structural relaxation in dental porcelain at high temperature to understand and identify root cause of undesired subsurface thermal stresses with overall aim of improving its integrity. This work, emphasizing structural relaxation for the first time in dental porcelain, provides an objective way forward for effective designing of dental restorations through development of appropriate heat treatment procedures and tailoring desired stress states.

The evidence-based critical literature review has shown that more efforts are required to standardize dental laboratory procedures, facilitating effective measures.

6.2 Limitations

Following limitations are identified for this study:

- Dental structures are usually crown shaped. However in this analysis, a rectangular structure was used. As per literature reviews, there is no consensus achieved so far on geometrical shapes of structures having an effect on stress states. Certain studies suggest that shape affects the stress states, while another study had shown no effect on stress states. However, this assumption is addressed as a future scope of work in section 6.3 of the thesis.

- Effect of radiation is not accounted in the finite element model. Only convective heat transfer mechanism is accounted to simulate the cooling rates. Data on radiation effects is not available in dental material literature.

- Phase transformation in dental porcelains were not addressed in research. Dental porcelains, such as Vita VM9, are feldspathic leucite-based porcelains containing leucite as crystalline phases to provide strength and suitable coefficient of thermal expansion behavior. Leucite transformation is more effective at higher temperature (e.g. 900-1000°C), however at lower temperatures such as in current research simulations at 700°C, the phase transformation may occur but at a lesser extent. This research has limitation of not addressing effect of phase transformation on structural relaxation and evolution of thermal stresses.

The process of phase transformation inclusion in numerical models requires extensive experimentation and development of subroutines which presents a critical challenge. However, it presents a tremendous scope of improvement to study various heat treatment protocols and devise measures to tailor the desired stresses in the dental porcelains.

To minimize the extent and magnitude of consequence of uncertainties in the model, extensive qualitative and quantitative validations of the model were performed. Quantitative validation of the model showed excellent agreement with physical reality. Qualitative validation showed expected material behavior ruling out any illogical outcomes of the model. In this way, confidence was gained to use the model for required analysis as presented within the scope of the thesis. Considering the current scope of thesis, current model provides a good conceptual understanding on the structural relaxation in dental porcelain and also shows its significance on subsurface thermal stresses.

The limitation in this study requires combination of extensive experimentation and numerical analysis in actual dental crown form which is then expected to bring a model to better physical reality with minimum uncertainties.

6.3 Recommendations

The primary cause for premature clinical failures of dental porcelains is associated with the defect initiation within the porcelain subsurface. It occurs primarily due to a combination of two main parameters – internal defects from manufacturing and the presence of residual tensile stresses in the subsurface:

a. Manufacturing Defects: They are induced due to the manufacturing process followed from raw materials until final dental laboratory preparation. Few examples include - the quality of materials, process parameters, surface treatment, and product realization.

Elimination of manufacturing defects is not entirely possible but can be minimized through process control. It can be controlled through appropriate manufacturing procedures.

b. Transient and Residual Thermal Stresses: Induced during the final glazing heat treatment through which dental materials are treated in the dental laboratories.

As seen in the present work, thermal gradients have to be adjusted to support adequate relaxation within dental porcelains to induce compressive stresses with minimum transient stresses. Based on these results, caution shall be exercised as structural relaxation is a factor that shall be considered only for dental porcelains with a positive CTC difference between 3Y-TZP and dental porcelains for the complete glassy stage. It is shown in Figure 5-9 when comparing Vita VM9 and IPS Empress2 that the later fictive temperature evolution is in better equilibrium than Vita VM9. Nevertheless, IPS Empress2 failed to induce compressive stresses in the subsurface region, mainly due to negative CTC difference, as exhibited in Figure 5-10.

Additionally, geometry serves as a critical factor in controlling the stress state, as discussed in the literature review.

The following pathway is recommended to tailor the desired stress state for veneered Y-TZP dental structures.

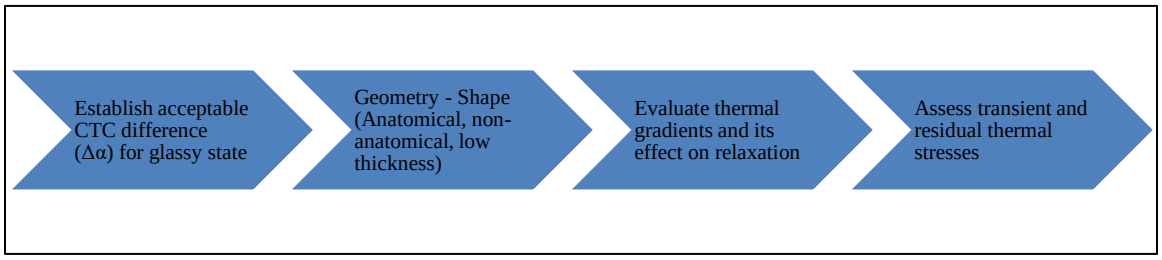

6.4 Future Scope

Present work presents the following opportunities from a design perspective which may yield to achieve an optimum solution for the unresolved issue of premature failure of veneered Y-TZP dental restorations:

Viscoelastic Properties:

Viscoelastic properties of a few dental porcelains are determined experimentally. Determining such properties for commercially available dental porcelains and using them

in the finite element model can provide insight into the development of new sustainable materials. Experiments are required to evaluate effect of structural relaxations on properties of dental porcelains. This will provide an effective understanding on structural relaxation in dental porcelains.

Crown shaped dental structures:

Dental structures are usually crown shaped. Further analysis by combination of experimental and finite element analysis using crown shaped specimen may facilitate in evaluating further progress in structural relaxation in dental porcelains.

Edge Chipping Experiments:

Edge chipping tests with quantification of internal volumetric defects may facilitate the use of that data to define a more accurate finite element model and evaluate their behavior with internal flaws.

Cooling Rates:

By evaluating various heat treatment protocols and their thermal gradient effects on the relaxation phenomenon.

Phase transformation in leucite-based feldspathic dental porcelains:

Leucite is the crystalline phase that is induced in feldspathic porcelain to improve its strength and mechanical properties. Such phase transformations can be defined in the finite element model to analyze its effects on the structural and stress relaxation, and its effect on the stress states.

Bibliography

[1] S.C. Bayne, J.L. Ferracane, G.W. Marshall, S.J. Marshall, R. van Noort, The Evolution of Dental Materials over the Past Century: Silver and Gold to Tooth Color and Beyond, J. Dent. Res. (2019). https://doi.org/10.1177/0022034518822808.

[2] D. Duraccio, F. Mussano, M.G. Faga, Biomaterials for dental implants: current and future trends, J. Mater. Sci. (2015). https://doi.org/10.1007/s10853-015-9056-3.

[3] C.J. Goodacre, G. Bernal, K. Rungcharassaeng, J.Y.K. Kan, Clinical complications in fixed prosthodontics, J. Prosthet. Dent. (2003). https://doi.org/10.1016/S0022-3913(03)00214-2.

[4] A. Della Bona, J.R. Kelly, The clinical success of all-ceramic restorations, J. Am. Dent. Assoc. (2008). https://doi.org/10.14219/jada.archive.2008.0361.

[5] R.P. Christensen, B.J. Ploeger, A clinical comparison of zirconia, metal and alumina fixed-prosthesis frameworks veneered with layered or pressed ceramic: A three-year report, J. Am. Dent. Assoc. (2010). https://doi.org/10.14219/jada.archive.2010.0076.

[6] S.P. Passos, B. Linke, P.W. Major, J.A. Nychka, Improving the compatibility of an Y-TZP/porcelain system using a new composite interlayer composition, J. Mech. Behav. Biomed. Mater. (2017). https://doi.org/10.1016/j.jmbbm.2016.07.032.

[7] J.B. Quinn, G.D. Quinn, V. Sundar, Fracture toughness of veneering ceramics for fused to metal (PFM) and zirconia dental restorative materials, J. Res. Natl. Inst. Stand. Technol. (2010). https://doi.org/10.6028/jres.115.024.

[8] F. Komine, J.R. Strub, H. Matsumura, Bonding between layering materials and zirconia frameworks, Jpn. Dent. Sci. Rev. (2012). https://doi.org/10.1016/j.jdsr.2012.06.001.

[9] M. V. Swain, Unstable cracking (chipping) of veneering porcelain on all-ceramic dental crowns and fixed partial dentures, Acta Biomater. (2009). https://doi.org/10.1016/j.actbio.2008.12.016.

[10] P. Benetti, F. Pelogia, L.F. Valandro, M.A. Bottino, A. Della Bona, The effect of porcelain thickness and surface liner application on the fracture behavior of a ceramic system, Dent. Mater. (2011). https://doi.org/10.1016/j.dental.2011.05.009.

[11] S. Dhital, C. Rodrigues, Y. Zhang, J. Kim, Viscoelastic finite element evaluation of transient and residual stresses in dental crowns: Design parametric study, J. Mech. Behav. Biomed. Mater. (2020). https://doi.org/10.1016/j.jmbbm.2019.103545.

[12] J. Fischer, B. Stawarczyk, M. Tomic, J.R. Strub, C.H.F. Hämmerle, Effect of thermal misfit between different veneering ceramics and zirconia frameworks on in vitro fracture load of single crowns, Dent. Mater. J. (2007). https://doi.org/10.4012/dmj.26.766.

[13] M.J. Tholey, M. V. Swain, N. Thiel, SEM observations of porcelain Y-TZP interface, Dent. Mater. (2009). https://doi.org/10.1016/j.dental.2009.01.006.

[14] P. Benetti, A. Della Bona, J.R. Kelly, Evaluation of thermal compatibility between core and veneer dental ceramics using shear bond strength test and contact angle measurement, Dent. Mater. (2010). https://doi.org/10.1016/j.dental.2010.03.019.

[15] M.N. Aboushelib, C.J. Kleverlaan, A.J. Feilzer, Microtensile bond strength of different components of core veneered all-ceramic restorations. Part 3: Double veneer technique, J. Prosthodont. (2008). https://doi.org/10.1111/j.1532-

849X.2007.00244.x.
[16] M.N. Aboushelib, M. De Kler, J.M. Van Der Zel, A.J. Feilzer, Microtensile bond strength and impact energy of fracture of CAD-veneered zirconia restorations, J. Prosthodont. (2009). https://doi.org/10.1111/j.1532-849X.2008.00412.x.
[17] A. Saito, F. Komine, M.B. Blatz, H. Matsumura, A comparison of bond strength of layered veneering porcelains to zirconia and metal, J. Prosthet. Dent. (2010). https://doi.org/10.1016/S0022-3913(10)60133-3.
[18] P.C. Guess, A. Kuliš, S. Witkowski, M. Wolkewitz, Y. Zhang, J.R. Strub, Shear bond strengths between different zirconia cores and veneering ceramics and their susceptibility to thermocycling, Dent. Mater. (2008). https://doi.org/10.1016/j.dental.2008.03.028.
[19] F.C. Lorenzoni, L.M. Martins, N.R.F.A. Silva, P.G. Coelho, P.C. Guess, E.A. Bonfante, V.P. Thompson, G. Bonfante, Fatigue life and failure modes of crowns systems with a modified framework design, J. Dent. (2010). https://doi.org/10.1016/j.jdent.2010.04.011.
[20] P.H. Corazza, S.A. Feitosa, A.L.S. Borges, A. Della Bona, Influence of convergence angle of tooth preparation on the fracture resistance of Y-TZP-based all-ceramic restorations, Dent. Mater. (2013). https://doi.org/10.1016/j.dental.2012.12.007.
[21] D. Fabris, J.C.M. Souza, F.S. Silva, M. Fredel, M. Gasik, B. Henriques, Influence of specimens' geometry and materials on the thermal stresses in dental restorative materials during thermal cycling, J. Dent. (2018). https://doi.org/10.1016/j.jdent.2017.08.017.
[22] P. Benetti, J.R. Kelly, A. Della Bona, Analysis of thermal distributions in veneered zirconia and metal restorations during firing, Dent. Mater. (2013). https://doi.org/10.1016/j.dental.2013.08.212.
[23] J.P. Tan, D. Sederstrom, J.R. Polansky, E.A. McLaren, S.N. White, The use of slow heating and slow cooling regimens to strengthen porcelain fused to zirconia, J. Prosthet. Dent. (2012). https://doi.org/10.1016/S0022-3913(12)60050-X.
[24] M.T. Marefati, A.M. Hadian, T. Hooshmand, B.E. Yekta, R. Koohkan, Wettability of zirconia by feldspathic veneer in dental restorations: Effect of firing atmosphere and surface roughness, Ceram. Int. (2018). https://doi.org/10.1016/j.ceramint.2017.12.020.
[25] V.G. Paula, F.C. Lorenzoni, E.A. Bonfante, N.R.F.A. Silva, V.P. Thompson, G. Bonfante, Slow cooling protocol improves fatigue life of zirconia crowns, Dent. Mater. (2015). https://doi.org/10.1016/j.dental.2014.10.005.
[26] S. Rues, E. Kröger, D. Müller, M. Schmitter, Effect of firing protocols on cohesive failure of all-ceramic crowns, J. Dent. (2010). https://doi.org/10.1016/j.jdent.2010.08.014.
[27] S. Zeighami, H. Mahgoli, F. Farid, A. Azari, The effect of multiple firings on microtensile bond strength of core-veneer zirconia-based all-ceramic restorations, J. Prosthodont. (2013). https://doi.org/10.1111/j.1532-849X.2012.00889.x.
[28] X. Tang, T. Nakamura, H. Usami, K. Wakabayashi, H. Yatani, Effects of multiple firings on the mechanical properties and microstructure of veneering ceramics for zirconia frameworks, J. Dent. (2012). https://doi.org/10.1016/j.jdent.2012.01.014.
[29] K. Wattanasirmkit, V. Srimaneepong, K. Kanchanatawewat, N. Monmaturapoj, P. Thunyakitpisal, S. Jinawath, Improving shear bond strength between feldspathic

porcelain and zirconia substructure with lithium disilicate glass-ceramic liner, Dent. Mater. J. (2015). https://doi.org/10.4012/dmj.2014-319.

[30] B. Śmielak, L. Klimek, R. Wojciechowski, M. Bąkała, Effect of zirconia surface treatment on its wettability by liquid ceramics, J. Prosthet. Dent. (2019). https://doi.org/10.1016/j.prosdent.2019.06.021.

[31] G. Göstemeyer, M. Jendras, L. Borchers, F.W. Bach, M. Stiesch, P. Kohorst, Effect of thermal expansion mismatch on the Y-TZP/veneer interfacial adhesion determined by strain energy release rate, J. Prosthodont. Res. (2012). https://doi.org/10.1016/j.jpor.2011.09.002.

[32] Z. Zhang, S. Zhou, Q. Li, W. Li, M. V. Swain, Sensitivity analysis of bi-layered ceramic dental restorations, Dent. Mater. (2012). https://doi.org/10.1016/j.dental.2011.11.012.

[33] C.B. Tanaka, R.Y. Ballester, G.M. De Souza, Y. Zhang, J.B.C. Meira, Influence of residual thermal stresses on the edge chipping resistance of PFM and veneered zirconia structures: Experimental and FEA study, Dent. Mater. (2019). https://doi.org/10.1016/j.dental.2018.11.034.

[34] V.M.G. de Figueiredo, S.M.B. Pereira, E. Bressiani, M.C. Valera, M.A. Bottino, Y. Zhang, R.M. de Melo, Effects of porcelain thickness on the flexural strength and crack propagation in a bilayered zirconia system, J. Appl. Oral Sci. (2017). https://doi.org/10.1590/1678-7757-2015-0479.

[35] P. Benetti, J.R. Kelly, M. Sanchez, A. Della Bona, Influence of thermal gradients on stress state of veneered restorations, Dent. Mater. (2014). https://doi.org/10.1016/j.dental.2014.02.020.

[36] L. Hallmann, P. Ulmer, S. Wille, M. Kern, Effect of differences in coefficient of thermal expansion of veneer and Y-TZP ceramics on interface phase transformation, J. Prosthet. Dent. (2014). https://doi.org/10.1016/j.prosdent.2013.11.009.

[37] Z. Zhang, M. Guazzato, T. Sornsuwan, S.S. Scherrer, C. Rungsiyakull, W. Li, M. V. Swain, Q. Li, Thermally induced fracture for core-veneered dental ceramic structures, Acta Biomater. (2013). https://doi.org/10.1016/j.actbio.2013.05.009.

[38] R. Belli, R. Frankenberger, A. Appelt, J. Schmitt, L.N. Baratieri, P. Greil, U. Lohbauer, Thermal-induced residual stresses affect the lifetime of zirconia-veneer crowns, in: Dent. Mater., 2013. https://doi.org/10.1016/j.dental.2012.11.015.

[39] A.K. Mainjot, G.S. Schajer, A.J. Vanheusden, M.J. Sadoun, Residual stress measurement in veneering ceramic by hole-drilling, Dent. Mater. (2011). https://doi.org/10.1016/j.dental.2010.12.002.

[40] G. Göstemeyer, M. Jendras, M.P. Dittmer, F.W. Bach, M. Stiesch, P. Kohorst, Influence of cooling rate on zirconia/veneer interfacial adhesion, Acta Biomater. (2010). https://doi.org/10.1016/j.actbio.2010.06.026.

[41] D. Longhini, C.O. de M. Rocha, I.S. Medeiros, R.G. Fonseca, G.L. Adabo, Effect of glaze cooling rate on mechanical properties of conventional and pressed porcelain on zirconia, Braz. Dent. J. (2016). https://doi.org/10.1590/0103-6440201600709.

[42] P.H. DeHoff, A.A. Barrett, R.B. Lee, K.J. Anusavice, Thermal compatibility of dental ceramic systems using cylindrical and spherical geometries, Dent. Mater. (2008). https://doi.org/10.1016/j.dental.2007.08.008.

[43] P.H. DeHoff, K.J. Anusavice, Creep functions of dental ceramics measured in a beam-bending viscometer, Dent. Mater. (2004). https://doi.org/10.1016/S0109-

5641(03)00107-6.
[44] J. Fischer, B. Stawarzcyk, A. Trottmann, C.H.F. Hämmerle, Impact of thermal misfit on shear strength of veneering ceramic/zirconia composites, Dent. Mater. (2009). https://doi.org/10.1016/j.dental.2008.09.003.
[45] B. Taskonak, G.A. Borges, J.J. Mecholsky, K.J. Anusavice, B.K. Moore, J. Yan, The effects of viscoelastic parameters on residual stress development in a zirconia/glass bilayer dental ceramic, Dent. Mater. (2008). https://doi.org/10.1016/j.dental.2008.01.004.
[46] P.J. Steiner, J.R. Kelly, A.A. Giuseppetti, Compatibility of Ceramic-Ceramic Systems for Fixed Prosthodontics, Int. J. Prosthodont. (1997).
[47] B.O. Mysen, P. Richet, Silicate Glasses and Melts: Properties and Structure, Elsevier Sci. (2005).
[48] C.T. Moynihan, A.J. Easteal, J. Wilder, J. Tucker, Dependence of the glass transition temperature on heating and cooling rate, J. Phys. Chem. (1974). https://doi.org/10.1021/j100619a008.
[49] B. Ananthasayanam, P.F. Joseph, D. Joshi, S. Gaylord, L. Petit, V.Y. Blouin, K.C. Richardson, D.L. Cler, M. Stairiker, M. Tardiff, Final shape of precision molded optics: Part I - Computational approach, material definitions and the effect of lens shape, J. Therm. Stress. (2012). https://doi.org/10.1080/01495739.2012.674830.
[50] Laurent Daudeville, Helene Carre, THERMAL TEMPERING SIMULATION OF GLASS PLATES: INNER AND EDGE RESIDUAL STRESSES, J. Therm. Stress. (1997).
[51] J.C. Mauro, R.J. Loucks, P.K. Gupta, Fictive temperature and the glassy state, J. Am. Ceram. Soc. (2009). https://doi.org/10.1111/j.1551-2916.2008.02851.x.
[52] O.S. NARAYANASWAMY, Stress and Structural Relaxation in Tempering Glass, J. Am. Ceram. Soc. (1978). https://doi.org/10.1111/j.1151-2916.1978.tb09259.x.
[53] O.S. NARAYANASWAMY, A Model of Structural Relaxation in Glass, J. Am. Ceram. Soc. (1971). https://doi.org/10.1111/j.1151-2916.1971.tb12186.x.
[54] O.S. NARAYANASWAMY, R. GARDON, Calculation of Residual Stresses in Glass, J. Am. Ceram. Soc. (1969). https://doi.org/10.1111/j.1151-2916.1969.tb09163.x.
[55] S.M. Rekhson, Thermal Stresses, Relaxation, and Hysteresis in Glass, J. Am. Ceram. Soc. (1993). https://doi.org/10.1111/j.1151-2916.1993.tb03728.x.
[56] J. Kim, S. Dhital, P. Zhivago, M.R. Kaizer, Y. Zhang, Viscoelastic finite element analysis of residual stresses in porcelain-veneered zirconia dental crowns, J. Mech. Behav. Biomed. Mater. (2018). https://doi.org/10.1016/j.jmbbm.2018.03.020.
[57] C.S. Rodrigues, S. Dhital, L.G. May, J. Kim, Y. Zhang, Residual stresses in bilayer crowns: a vfem study, Dent. Mater. (2019). https://doi.org/10.1016/j.dental.2019.08.094.
[58] P.H. DeHoff, K.J. Anusavice, N. Götzen, Viscoelastic finite element analysis of an all-ceramic fixed partial denture, J. Biomech. (2006). https://doi.org/10.1016/j.jbiomech.2004.11.007.
[59] P.H. DeHoff, K.J. Anusavice, Shear stress relaxation of dental ceramics determined from creep behavior, Dent. Mater. (2004). https://doi.org/10.1016/j.dental.2003.10.005.
[60] H. Snyder, Literature review as a research methodology: An overview and

guidelines, J. Bus. Res. (2019). https://doi.org/10.1016/j.jbusres.2019.07.039.
[61] G. Wong, T. Greenhalgh, G. Westhorp, J. Buckingham, R. Pawson, RAMESES publication standards: Meta-narrative reviews, J. Adv. Nurs. (2013). https://doi.org/10.1111/jan.12092.
[62] R.J. Torraco, Writing Integrative Literature Reviews: Guidelines and Examples, Hum. Resour. Dev. Rev. (2005). https://doi.org/10.1177/1534484305278283.
[63] Y. Zhang, B.R. Lawn, Evaluating dental zirconia, Dent. Mater. (2019). https://doi.org/10.1016/j.dental.2018.08.291.
[64] N. Juntavee, C. Dangsuwan, Role of coefficient of thermal expansion on bond strength of ceramic veneered yttrium-stabilized zirconia, J. Clin. Exp. Dent. (2018). https://doi.org/10.4317/jced.54605.
[65] A.K. Mainjot, A. Najjar, B.D. Jakubowicz-Kohen, M.J. Sadoun, Influence of thermal expansion mismatch on residual stress profile in veneering ceramic layered on zirconia: Measurement by hole-drilling, Dent. Mater. (2015). https://doi.org/10.1016/j.dental.2015.06.017.
[66] M. Wendler, R. Belli, A. Petschelt, U. Lohbauer, Characterization of residual stresses in zirconia veneered bilayers assessed via sharp and blunt indentation, Dent. Mater. (2015). https://doi.org/10.1016/j.dental.2015.05.001.
[67] G. Aktas, E. Sahin, P. Vallittu, M. Özcan, L. Lassila, Effect of colouring green stage zirconia on the adhesion of veneering ceramics with different thermal expansion coefficients, Int. J. Oral Sci. (2013). https://doi.org/10.1038/ijos.2013.66.
[68] J.B.C. Meira, B.R. Reis, C.B. Tanaka, R.Y. Ballester, P.F. Cesar, A. Versluis, M. V. Swain, Residual stresses in Y-TZP crowns due to changes in the thermal contraction coefficient of veneers, Dent. Mater. (2013). https://doi.org/10.1016/j.dental.2013.03.012.
[69] M.N. Aboushelib, A.J. Feilzer, N. De Jager, C.J. Kleverlaan, Prestresses in bilayered all-ceramic restorations, J. Biomed. Mater. Res. - Part B Appl. Biomater. (2008). https://doi.org/10.1002/jbm.b.31083.
[70] M.N. Aboushelib, N. De Jager, C.J. Kleverlaan, A.J. Feilzer, Microtensile bond strength of different components of core veneered all-ceramic restorations, Dent. Mater. (2005). https://doi.org/10.1016/j.dental.2005.03.013.
[71] M. V. Swain, V. Mercurio, J.E. Tibballs, M. Tholey, Thermal induced deflection of a porcelain–zirconia bilayer: Influence of cooling rate, Dent. Mater. (2019). https://doi.org/10.1016/j.dental.2019.01.019.
[72] D. Fabris, J.C.M. Souza, F.S. Silva, M. Fredel, J. Mesquita-Guimarães, Y. Zhang, B. Henriques, Thermal residual stresses in bilayered, trilayered and graded dental ceramics, Ceram. Int. (2017). https://doi.org/10.1016/j.ceramint.2016.11.209.
[73] M. Sebastiani, F. Massimi, G. Merlati, E. Bemporad, Residual micro-stress distributions in heat-pressed ceramic on zirconia and porcelain-fused to metal systems: Analysis by FIB-DIC ring-core method and correlation with fracture toughness, Dent. Mater. (2015). https://doi.org/10.1016/j.dental.2015.08.158.
[74] R. Belli, S. Monteiro, L.N. Baratieri, H. Katte, A. Petschelt, U. Lohbauer, A photoelastic assessment of residual stresses in zirconia-veneer crowns, J. Dent. Res. (2012). https://doi.org/10.1177/0022034511435100.
[75] M. Inokoshi, K. Yoshihara, N. Nagaoka, M. Nakanishi, J. De Munck, S. Minakuchi, K. Vanmeensel, F. Zhang, Y. Yoshida, J. Vleugels, I. Naert, B. Van Meerbeek,

Structural and Chemical Analysis of the Zirconia-Veneering Ceramic Interface, J. Dent. Res. (2016). https://doi.org/10.1177/0022034515608825.

[76] A.N. Jikihara, C.B. Tanaka, R.Y. Ballester, M. V. Swain, A. Versluis, J.B.C. Meira, Why a zero CTE mismatch may be better for veneered Y-TZP structures, J. Mech. Behav. Biomed. Mater. (2019). https://doi.org/10.1016/j.jmbbm.2019.04.049.

[77] M. De Kler, N. De Jager, M. Meegdes, J.M. Van Der Zel, Influence of thermal expansion mismatch and fatigue loading on phase changes in porcelain veneered Y-TZP zirconia discs, J. Oral Rehabil. (2007). https://doi.org/10.1111/j.1365-2842.2006.01675.x.

[78] J.P. Nielsen, J.J. Tuccillo, Calculation of Interfacial Stress in Dental Porcelain Bonded to Gold Alloy Substrate, J. Dent. Res. (1972). https://doi.org/10.1177/00220345720510040901.

[79] J.S. Shell, J.P. Nielsen, Study of the Bond between Gold Alloys and Porcelain, J. Dent. Res. (1962). https://doi.org/10.1177/00220345620410062101.

[80] P.H. Dehoff, K.J. Anusavice, Viscoelastic finite element stress analysis of the thermal compatibility of dental bilayer ceramic systems, Int. J. Prosthodont. (2009).

[81] H.M. Al-Dohan, P. Yaman, J.B. Dennison, M.E. Razzoog, B.R. Lang, Shear strength of core-veneer interface in bi-layered ceramics, J. Prosthet. Dent. (2004). https://doi.org/10.1016/j.prosdent.2004.02.009.

[82] M.D. Peng, J.Q. Wei, Y.N. Wang, Q. Li, Microstructure and nanoindentation analyses of low-temperature aging on the zirconia-porcelain interface, J. Mech. Behav. Biomed. Mater. (2017). https://doi.org/10.1016/j.jmbbm.2016.11.010.

[83] S.N. White, V.G. Miklus, E.A. McLaren, L.A. Lang, A.A. Caputo, Flexural strength of a layered zirconia and porcelain dental all-ceramic system, J. Prosthet. Dent. (2005). https://doi.org/10.1016/j.prosdent.2005.05.007.

[84] M. Borba, M.D. De Araújo, E. De Lima, H.N. Yoshimura, P.F. Cesar, J.A. Griggs, Á. Della Bona, Flexural strength and failure modes of layered ceramic structures, Dent. Mater. (2011). https://doi.org/10.1016/j.dental.2011.09.008.

[85] R.K. Chintapalli, A. Mestra Rodriguez, F. Garcia Marro, M. Anglada, Effect of sandblasting and residual stress on strength of zirconia for restorative dentistry applications, J. Mech. Behav. Biomed. Mater. (2014). https://doi.org/10.1016/j.jmbbm.2013.09.004.

[86] J. Yang, M. Shahid, C. Wan, F. Jing, W. Pan, Anisotropy in elasticity, sound velocities and minimum thermal conductivity of zirconia from first-principles calculations, J. Eur. Ceram. Soc. (2017). https://doi.org/10.1016/j.jeurceramsoc.2016.08.034.

[87] U. Lohbauer, S.S. Scherrer, A. Della Bona, M. Tholey, R. van Noort, A. Vichi, J.R. Kelly, P.F. Cesar, ADM guidance-Ceramics: all-ceramic multilayer interfaces in dentistry, Dent. Mater. (2017). https://doi.org/10.1016/j.dental.2017.03.005.

[88] B.A. Cottom, M.J. Mayo, Fracture toughness of nanocrystalline ZrO2-3mol% y2o3 determined by vickers indentation, Scr. Mater. (1996). https://doi.org/10.1016/1359-6462(95)00587-0.

[89] I. Denry, J.R. Kelly, Emerging ceramic-based materials for dentistry, J. Dent. Res. (2014). https://doi.org/10.1177/0022034514553627.

[90] J. Chevalier, S. Deville, E. Münch, R. Jullian, F. Lair, Critical effect of cubic phase on aging in 3 mol% yttria-stabilized zirconia ceramics for hip replacement

prosthesis, Biomaterials. (2004). https://doi.org/10.1016/j.biomaterials.2004.01.002.
[91] E. a Mclaren, P.T. Cao, Ceramics in Dentistry—Part I: Classes of Materials, Insid. Dent. (2009).
[92] I.L. Denry, J. Mackert, J.A. Holloway, S.F. Rosenstiel, Effect of cubic leucite stabilization on the flexural strength of feldspathic dental porcelain, J. Dent. Res. (1996). https://doi.org/10.1177/00220345960750120301.
[93] J. Mackert, A.L. Williams, Microcracks in dental porcelain and their behavior during multiple firing, J. Dent. Res. (1996). https://doi.org/10.1177/00220345960750070801.
[94] J.C. Durand, B. Jacquot, H. Salehi, M. Fages, J. Margerit, F.J.G. Cuisinier, Confocal Raman microscopic analysis of the zirconia/feldspathic ceramic interface, Dent. Mater. (2012). https://doi.org/10.1016/j.dental.2012.02.013.
[95] Y. Zhang, H. Chai, J.J.W. Lee, B.R. Lawn, Chipping resistance of graded zirconia ceramics for dental crowns, J. Dent. Res. (2012). https://doi.org/10.1177/0022034511434356.
[96] H. Chai, J.J.W. Lee, A.J. Mieleszko, S.J. Chu, Y. Zhang, On the interfacial fracture of porcelain/zirconia and graded zirconia dental structures, Acta Biomater. (2014). https://doi.org/10.1016/j.actbio.2014.04.016.
[97] S. Roedel, J. Mesquita-Guimarães, J.C.M. Souza, F.S. Silva, M.C. Fredel, B. Henriques, Production and characterization of zirconia structures with a porous surface, Mater. Sci. Eng. C. (2019). https://doi.org/10.1016/j.msec.2019.03.087.
[98] V. Rosa, C. Fredericci, M.F. Moreira, H.N. Yoshimura, P.F. Cesar, Effect of ion-exchange temperature on mechanical properties of a dental porcelain, Ceram. Int. (2010). https://doi.org/10.1016/j.ceramint.2010.05.007.
[99] N. Su, Y. Liao, H. Zhang, L. Yue, X. Lu, J. Shen, H. Wang, Effects of core-to-dentin thickness ratio on the biaxial flexural strength, reliability, and fracture mode of bilayered materials of zirconia core (Y-TZP) and veneer indirect composite resins, J. Prosthet. Dent. (2017). https://doi.org/10.1016/j.prosdent.2016.04.017.
[100] P. Sinthuprasirt, R. Van Noort, R. Moorehead, S. Pollington, Evaluation of a novel multiple phase veneering ceramic, Dent. Mater. (2015). https://doi.org/10.1016/j.dental.2015.01.012.
[101] T. Nakamura, T. Sugano, H. Usami, K. Wakabayashi, H. Ohnishi, T. Sekino, H. Yatani, Shear bond strength of veneering porcelain to porous zirconia, Dent. Mater. J. (2014). https://doi.org/10.4012/dmj.2013-191.
[102] M. Borba, M.D. De Araújo, K.A. Fukushima, H.N. Yoshimura, P.F. Cesar, J.A. Griggs, Á. Della Bona, Effect of the microstructure on the lifetime of dental ceramics, Dent. Mater. (2011). https://doi.org/10.1016/j.dental.2011.04.003.
[103] I. Denry, J.R. Kelly, State of the art of zirconia for dental applications, Dent. Mater. (2008). https://doi.org/10.1016/j.dental.2007.05.007.
[104] R.C. Garvie, R.H. Hannink, R.T. Pascoe, Ceramic steel?, Nature. (1975). https://doi.org/10.1038/258703a0.
[105] R.C. GARVIE, P.S. NICHOLSON, Phase Analysis in Zirconia Systems, J. Am. Ceram. Soc. (1972). https://doi.org/10.1111/j.1151-2916.1972.tb11290.x.
[106] M. Allahkarami, J.C. Hanan, Mapping the tetragonal to monoclinic phase transformation in zirconia core dental crowns, Dent. Mater. (2011).

https://doi.org/10.1016/j.dental.2011.09.004.
[107] E.C. Subbarao, ZIRCONIA - AN OVERVIEW., in: Adv. Ceram., 1981.
[108] A.H. HEUER, N. CLAUSSEN, W.M. KRIVEN, M. RUHLE, Stability of Tetragonal ZrO2 Particles in Ceramic Matrices, J. Am. Ceram. Soc. (1982). https://doi.org/10.1111/j.1151-2916.1982.tb09946.x.
[109] M. Inokoshi, F. Zhang, J. De Munck, S. Minakuchi, I. Naert, J. Vleugels, B. Van Meerbeek, K. Vanmeensel, Influence of sintering conditions on low-temperature degradation of dental zirconia, Dent. Mater. (2014). https://doi.org/10.1016/j.dental.2014.03.005.
[110] E. Siarampi, E. Kontonasaki, K.S. Andrikopoulos, N. Kantiranis, G.A. Voyiatzis, T. Zorba, K.M. Paraskevopoulos, P. Koidis, Effect of in vitro aging on the flexural strength and probability to fracture of Y-TZP zirconia ceramics for all-ceramic restorations, Dent. Mater. (2014). https://doi.org/10.1016/j.dental.2014.05.033.
[111] H. Xie, Y. Gu, Q. Li, M. Qian, F. Zhang, F.R. Tay, C. Chen, Effects of multiple firings on the low-temperature degradation of dental yttria-stabilized tetragonal zirconia, J. Prosthet. Dent. (2016). https://doi.org/10.1016/j.prosdent.2015.08.029.
[112] L.M. Miragaya, R.B. Guimarães, R.O. de A. e. Souza, G. dos Santos Botelho, J.G. Antunes Guimarães, E.M. da Silva, Effect of intra-oral aging on t→m phase transformation, microstructure, and mechanical properties of Y-TZP dental ceramics, J. Mech. Behav. Biomed. Mater. (2017). https://doi.org/10.1016/j.jmbbm.2017.04.014.
[113] M. Kelch, J. Schulz, D. Edelhoff, B. Sener, B. Stawarczyk, Impact of different pretreatments and aging procedures on the flexural strength and phase structure of zirconia ceramics, Dent. Mater. (2019). https://doi.org/10.1016/j.dental.2019.07.020.
[114] S.F. Poole, G.K. Rocha Pereira, I.C.M. Moris, A.G. Marques, R.F. Ribeiro, E.A. Gomes, Physical properties of conventional and monolithic yttria-zirconia materials after low-temperature degradation, Ceram. Int. (2019). https://doi.org/10.1016/j.ceramint.2019.07.012.
[115] H.A. Vidotti, J.R. Pereira, E. Insaurralde, L.F. Plaça, J.R. Delben, A.L. do Valle, Influence of thermal and mechanical fatigue on the shear bond strength of different all-ceramic systems, J. Clin. Exp. Dent. (2017). https://doi.org/10.4317/jced.53728.
[116] C.M. Ramos, P.F. Cesar, R.F. Lia Mondelli, A.S. Tabata, J. De Souza Santos, A.F. Sanches Borges, Bond strength and Raman analysis of the zirconia-feldspathic porcelain interface, J. Prosthet. Dent. (2014). https://doi.org/10.1016/j.prosdent.2014.02.009.
[117] H.M. Ashkanani, A.J. Raigrodski, B.D. Flinn, H. Heindl, L.A. Mancl, Flexural and shear strengths of ZrO2 and a high-noble alloy bonded to their corresponding porcelains, J. Prosthet. Dent. (2008). https://doi.org/10.1016/S0022-3913(08)60206-1.
[118] V. Preis, M. Behr, S. Hahnel, G. Handel, M. Rosentritt, In vitro failure and fracture resistance of veneered and full-contour zirconia restorations, J. Dent. (2012). https://doi.org/10.1016/j.jdent.2012.07.010.
[119] R.O.A. Souza, L.F. Valandro, R.M. Melo, J.P.B. Machado, M.A. Bottino, M. Özcan, Air-particle abrasion on zirconia ceramic using different protocols: Effects on biaxial flexural strength after cyclic loading, phase transformation and surface

topography, J. Mech. Behav. Biomed. Mater. (2013). https://doi.org/10.1016/j.jmbbm.2013.04.018.
[120] H.A. Vidotti, J.R. Pereira, E. Insaurralde, A.L.P.F. De Almeida, A.L. Do Valle, Thermo and mechanical cycling and veneering method do not influence Y-TZP core/veneer interface bond strength, J. Dent. (2013). https://doi.org/10.1016/j.jdent.2012.12.001.
[121] C.W. Cheng, C.C. Yang, M. Yan, Bond strength of heat-pressed veneer ceramics to zirconia with various blasting conditions, J. Dent. Sci. (2018). https://doi.org/10.1016/j.jds.2018.03.002.
[122] L. Sreekala, J. Varghese, A. Zainaba Fathima, S. Eerali, S. Eerali, M. Narayanan, Comparative evaluation of shear bond strengths of veneering porcelain to base metal alloy and zirconia substructures before and after aging - An in vitro study , J. Int. Soc. Prev. Community Dent. (2015). https://doi.org/10.4103/2231-0762.171590.
[123] M. Schmitter, D. Mueller, S. Rues, In vitro chipping behaviour of all-ceramic crowns with a zirconia framework and feldspathic veneering: Comparison of CAD/CAM-produced veneer with manually layered veneer, J. Oral Rehabil. (2013). https://doi.org/10.1111/joor.12061.
[124] M.S. Chaar, S. Witkowski, J.R. Strub, W. Att, Effect of veneering technique on the fracture resistance of zirconia fixed dental prostheses, J. Oral Rehabil. (2013). https://doi.org/10.1111/j.1365-2842.2012.02323.x.
[125] M. Schmitter, G. Lotze, W. Bömicke, S. Rues, Influence of surface treatment on the in-vitro fracture resistance of zirconia-based all-ceramic anterior crowns, Dent. Mater. (2015). https://doi.org/10.1016/j.dental.2015.10.003.
[126] H.I. Yoon, I.S. Yeo, Y.J. Yi, S.H. Kim, J.B. Lee, J.S. Han, Effect of various intermediate ceramic layers on the interfacial stability of zirconia core and veneering ceramics, Acta Odontol. Scand. (2015). https://doi.org/10.3109/00016357.2014.986755.
[127] B. Ebadian, R. Mosharraf, M. Abbasi, Effect of ceramic cooling protocols and zirconia coloring on fracture load of zirconia based restorations, Dent. Res. J. (Isfahan). (2018). https://doi.org/10.4103/1735-3327.223612.
[128] G. Pradíes, L. Godoy-Ruiz, M. Özcan, I. Moreno-Hay, F. Martínez-Rus, Analysis of Surface Roughness, Fracture Toughness, and Weibull Characteristics of Different Framework—Veneer Dental Ceramic Assemblies after Grinding, Polishing, and Glazing, J. Prosthodont. (2019). https://doi.org/10.1111/jopr.12653.
[129] D.J.H. Mahmood, E.H. Linderoth, A. Wennerberg, P.V. Von Steyern, Influence of core design, production technique, and material selection on fracture behavior of yttria-stabilized tetragonal zirconia polycrystal fixed dental prostheses produced using different multilayer techniques: Split-file, over-pressing, and manuall, in: Clin. Cosmet. Investig. Dent., 2016. https://doi.org/10.2147/CCIDE.S94343.
[130] A.G. Turk, M. Ulusoy, M. Yuce, H. Akin, Effect of different veneering techniques on the fracture strength of metal and zirconia frameworks, J. Adv. Prosthodont. (2015). https://doi.org/10.4047/jap.2015.7.6.454.
[131] J.W. Oh, K.Y. Song, S.G. Ahn, J.M. Park, M.H. Lee, J.M. Seo, Effects of core characters and veneering technique on biaxial flexural strength in porcelain fused to metal and porcelain veneered zirconia, J. Adv. Prosthodont. (2015). https://doi.org/10.4047/jap.2015.7.5.349.

[132] C. Larsson, M. Drazic, E. Nilsson, P. Vult von Steyern, Fracture of porcelain-veneered gold-alloy and zirconia molar crowns using a modified test set-up., Acta Biomater. Odontol. Scand. (2015). https://doi.org/10.3109/23337931.2015.1057825.
[133] V. Preis, T. Dowerk, M. Behr, C. Kolbeck, M. Rosentritt, Influence of cusp inclination and curvature on the in vitro failure and fracture resistance of veneered zirconia crowns, Clin. Oral Investig. (2014). https://doi.org/10.1007/s00784-013-1029-9.
[134] M. Ishibe, A.J. Raigrodski, B.D. Flinn, K.H. Chung, C. Spiekerman, R.R. Winter, Shear bond strengths of pressed and layered veneering ceramics to high-noble alloy and zirconia cores, J. Prosthet. Dent. (2011). https://doi.org/10.1016/S0022-3913(11)60090-5.
[135] C. Larsson, S. El Madhoun, A. Wennerberg, P. Vult von Steyern, Fracture strength of yttria-stabilized tetragonal zirconia polycrystals crowns with different design: An in vitro study, Clin. Oral Implants Res. (2012). https://doi.org/10.1111/j.1600-0501.2011.02224.x.
[136] H.I. Yoon, I.S. Yeo, J.S. Han, Effect of various surface treatments on the interfacial adhesion between zirconia cores and porcelain veneers, Int. J. Adhes. Adhes. (2016). https://doi.org/10.1016/j.ijadhadh.2016.03.019.
[137] K.C. Li, J.N. Waddell, D.J. Prior, S. Ting, L. Girvan, L.J. Van Vuuren, M. V. Swain, Effect of autoclave induced low-temperature degradation on the adhesion energy between yttria-stabilized zirconia veneered with porcelain, Dent. Mater. (2013). https://doi.org/10.1016/j.dental.2013.08.204.
[138] H.P. Papanagiotou, S.M. Morgano, R.A. Giordano, R. Pober, In vitro evaluation of low-temperature aging effects and finishing procedures on the flexural strength and structural stability of Y-TZP dental ceramics, J. Prosthet. Dent. (2006). https://doi.org/10.1016/j.prosdent.2006.08.004.
[139] V. Lughi, V. Sergo, Low temperature degradation -aging- of zirconia: A critical review of the relevant aspects in dentistry, Dent. Mater. (2010). https://doi.org/10.1016/j.dental.2010.04.006.
[140] M. Cattani-Lorente, S.S. Scherrer, P. Ammann, M. Jobin, H.W.A. Wiskott, Low temperature degradation of a Y-TZP dental ceramic, Acta Biomater. (2011). https://doi.org/10.1016/j.actbio.2010.09.020.
[141] B. Stawarczyk, M. Özcan, A. Trottmann, C.H.F. Hämmerle, M. Roos, Evaluation of flexural strength of hipped and presintered zirconia using different estimation methods of Weibull statistics, J. Mech. Behav. Biomed. Mater. (2012). https://doi.org/10.1016/j.jmbbm.2012.01.020.
[142] S.S. Scherrer, M. Cattani-Lorente, S. Yoon, L. Karvonen, S. Pokrant, F. Rothbrust, J. Kuebler, Post-hot isostatic pressing: A healing treatment for process related defects and laboratory grinding damage of dental zirconia?, Dent. Mater. (2013). https://doi.org/10.1016/j.dental.2013.04.014.
[143] S. Deville, J. Chevalier, L. Gremillard, Influence of surface finish and residual stresses on the ageing sensitivity of biomedical grade zirconia, Biomaterials. (2006). https://doi.org/10.1016/j.biomaterials.2005.11.021.
[144] M.N. Aboushelib, C.J. Kleverlaan, A.J. Feilzer, Effect of zirconia type on its bond strength with different veneer ceramics, J. Prosthodont. (2008).

https://doi.org/10.1111/j.1532-849X.2008.00306.x.
[145] R. Mosharraf, M. Rismanchian, O. Savabi, A.H. Ashtiani, Influence of surface modification techniques on shear bond strength between different zirconia cores and veneering ceramics, J. Adv. Prosthodont. (2011). https://doi.org/10.4047/jap.2011.3.4.221.
[146] O.S. Abd El-Ghany, A.H. Sherief, Zirconia based ceramics, some clinical and biological aspects: Review, Futur. Dent. J. (2016). https://doi.org/10.1016/j.fdj.2016.10.002.
[147] M.J. Heffernan, S.A. Aquilino, A.M. Diaz-Arnold, D.R. Haselton, C.M. Stanford, M.A. Vargas, Relative translucency of six all-ceramic systems. Part II: Core and veneer materials, J. Prosthet. Dent. (2002). https://doi.org/10.1016/S0022-3913(02)00041-0.
[148] P. Pittayachawan, A. McDonald, A. Petrie, J.C. Knowles, The biaxial flexural strength and fatigue property of Lava™ Y-TZP dental ceramic, Dent. Mater. (2007). https://doi.org/10.1016/j.dental.2006.09.003.
[149] B.I. Ardlin, Transformation-toughened zirconia for dental inlays, crowns and bridges: Chemical stability and effect of low-temperature aging on flexural strength and surface structure, Dent. Mater. (2002). https://doi.org/10.1016/S0109-5641(01)00095-1.
[150] J. Hjerppe, T. Närhi, K. Fröberg, P.K. Vallittu, L.V.J. Lassila, Effect of shading the zirconia framework on biaxial strength and surface microhardness, Acta Odontol. Scand. (2008). https://doi.org/10.1080/00016350802247123.
[151] M. Reis, R. Sgura, B.A. Serinhano, M. Dutra-Correa, F. Taddeo, I.S. Medeiros, Mechanical properties of a zirconia veneering porcelain irradiated with CO2 laser, Dent. Mater. (2013). https://doi.org/10.1016/j.dental.2013.08.050.
[152] E. Roitero, F. Lasserre, M. Anglada, F. Mücklich, E. Jiménez-Piqué, A parametric study of laser interference surface patterning of dental zirconia: Effects of laser parameters on topography and surface quality, Dent. Mater. (2017). https://doi.org/10.1016/j.dental.2016.09.040.
[153] B. Henriques, D. Fabris, J.C.M. Souza, F.S. Silva, Ó. Carvalho, M.C. Fredel, J. Mesquita-Guimarães, Bond strength enhancement of zirconia-porcelain interfaces via Nd:YAG laser surface structuring, J. Mech. Behav. Biomed. Mater. (2018). https://doi.org/10.1016/j.jmbbm.2018.02.031.
[154] S. Kurtulmus-Yilmaz, H. Aktore, Effect of the application of surface treatments before and after sintering on the flexural strength, phase transformation and surface topography of zirconia, J. Dent. (2018). https://doi.org/10.1016/j.jdent.2018.02.006.
[155] A.O. Abdullah, H. Yu, S. Pollington, F.K. Muhammed, S. Xudong, Y. Liu, Effect of repeated laser surface treatments on shear bond strength between zirconia and veneering ceramic, J. Prosthet. Dent. (2020). https://doi.org/10.1016/j.prosdent.2019.10.007.
[156] C. Monaco, A. Tucci, L. Esposito, R. Scotti, Adhesion mechanisms at the interface between Y-TZP and veneering ceramic with and without modifier, J. Dent. (2014). https://doi.org/10.1016/j.jdent.2014.07.019.
[157] E. Camposilvan, Q. Flamant, M. Anglada, Surface roughened zirconia: Towards hydrothermal stability, J. Mech. Behav. Biomed. Mater. (2015). https://doi.org/10.1016/j.jmbbm.2015.03.017.

[158] E. Camposilvan, F.G. Marro, A. Mestra, M. Anglada, Enhanced reliability of yttria-stabilized zirconia for dental applications, Acta Biomater. (2015). https://doi.org/10.1016/j.actbio.2015.01.023.
[159] S.B. Her, K.H. Kim, S.E. Park, E.J. Park, The effect of zirconia surface architecturing technique on the zirconia/veneer interfacial bond strength, J. Adv. Prosthodont. (2018). https://doi.org/10.4047/jap.2018.10.4.259.
[160] N.A. Bastos, P.N. Lisboa-Filho, A. Tabata, P.A.S. Francisconi, A.Y. Furuse, H.M. Honório, A.F.S. Borges, Effect of alternative sonochemical treatment on zirconia surface and bond strength with veneering ceramic, Mater. Sci. Eng. B Solid-State Mater. Adv. Technol. (2020). https://doi.org/10.1016/j.mseb.2019.114473.
[161] C. Anunmana, W. Wansom, Bonding measurement —Strength and fracture mechanics approaches, Dent. Mater. J. (2017). https://doi.org/10.4012/dmj.2016-193.
[162] M. Yan, A. Csík, C.C. Yang, Y. Luo, T. Fodor, S.J. Ding, Synergistic reinforcement of surface modification on improving the bonding of veneering ceramics to zirconia, Ceram. Int. (2018). https://doi.org/10.1016/j.ceramint.2018.07.218.
[163] T. Sawada, C. Schille, J. Zöldföldi, E. Schweizer, J. Geis-Gerstorfer, S. Spintzyk, Influence of a surface conditioner to pre-sintered zirconia on the biaxial flexural strength and phase transformation, Dent. Mater. (2018). https://doi.org/10.1016/j.dental.2017.12.004.
[164] T. Ghaffari, E. Moslehifard, M. Motiei, Effect of thermal and mechanical cycles on shear bond strength of zirconia core to porcelain veneer under different surface treatments, J. Dent. Res. Dent. Clin. Dent. Prospects. (2019). https://doi.org/10.15171/joddd.2019.035.
[165] P. Yadav, N. Dabas, S.S. Phukela, P. Malhotra, S. Drall, P.K. Ritwal, A comparative evaluation of the effect of liners on the shear bond strength of veneered zirconia block: An in vitro study, J. Indian Prosthodont. Soc. (2019). https://doi.org/10.4103/jips.jips_103_19.
[166] S. Nikzadjamnani, S. Zarrati, M. Rostamzadeh, Microtensile Bond Strength Between Zirconia Core and Veneering Porcelain After Different Surface Treatments., J. Dent. (Tehran). (2017).
[167] H.A. Prasad, N. Pasha, M. Hilal, G.S. Amarnath, V. Kundapur, M. Anand, S. Singh, To Evaluate Effect of Airborne Particle Abrasion using Different Abrasives Particles and Compare Two Commercial Available Zirconia on Flexural Strength on Heat Treatment., Int. J. Biomed. Sci. (2017).
[168] O. Kirmali, A. Kapdan, A. Kustarci, K. Er, Veneer Ceramic to Y-TZP Bonding: Comparison of Different Surface Treatments, J. Prosthodont. (2016). https://doi.org/10.1111/jopr.12304.
[169] M. Bankoɬlu Güngör, H. Yilmaz, S. Karakoca Nemli, B. Turhan Bal, C. Aydin, Effect of surface treatments on the biaxial flexural strength, phase transformation, and surface roughness of bilayered porcelain/zirconia dental ceramics, J. Prosthet. Dent. (2015). https://doi.org/10.1016/j.prosdent.2014.12.002.
[170] H. in Yoon, I. sung Yeo, Y. jin Yi, S. hun Kim, J. bong Lee, J. suk Han, Effect of surface treatment and liner material on the adhesion between veneering ceramic and zirconia, J. Mech. Behav. Biomed. Mater. (2014). https://doi.org/10.1016/j.jmbbm.2014.09.017.

[171] G. Wang, S. Zhang, C. Bian, H. Kong, Effect of zirconia surface treatment on zirconia/veneer interfacial toughness evaluated by fracture mechanics method, J. Dent. (2014). https://doi.org/10.1016/j.jdent.2014.04.005.
[172] A. Grigore, S. Spallek, A. Petschelt, B. Butz, E. Spiecker, U. Lohbauer, Microstructure of veneered zirconia after surface treatments: A TEM study, Dent. Mater. (2013). https://doi.org/10.1016/j.dental.2013.07.022.
[173] M.N. Aboushelib, H. Wang, Influence of crystal structure on debonding failure of zirconia veneered restorations, Dent. Mater. (2013). https://doi.org/10.1016/j.dental.2013.04.008.
[174] A.B. Harding, B.K. Norling, E.C. Teixeira, The Effect of Surface Treatment of the Interfacial Surface on Fatigue-Related Microtensile Bond Strength of Milled Zirconia to Veneering Porcelain, J. Prosthodont. (2012). https://doi.org/10.1111/j.1532-849X.2012.00843.x.
[175] T. Nakamura, K. Wakabayashi, C. Zaima, H. Nishida, S. Kinuta, H. Yatani, Tensile bond strength between tooth-colored porcelain and sandblasted zirconia framework, J. Prosthodont. Res. (2009). https://doi.org/10.1016/j.jpor.2009.02.007.
[176] H.J. Kim, H.P. Lim, Y.J. Park, M.S. Vang, Effect of zirconia surface treatments on the shear bond strength of veneering ceramic, J. Prosthet. Dent. (2011). https://doi.org/10.1016/S0022-3913(11)60060-7.
[177] M. Guazzato, L. Quach, M. Albakry, M. V. Swain, Influence of surface and heat treatments on the flexural strength of Y-TZP dental ceramic, J. Dent. (2005). https://doi.org/10.1016/j.jdent.2004.07.001.
[178] R.G. Luthardt, M.S. Holzhüter, H. Rudolph, V. Herold, M.H. Walter, CAD/CAM-machining effects on Y-TZP zirconia, Dent. Mater. (2004). https://doi.org/10.1016/j.dental.2003.08.007.
[179] M.N. Aboushelib, H. Wang, Effect of surface treatment on flexural strength of zirconia bars, J. Prosthet. Dent. (2010). https://doi.org/10.1016/S0022-3913(10)60100-X.
[180] C. Mochales, A. Maerten, A. Rack, P. Cloetens, W.D. Mueller, P. Zaslansky, C. Fleck, Monoclinic phase transformations of zirconia-based dental prostheses, induced by clinically practised surface manipulations, Acta Biomater. (2011). https://doi.org/10.1016/j.actbio.2011.04.007.
[181] I.L. Aurélio, A.M.E. Marchionatti, A.F. Montagner, L.G. May, F.Z.M. Soares, Does air particle abrasion affect the flexural strength and phase transformation of Y-TZP? A systematic review and meta-analysis, Dent. Mater. (2016). https://doi.org/10.1016/j.dental.2016.03.021.
[182] R.K. Chintapalli, F.G. Marro, E. Jimenez-Pique, M. Anglada, Phase transformation and subsurface damage in 3Y-TZP after sandblasting, Dent. Mater. (2013). https://doi.org/10.1016/j.dental.2013.03.005.
[183] M.T. Marefati, A.M. Hadian, T. Hooshmand, A. Hadian, B.E. Yekta, Wetting Characteristics of a Nano Y-TZP Dental Ceramic by a Molten Feldspathic Veneer, Procedia Mater. Sci. (2015). https://doi.org/10.1016/j.mspro.2015.11.038.
[184] G. Wang, S. Zhang, C. Bian, H. Kong, Interface toughness of a zirconia-veneer system and the effect of a liner application, J. Prosthet. Dent. (2014). https://doi.org/10.1016/j.prosdent.2013.12.010.
[185] S.P. Passos, B. Linke, P.W. Major, J.A. Nychka, The effect of air-abrasion and heat

treatment on the fracture behavior of Y-TZP, Dent. Mater. (2015). https://doi.org/10.1016/j.dental.2015.05.008.
[186] A. Nishigori, T. Yoshida, M.C. Bottino, J.A. Platt, Influence of zirconia surface treatment on veneering porcelain shear bond strength after cyclic loading, J. Prosthet. Dent. (2014). https://doi.org/10.1016/j.prosdent.2014.05.029.
[187] L. Hallmann, P. Ulmer, E. Reusser, C.H.F. Hämmerle, Effect of blasting pressure, abrasive particle size and grade on phase transformation and morphological change of dental zirconia surface, Surf. Coatings Technol. (2012). https://doi.org/10.1016/j.surfcoat.2012.04.043.
[188] C. Monaco, A. Tucci, L. Esposito, R. Scotti, Microstructural changes produced by abrading Y-TZP in presintered and sintered conditions, J. Dent. (2013). https://doi.org/10.1016/j.jdent.2012.06.009.
[189] U. Işeri, Z. Özkurt, A. Yalniz, E. Kazazoglu, Comparison of different grinding procedures on the flexural strength of zirconia, J. Prosthet. Dent. (2012). https://doi.org/10.1016/S0022-3913(12)60081-X.
[190] Y. tao Jian, T. yu Tang, M. V. Swain, X. dong Wang, K. Zhao, Effect of core ceramic grinding on fracture behaviour of bilayered zirconia veneering ceramic systems under two loading schemes, Dent. Mater. (2016). https://doi.org/10.1016/j.dental.2016.06.007.
[191] T. Kondo, F. Komine, J. Honda, H. Takata, Y. Moriya, Effect of veneering materials on fracture loads of implant-supported zirconia molar fixed dental prostheses, J. Prosthodont. Res. (2019). https://doi.org/10.1016/j.jpor.2018.10.006.
[192] P. Zhao, P. Yu, Y. Xiong, L. Yue, D. Arola, S. Gao, Does the bond strength of highly translucent zirconia show a different dependence on the airborne-particle abrasion parameters in comparison to conventional zirconia?, J. Prosthodont. Res. (2020). https://doi.org/10.1016/j.jpor.2019.04.008.
[193] A.R. Alao, R. Stoll, X.F. Song, T. Miyazaki, Y. Hotta, Y. Shibata, L. Yin, Surface quality of yttria-stabilized tetragonal zirconia polycrystal in CAD/CAM milling, sintering, polishing and sandblasting processes, J. Mech. Behav. Biomed. Mater. (2017). https://doi.org/10.1016/j.jmbbm.2016.08.021.
[194] G.R. Hatanaka, G.S. Polli, L.M.G. Fais, J.M. dos S.N. Reis, L.A.P. Pinelli, Zirconia changes after grinding and regeneration firing, J. Prosthet. Dent. (2017). https://doi.org/10.1016/j.prosdent.2016.09.026.
[195] M.G. Botelho, S. Dangay, K. Shih, W.Y.H. Lam, The effect of surface treatments on dental zirconia: An analysis of biaxial flexural strength, surface roughness and phase transformation, J. Dent. (2018). https://doi.org/10.1016/j.jdent.2018.05.016.
[196] G.K.R. Pereira, S. Fraga, A.F. Montagner, F.Z.M. Soares, C.J. Kleverlaan, L.F. Valandro, The effect of grinding on the mechanical behavior of Y-TZP ceramics: A systematic review and meta-analyses, J. Mech. Behav. Biomed. Mater. (2016). https://doi.org/10.1016/j.jmbbm.2016.06.028.
[197] A. Piosik, K. Żurowski, Z. Pietralik, W. Hędzelek, M. Kozak, Structural studies of degradation process of zirconium dioxide tetragonal phase induced by grinding with dental bur, Nucl. Instruments Methods Phys. Res. Sect. B Beam Interact. with Mater. Atoms. (2017). https://doi.org/10.1016/j.nimb.2017.07.024.
[198] C.M.B. Ho, H. Ding, X. Chen, J.K.H. Tsoi, M.G. Botelho, The effects of dry and wet grinding on the strength of dental zirconia, Ceram. Int. (2018).

https://doi.org/10.1016/j.ceramint.2018.03.062.
[199] D.Y. Toyama, L.M.M. Alves, G.F. Ramos, T.M.B. Campos, G. de Vasconcelos, A.L.S. Borges, R.M. de Melo, Bioinspired silica-infiltrated zirconia bilayers: Strength and interfacial bonding, J. Mech. Behav. Biomed. Mater. (2019). https://doi.org/10.1016/j.jmbbm.2018.09.013.
[200] J. Teng, H. Wang, Y. Liao, X. Liang, Evaluation of a conditioning method to improve core-veneer bond strength of zirconia restorations, J. Prosthet. Dent. (2012). https://doi.org/10.1016/S0022-3913(12)60095-X.
[201] A. Oliveira-Ogliari, C.S. Vasconcelos, R.C. Bruschi, A.P. Gonçalves, F.A. Ogliari, R.R. Moraes, Thermal silicatization: A new approach for bonding to zirconia ceramics, Int. J. Adhes. Adhes. (2014). https://doi.org/10.1016/j.ijadhadh.2013.09.048.
[202] K. Kvam, High temperature silicatization of zirconia-surface to improve veneering strength, Dent. Mater. (2017). https://doi.org/10.1016/j.dental.2017.08.087.
[203] S.B. Bitencourt, D.M. dos Santos, E.V.F. da Silva, V.A.R. Barão, E.C. Rangel, N.C. da Cruz, G.M. de Souza, M.C. Goiato, A.A. Pesqueira, Characterisation of a new plasma-enhanced film to improve shear bond strength between zirconia and veneering ceramic, Mater. Sci. Eng. C. (2018). https://doi.org/10.1016/j.msec.2018.06.052.
[204] F.A. Farhan, E. Sulaiman, M.G. Kutty, Application of zirconia surface coating to improve fracture resistance and stress distribution of zirconia ceramic restorations, Ceram. Int. (2018). https://doi.org/10.1016/j.ceramint.2018.08.246.
[205] R.L.P. Santos, F.S. Silva, R.M. Nascimento, J.C.M. Souza, F. V. Motta, O. Carvalho, B. Henriques, Shear bond strength of veneering porcelain to zirconia: Effect of surface treatment by CNC-milling and composite layer deposition on zirconia, J. Mech. Behav. Biomed. Mater. (2016). https://doi.org/10.1016/j.jmbbm.2016.03.015.
[206] E.C. Teixeira, J.R. Piascik, B.R. Stoner, J.Y. Thompson, Zirconia-parylene multilayer thin films for enhanced fracture resistance of dental ceramics, in: Proc. Inst. Mech. Eng. Part H J. Eng. Med., 2009. https://doi.org/10.1243/09544119JEIM543.
[207] Y.C. Liu, J.P. Hsieh, Y.C. Chen, L.L. Kang, C.S. Hwang, S.F. Chuang, Promoting porcelain–zirconia bonding using different atmospheric pressure gas plasmas, Dent. Mater. (2018). https://doi.org/10.1016/j.dental.2018.05.004.
[208] F.A. Farhan, E. Sulaiman, M.G. Kutty, Effect of new zirconia surface coatings on the surface properties and bonding strength of veneering zirconia substrate, Surf. Coatings Technol. (2018). https://doi.org/10.1016/j.surfcoat.2017.10.030.
[209] M.N. Aboushelib, C.J. Kleverlaan, A.J. Feilzer, Microtensile bond strength of different components of core veneered all-ceramic restorations. Part II: Zirconia veneering ceramics, Dent. Mater. (2006). https://doi.org/10.1016/j.dental.2005.11.014.
[210] M.H. Lee, B.K. Min, J.S. Son, T.Y. Kwon, Influence of different post-plasma treatment storage conditions on the shear bond strength of veneering porcelain to zirconia, Materials (Basel). (2016). https://doi.org/10.3390/ma9010043.
[211] M. Cattani Lorente, S.S. Scherrer, J. Richard, R. Demellayer, M. Amez-Droz, H.W.A. Wiskott, Surface roughness and EDS characterization of a Y-TZP dental

ceramic treated with the CoJet™ Sand, Dent. Mater. (2010). https://doi.org/10.1016/j.dental.2010.06.005.
[212] A.C. Diniz, R.M. Nascimento, J.C.M. Souza, B.B. Henriques, A.F.P. Carreiro, Fracture and shear bond strength analyses of different dental veneering ceramics to zirconia, Mater. Sci. Eng. C. (2014). https://doi.org/10.1016/j.msec.2014.01.032.
[213] J.E. Choi, J.N. Waddell, B. Torr, M.V. Swain, Pressed ceramics onto zirconia. Part 1: Comparison of crystalline phases present, adhesion to a zirconia system and flexural strength, Dent. Mater. (2011). https://doi.org/10.1016/j.dental.2011.08.006.
[214] M. Øilo, K. Kvam, N.R. Gjerdet, Simulation of clinical fractures for three different all-ceramic crowns, Eur. J. Oral Sci. (2014). https://doi.org/10.1111/eos.12128.
[215] Y.S. Choi, S.H. Kim, J.B. Lee, J.S. Han, I.S. Yeo, In vitro evaluation of fracture strength of zirconia restoration veneered with various ceramic materials, J. Adv. Prosthodont. (2012). https://doi.org/10.4047/jap.2012.4.3.162.
[216] L. Porojan, F. Topală, S. Porojan, C. Savencu, Effect of frame design and veneering material on biomechanical behavior of zirconia dental crowns veneered with overpressing ceramics, Dent. Mater. J. (2017). https://doi.org/10.4012/dmj.2016-096.
[217] M.J. Tholey, C. Berthold, M. V. Swain, N. Thiel, XRD2 micro-diffraction analysis of the interface between Y-TZP and veneering porcelain: Role of application methods, Dent. Mater. (2010). https://doi.org/10.1016/j.dental.2010.02.002.
[218] A. Brijawi, A. Samran, A. Samran, A. Alqerban, M. Murad, Effect of different core design made of computer-aided design/computer-aided manufacturing system and veneering technique on the fracture resistance of zirconia crowns: A laboratory study, J. Conserv. Dent. (2019). https://doi.org/10.4103/JCD.JCD_426_18.
[219] A.M.E. Marchionatti, I.L. Aurélio, L.G. May, Does veneering technique affect the flexural strength or load-to-failure of bilayer Y-TZP? A systematic review and meta-analysis, J. Prosthet. Dent. (2018). https://doi.org/10.1016/j.prosdent.2017.11.013.
[220] B. Stawarczyk, M. Özcan, M. Roos, A. Trottmann, I. Sailer, C.H.F. Hämmerle, Load-bearing capacity and failure types of anterior zirconia crowns veneered with overpressing and layering techniques, Dent. Mater. (2011). https://doi.org/10.1016/j.dental.2011.07.006.
[221] M. Eisenburger, T. Mache, L. Borchers, M. Stiesch, Fracture stability of anterior zirconia crowns with different core designs and veneered using the layering or the press-over technique, Eur. J. Oral Sci. (2011). https://doi.org/10.1111/j.1600-0722.2011.00829.x.
[222] High strength CAD/CAM fabricated veneering material sintered to zirconia copings – A new fabrication mode for all-ceramic restorations, J. Prosthet. Dent. (2009). https://doi.org/10.1016/s0022-3913(09)60140-2.
[223] J.M.C. Lima, A.C.O. Souza, L.C. Anami, M.A. Bottino, R.M. Melo, R.O.A. Souza, Effects of thickness, processing technique, and cooling rate protocol on the flexural strength of a bilayer ceramic system, Dent. Mater. (2013). https://doi.org/10.1016/j.dental.2013.07.019.
[224] M. Subash, D. Vijitha, S. Deb, A. Satish, N. Mahendirakumar, Evaluation of shear bond strength between zirconia core and ceramic veneers fabricated by pressing and layering techniques: In vitro study, J. Pharm. Bioallied Sci. (2015). https://doi.org/10.4103/0975-7406.163568.

[225] A. Vichi, M. Sedda, G. Bonadeo, M. Bosco, A. Barbiera, N. Tsintsadze, M. Carrabba, M. Ferrari, Effect of repeated firings on flexural strength of veneered zirconia, Dent. Mater. (2015). https://doi.org/10.1016/j.dental.2015.04.012.
[226] B. Kanat-Ertürk, E.M. Çömlekoğlu, M. Dündar-Çömlekoğlu, M. Özcan, M.A. Güngör, Effect of Veneering Methods on Zirconia Framework-Veneer Ceramic Adhesion and Fracture Resistance of Single Crowns, J. Prosthodont. (2015). https://doi.org/10.1111/jopr.12236.
[227] B. Kanat, E.M. Çömlekoğlu, M. Dündar-Çömlekoğlu, B. Hakan Sen, M. Özcan, M. Ali Güngör, Effect of Various Veneering Techniques on Mechanical Strength of Computer-Controlled Zirconia Framework Designs, J. Prosthodont. (2014). https://doi.org/10.1111/jopr.12130.
[228] P.C. Guess, E.A. Bonfante, N.R.F.A. Silva, P.G. Coelho, V.P. Thompson, Effect of core design and veneering technique on damage and reliability of Y-TZP-supported crowns, Dent. Mater. (2013). https://doi.org/10.1016/j.dental.2012.11.012.
[229] W.S. Lin, C. Ercoli, C. Feng, D. Morton, The Effect of Core Material, Veneering Porcelain, and Fabrication Technique on the Biaxial Flexural Strength and Weibull Analysis of Selected Dental Ceramics, J. Prosthodont. (2012). https://doi.org/10.1111/j.1532-849X.2012.00845.x.
[230] R. Ansong, B. Flinn, K.H. Chung, L. Mancl, M. Ishibe, A.J. Raigrodski, Fracture toughness of heat-pressed and layered ceramics, J. Prosthet. Dent. (2013). https://doi.org/10.1016/S0022-3913(13)60051-7.
[231] A.K.F. Costa, A.L.S. Borges, G.J.P. Fleming, O. Addison, The strength of sintered and adhesively bonded zirconia/veneer-ceramic bilayers, J. Dent. (2014). https://doi.org/10.1016/j.jdent.2014.08.001.
[232] F. Beuer, J. Schweiger, M. Eichberger, H.F. Kappert, W. Gernet, D. Edelhoff, High-strength CAD/CAM-fabricated veneering material sintered to zirconia copings - A new fabrication mode for all-ceramic restorations, Dent. Mater. (2009). https://doi.org/10.1016/j.dental.2008.04.019.
[233] C. Riedel, M. Wendler, R. Belli, A. Petschelt, U. Lohbauer, In vitro lifetime of zirconium dioxide-based crowns veneered using Rapid Layer Technology, Eur. J. Oral Sci. (2019). https://doi.org/10.1111/eos.12604.
[234] J.Y. Sim, W.S. Lee, J.H. Kim, H.Y. Kim, W.C. Kim, Evaluation of shear bond strength of veneering ceramics and zirconia fabricated by the digital veneering method, J. Prosthodont. Res. (2016). https://doi.org/10.1016/j.jpor.2015.11.001.
[235] S. Tangsatchatham, N. Juntavee, Flexural strength of various types of computerized machinable ceramic veneered to yttria stabilized tetragonal zirconia polycrystalline ceramic upon different hybridized techniques, Clin. Cosmet. Investig. Dent. (2019). https://doi.org/10.2147/CCIDE.S196297.
[236] C. da S. Rodrigues, I.L. Aurélio, M. da R. Kaizer, Y. Zhang, L.G. May, Do thermal treatments affect the mechanical behavior of porcelain-veneered zirconia? A systematic review and meta-analysis, Dent. Mater. (2019). https://doi.org/10.1016/j.dental.2019.02.016.
[237] P.D. Meirelles, Y.O. Spigolon, M. Borba, P. Benetti, Leucite and cooling rate effect on porcelain–zirconia mechanical behavior, Dent. Mater. (2016). https://doi.org/10.1016/j.dental.2016.09.018.
[238] C.B. Tanaka, H. Harisha, M. Baldassarri, M.S. Wolff, H. Tong, J.B.C. Meira, Y.

Zhang, Experimental and finite element study of residual thermal stresses in veneered Y-TZP structures, Ceram. Int. (2016). https://doi.org/10.1016/j.ceramint.2016.03.018.

[239] B. Al-Amleh, J. Neil Waddell, K. Lyons, M. V. Swain, Influence of veneering porcelain thickness and cooling rate on residual stresses in zirconia molar crowns, Dent. Mater. (2014). https://doi.org/10.1016/j.dental.2013.11.011.

[240] A.K. Mainjot, G.S. Schajer, A.J. Vanheusden, M.J. Sadoun, Influence of veneer thickness on residual stress profile in veneering ceramic: Measurement by hole-drilling, Dent. Mater. (2012). https://doi.org/10.1016/j.dental.2011.11.008.

[241] J.E. Choi, J.N. Waddell, M. V. Swain, Pressed ceramics onto zirconia. Part 2: Indentation fracture and influence of cooling rate on residual stresses, Dent. Mater. (2011). https://doi.org/10.1016/j.dental.2011.08.003.

[242] M.J. Tholey, M. V. Swain, N. Thiel, Thermal gradients and residual stresses in veneered Y-TZP frameworks, Dent. Mater. (2011). https://doi.org/10.1016/j.dental.2011.08.001.

[243] A.K. Mainjot, G.S. Schajer, A.J. Vanheusden, M.J. Sadoun, Influence of cooling rate on residual stress profile in veneering ceramic: Measurement by hole-drilling, Dent. Mater. (2011). https://doi.org/10.1016/j.dental.2011.05.005.

[244] A.K. Mainjot, G.S. Schajer, A.J. Vanheusden, M.J. Sadoun, Influence of zirconia framework thickness on residual stress profile in veneering ceramic: Measurement by hole-drilling, Dent. Mater. (2012). https://doi.org/10.1016/j.dental.2011.11.009.

[245] A.A. Almeida-Júnior, D. Longhini, N.B. Domingues, C. Santos, G.L. Adabo, Effects of extreme cooling methods on mechanical properties and shear bond strength of bilayered porcelain/3Y-TZP specimens, J. Dent. (2013). https://doi.org/10.1016/j.jdent.2013.01.005.

[246] C.S. Rodrigues, I.L. Aurélio, S. Fraga, L.G. May, Glaze firings on veneered zirconia: Residual stresses and optical aspects, Dent. Mater. (2018). https://doi.org/10.1016/j.dental.2018.08.204.

[247] C.B. Tanaka, N.H.B. Ahmad, A. Ellakwa, J.J. Kruzic, Effect of cooling protocol on mechanical properties and microstructure of dental veneering ceramics, Dent. Mater. (2019). https://doi.org/10.1016/j.dental.2019.07.011.

[248] S. Yamauchi, S. Miura, S. Kasahara, J. Sun, H. Egusa, A thick frame decreases the fracture toughness of veneering ceramics used for zirconia-based all-ceramic restorations, J. Prosthodont. Res. (2019). https://doi.org/10.1016/j.jpor.2018.11.007.

[249] S.S. Scherrer, U. Lohbauer, A. Della Bona, A. Vichi, M.J. Tholey, J.R. Kelly, R. van Noort, P.F. Cesar, ADM guidance—Ceramics: guidance to the use of fractography in failure analysis of brittle materials, Dent. Mater. (2017). https://doi.org/10.1016/j.dental.2017.03.004.

[250] M. Baldassarri, C.F.J. Stappert, M.S. Wolff, V.P. Thompson, Y. Zhang, Residual stresses in porcelain-veneered zirconia prostheses, Dent. Mater. (2012). https://doi.org/10.1016/j.dental.2012.04.019.

[251] G. Ramos, E. Monteiro, M. Bottino, Y. Zhang, R. Marques de Melo, Failure Probability of Three Designs of Zirconia Crowns, Int. J. Periodontics Restorative Dent. (2015). https://doi.org/10.11607/prd.2448.

[252] A. Skjold, C. Schriwer, M. Øilo, Effect of margin design on fracture load of zirconia crowns, Eur. J. Oral Sci. (2019). https://doi.org/10.1111/eos.12593.

[253] Y. Liu, H. Feng, Y. Bao, Y. Qiu, N. Xing, Z. Shen, Fracture and interfacial delamination origins of bilayer ceramic composites for dental restorations, J. Eur. Ceram. Soc. (2010). https://doi.org/10.1016/j.jeurceramsoc.2009.11.019.
[254] N.R.F.A. Silva, E. Bonfante, B.T. Rafferty, R.A. Zavanelli, L.L. Martins, E.D. Rekow, V.P. Thompson, P.G. Coehlo, Conventional and Modified Veneered Zirconia vs. Metalloceramic: Fatigue and Finite Element Analysis, J. Prosthodont. (2012). https://doi.org/10.1111/j.1532-849X.2012.00861.x.
[255] M.N. Aboushelib, Fatigue and Fracture Resistance of Zirconia Crowns Prepared with Different Finish Line Designs, J. Prosthodont. (2012). https://doi.org/10.1111/j.1532-849X.2011.00787.x.
[256] J.H. Kim, J.H. Park, Y.B. Park, H.S. Moon, Fracture load of zirconia crowns according to the thickness and marginal design of coping, J. Prosthet. Dent. (2012). https://doi.org/10.1016/S0022-3913(12)60114-0.
[257] Y. Zhang, M. Allahkarami, J.C. Hanan, Measuring residual stress in ceramic zirconia-porcelain dental crowns by nanoindentation, J. Mech. Behav. Biomed. Mater. (2012). https://doi.org/10.1016/j.jmbbm.2011.11.006.
[258] C.S. Millen, R.L. Reuben, R.J. Ibbetson, The effect of coping/veneer thickness on the fracture toughness and residual stress of implant supported, cement retained zirconia and metal-ceramic crowns, Dent. Mater. (2012). https://doi.org/10.1016/j.dental.2012.06.008.
[259] S.R. Ha, S.H. Kim, J.B. Lee, J.S. Han, I.S. Yeo, S.H. Yoo, Effects of coping designs on stress distributions in zirconia crowns: Finite element analysis, Ceram. Int. (2016). https://doi.org/10.1016/j.ceramint.2015.12.007.
[260] V.P. Fardin, E.A. Bonfante, P.G. Coelho, M.N. Janal, N. Tovar, L. Witek, D. Bordin, G. Bonfante, Residual stress of porcelain-fused to zirconia 3-unit fixed dental prostheses measured by nanoindentation, Dent. Mater. (2018). https://doi.org/10.1016/j.dental.2017.11.013.
[261] M. Øilo, K. Kvam, N.R. Gjerdet, Load at fracture of monolithic and bilayered zirconia crowns with and without a cervical zirconia collar, J. Prosthet. Dent. (2016). https://doi.org/10.1016/j.prosdent.2015.11.017.
[262] H. Scholze, Scholze, Horst (1991). Glass – Nature, Structure, and Properties. Springer. pp. 3–5. ISBN 978-0-387-97396-8., 2020.
[263] D. Kennedy, C. Norman, What don't we know?, Science (80-.). (2005). https://doi.org/10.1126/science.309.5731.75.
[264] George W. Scherer, Relaxation in Glass and Composites, Wiley, New York, 1986.
[265] ABAQUS, Abaqus 6.14, Abaqus 6.14 Anal. User's Guid. (2014).
[266] R. Gardon, Thermal Tempering of Glass, in: 1980. https://doi.org/10.1016/b978-0-12-706705-6.50010-2.
[267] A.Q. Tool, RELATION BETWEEN INELASTIC DEFORMABILITY AND THERMAL EXPANSION OF GLASS IN ITS ANNEALING RANGE, J. Am. Ceram. Soc. (1946). https://doi.org/10.1111/j.1151-2916.1946.tb11592.x.
[268] A. Markovsky, T.F. Soules, D.C. Boyd, An Efficient and Stable Algorithm for Calculating Fictive Temperatures, J. Am. Ceram. Soc. (1984). https://doi.org/10.1111/j.1151-2916.1984.tb18826.x.
[269] V.L. Indenbom, L.I. Vidro, Thermoplastic and Structrual Stresses in Solids, Sov. Phys. - Solid State (Engl. Transl.). (1964).

Appendices

Appendix A:

This appendix contains few novel methods and developments explored in the field of zirconia-based bilayer dental materials for performance improvement. This appendix is provided for ready reference of related studies.

Type of Novel Methods / Developments	References
Examples of surface treatment: Various Laser Treatments, Non-Thermal Plasma, Silica Coating, Enriched Ce-Layer deposition, Zirconia Surface Architecturing, Sonochemical Treatment, Atmospheric Pressure Glass Plasma Treatment, Si_3N_4 Treatment, Conditioner, Tribochemical Grit Blasting, CH_2Cl_2 Cleaning	[146,151–160,162,163,166,168,172,207,210,211]
Examples of bonding enhancement: Silica Infiltration, Hybrid Interlayer, Powder Coating, Thermal Silicatization, Plasma Enhanced Chemical Vapor Deposition Technique, Glaze Ceramic Coating, Interlayer Deposition, Parylene Multilayer)	[6,199–203,205,206,208]
Examples of veneering technique: Rapid Layer Technology, Digital Veneering Method, Hybridization	[233–235]
Examples of material development: Infiltration, Graded Structure, Porous Structure, Ion Exchange, Indirect Composite Resins, Novel Veneer Material	[95–101]

Appendix B:

This appendix contains sensitivity analysis performed to evaluate the effect of change in structural relaxation times on maximum principle stresses. Structural relaxation times are changed as 1/4th, 1/10th and 1/20th of shear relaxation times. The effect of change in structural relaxation times is evaluated on resulting maximum principal stresses. Based on this sensitivity analysis, it is observed that structural relaxation times within 1/4th to 1/20th of shear relaxation times are causing minor changes in the stress values. Difference of 3 to 4 MPa was observed by changing structural relaxation times.

(thickness = 0.7 mm 3Y-TZP + 1.5 mm Vita VM9; cooling rate = 200°C/min, material properties are referred from section 4 of this thesis)

Sr. No.	Structural relaxation time	Maximum Principal Stress (MPa)
1	1/4th of shear relaxation times	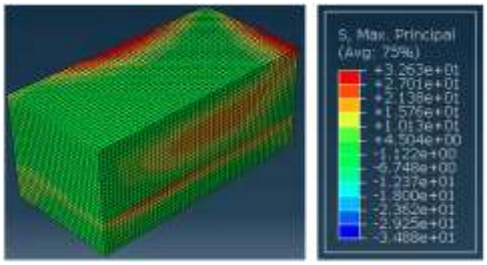
2	1/10th of shear relaxation times	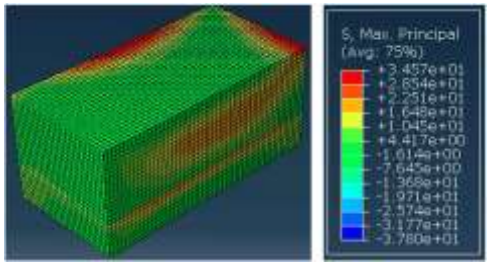
3	1/20th of shear relaxation times	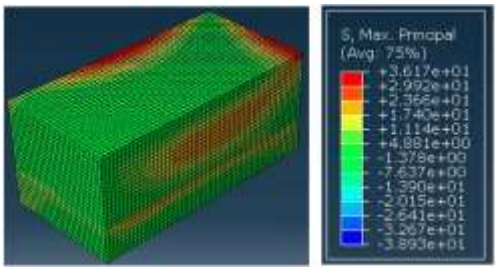

Curriculum Vitae

Name:	Prashant Satishkumar Shelar
Post-secondary Education and Degrees:	The Maharaja Sayajirao University of Baroda Vadodara, Gujarat, India 2003-2007 Bachelor of Engineering (Metallurgy) The University of Western Ontario London, Ontario, Canada 2019-2021 Master of Engineering Science (MME)
Honours and Awards:	Western Graduate Research Scholarship 2019-2020
Related Work Experience	Teaching Assistant / Research Assistant The University of Western Ontario 2019-2020 Senior Welding / Material Engineer Petrofac International Limited 2013-2019 Welding Engineer Lamprell Energy Limited 2011-2013 Welding Engineer Quality International Limited 2010-2011 Senior Executive (Welding) Godrej and Boyce Manufacturing Limited 2009-2010 Project Engineer Essar Steel Limited 2007-2009